Politecnico di Milano

School of Industrial and Information Engineering
Master of Science in Mathematical Engineering

MASTER THESIS

The DRPM Strikes Back: More Flexibility for a Bayesian Spatio-Temporal Clustering Model

Advisor
Prof. Alessandra Guglielmi

Coadvisor
Prof. Alessandro Carminati

Candidate
Federico Angelo Mor
Matr. 221429

Academic Year 2023–2024

to my cats Otto
and La Micia

Abstract

Clustering is a key technique for identifying patterns and structures in complex datasets, whose relevance is intensified in spatio-temporal contexts where observations are simultaneously influenced by multiple factors such as space, time, and covariates. This complexity can be effectively tamed by model-based clustering methods, which often provide more accurate and interpretable results with respect to traditional frequentist approaches thanks to the possibility of encoding data information directly inside the model. To this end, the Dependent Random Partition Model (G. L. Page et al., 2022) is one of the most relevant Bayesian models due to its explicit consideration of temporal dependence in the partitions. However, the current formulation of the model and the implementation of the associated MCMC algorithm lack of the inclusion of covariates, the handling of missing data, and the efficiency in execution times. Therefore, in this work we improve the original DRPM by addressing those issues through updates on the model formulation and a brand new implementation in Julia. These advancements are then tested on synthetic and real-world datasets, including air quality data from the AgrImOnIA project (Fassò et al., 2023) in Lombardy, Italy.

KEYWORDS: Bayesian modelling, clustering, spatio-temporal data, MCMC, Julia

Sommario

Il clustering è una tecnica fondamentale per identificare strutture e pattern in dataset complessi, la cui importanza è intensificata nei contesti spazio-temporali in cui le osservazioni sono influenzate simultaneamente da molteplici fattori come spazio, tempo e covariate. Questa complessità può essere efficacemente gestita da metodi di clustering basati su modelli, che spesso forniscono risultati più precisi e interpretabili rispetto agli approcci frequentisti tradizionali grazie alla possibilità di inserire informazioni riguardo ai dati direttamente all'interno del modello. In tal senso, il Dependent Random Partition Model (G. L. Page et al., 2022) è uno dei modelli bayesiani più rilevanti in quanto tiene conto in modo esplicito della dipendenza temporale delle partizioni. Tuttavia, l'attuale formulazione del modello e la sua corrispondente implementazione dell'algoritmo di campionamento mancano dell'inclusione di covariate, della gestione dei dati mancanti, e di efficienza nei tempi di esecuzione. In questo lavoro abbiamo quindi migliorato l'originale DRPM affrontando tali problemi tramite aggiornamenti sulla formulazione del modello e una fiammante implementazione in Julia. Questi sviluppi sono stati poi testati su dataset sintetici e reali, compresi i dati sulla qualità dell'aria in Lombardia del progetto AgrImOnIA (Fassò et al., 2023).

Parole chiave: modellistica bayesiana, clustering, dati spazio-temporali, MCMC, Julia

Contents

List of Figures

List of Tables

Introduction

Clustering is a fundamental technique of unsupervised learning where a set of data points has to be divided into homogenous groups of units which exhibit a similar behaviour relative to a target variable. It has long been a powerful tool for identifying structures and patterns in data, especially in contexts where relationships between observations are complex, such as when the target variable is affected by multiple factors simultaneously. For this reason, clustering methods have become increasingly popular across a variety of scientific fields, including social sciences, climate and environmental analysis, economics, and healthcare.

Clustering approaches are generally divided into two main categories: algorithmic and model-based methods.

Algorithmic methods such as hierarchical, partition-based, or density-based methods, address the clustering problem as an optimization problem where a certain metric has to be minimised (or maximised). For instance, partition-based methods like k-means generate clusters around a set of centroids which are iteratively updated to minimize the within-cluster variance, i.e. the mean squared distance of the units from their assigned cluster centroid. However, these methods require to specify the desired number k of clusters in advance and are limited to numerical data. Hierarchical clustering methods, on the other hand, build a tree-like structure of clustering solutions, represented as a dendrogram, which captures the relationships among potential clusters. This is done through either an agglomerative (bottom-up) strategy, where each unit starts in her own cluster that gets iteratively combined with other units or clusters, or in a divisive (top-down) strategy, where units start in a single cluster that is iteratively subdivided. These methods do not necessitate a predefined number of clusters, but they are highly sensitive to the choice of the distance metric, which drives all merging and splitting decisions. Density based methods, such as DBSCAN, define clusters through a density metric which can produce more flexible structures with clusters of varying shapes. However, these methods remain sensitive to the choice of the density parameters and may yield less interpretable and irregular clusters. In summary, these algorithmic approaches are largely heuristic, performing well only with well-separated clusters or standard geometric forms, but often failing in more complex scenarios. Furthermore, lacking a solid statistical foundation, these methods can lead to unsatisfactory results and provide no assessment about clustering uncertainty.

An alternative and more flexible approach is therefore proposed by model-based methods, which assume a probabilistic modelling of the data. This is typically done through a mixture model, where each mixture component corresponds to a cluster

with its specific cluster parameters (Wade, 2023) (Gormley et al., 2022). In this way, each observation is assumed to have arisen from one of J possible groups which are mixed together in various proportions. More formally, for each unit $i = 1, \dots, n$ we have that

$$f(y_i|\boldsymbol{\pi}, \boldsymbol{\vartheta}_1^\star, \dots, \boldsymbol{\vartheta}_J^\star) = \sum_{j=1}^{J} \pi_j f_j(y_j|\boldsymbol{\vartheta}_j^\star) \tag{1}$$

where y_i is the data point of the i-th observation, $\boldsymbol{\pi}$ is the set of weights satisfying $\pi_j \in [0, 1]$ for $j = 1, \dots, J$ and $\sum_{j=1}^{J} \pi_j = 1$, $\boldsymbol{\vartheta}_j^\star$ are the cluster-specific parameters, and $f_j(\cdot, |\vartheta_j^\star)$ is the density of the j-th cluster. A common modelling choice is a gaussian mixture model (GMM), where each cluster follows a normal distribution and thus making $\boldsymbol{\vartheta}_{\boldsymbol{j}}^\star = (\mu_j^\star, \sigma_j^{2\star})$, or $\boldsymbol{\vartheta}_{\boldsymbol{j}}^\star = (\boldsymbol{\mu}_j^\star, \Sigma_j^\star)$ in the multivariate case. This choice is flexible and effective since, especially in the multivariate case, gaussian distribution are able to capture very different clustering structures. Anyway, in this model-based approach, the goal is to estimate the cluster-specific parameters $\boldsymbol{\vartheta}_1, \dots, \boldsymbol{\vartheta}_J$ and the mixing proportions $\pi_1, \dots, \pi_J$. The estimation step is often performed through the Expectation-Maximization (EM) algorithm, which iteratively refines the estimates of the parameters via maximum likelihood estimation (MLE). Once the cluster-specific parameters are estimated, each observation can be assigned to a component, i.e. to a cluster, based on the highest posterior probability of belonging to that component, which can be computed through the Bayes rule.

This approach of mixture model can be naturally moved in a Bayesian framework where to each parameter is treated as a random variable with a corresponding prior distribution (Franzén, 2008). This leads (1) to be reformulated into

$$\begin{aligned} y_i|c_i, \boldsymbol{\pi}, \boldsymbol{\vartheta}_1^\star, \dots, \boldsymbol{\vartheta}_J^\star &\overset{\text{iid}}{\sim} f_{c_i}(y_i|\boldsymbol{\vartheta}_{c_i}^\star) \\ c_1, \dots, c_n &\sim \text{Cat}(\pi_1, \dots, \pi_J) \\ \boldsymbol{\vartheta}_1^\star, \dots, \boldsymbol{\vartheta}_J^\star &\overset{\text{iid}}{\sim} F_0 \\ \pi_1, \dots, \pi_J &\sim \text{Dir}(\gamma, \dots, \gamma) \end{aligned} \tag{2}$$

where the cluster labels $c_1, \dots, c_n$ are assigned a multinomial distribution with probabilities given by the vector of weights $\boldsymbol{\pi}$, the cluster-specific parameters $\boldsymbol{\vartheta}_j^\star$ are assigned a prior distribution F_0, while the weights are assigned a Dirichlet distribution, where e.g. all parameters are the same $\gamma_j = \gamma$ if no prior information about cluster assignments is wished to be inserted into the model.

The Bayesian framework is however much powerful and allows for even more complex formulations. In fact, moving to a Bayesian non-parametric approach, an infinite mixture model (i.e. that does not require a predetermined number J of components) can be introduced. This extension often relies on the Dirichlet Process (DP) (Ferguson, 1973), which leads to a model formulation in the form

$$\begin{aligned} y_i|\boldsymbol{\vartheta}_i &\overset{\text{ind}}{\sim} f(y_i|\boldsymbol{\vartheta}_i) \\ \boldsymbol{\vartheta}_1, \dots, \boldsymbol{\vartheta}_n|P &\overset{\text{iid}}{\sim} P \\ P &\sim \text{discrete RPM} \end{aligned}$$

where RPM denotes a random probability measure. The discreteness of P implies the presence of ties among the atoms of the process $\boldsymbol{\vartheta}_1, \ldots, \boldsymbol{\vartheta}_n$. These ties therefore induce a partition ρ_n which can be identified by the units manifesting the same values of the parameter $\boldsymbol{\vartheta}_i$. That is, denoting with $\boldsymbol{\vartheta}_1^\star, \ldots, \boldsymbol{\vartheta}_K^\star$ the unique values of $\boldsymbol{\vartheta}_1, \ldots, \boldsymbol{\vartheta}_n$, the generic h-cluster can be defined as $S_h = \{i \in \{1, \ldots, n\} : \boldsymbol{\vartheta}_i = \boldsymbol{\vartheta}_h^\star\}$. The Dirichlet Process plays a significant role in general in Bayesian nonparametrics (Grazian, 2023), but especially in clustering, thanks to its computationally manageable implementation through the stick-breaking representation (Teh, 2010), the Pólya urn representation (Blackwell et al., 1973), and the Chinese restaurant process (CRP) (Aldous, 1985).

However, implementing Bayesian methods often requires the design of Markov Chain Monte Carlo (MCMC) algorithms, which can often be complex and computationally intensive. MCMC techniques, such as the Metropolis-Hastings and Gibbs sampling algorithms, are essential for approximating the posterior distributions of the model parameters and to allow inference on the generated clusters. These algorithms work by constructing a Markov chain that eventually generates samples from the target distribution; a process that requires a certain tuning of the hyperparameters and final convergence diagnostics to ensure reliability of the results. The iterative nature of MCMC also implies that considerable computational resources may be needed, particularly for models with an high-dimensional parameter space or simply when working with large datasets. Consequently, while Bayesian methods provide a robust framework for modeling uncertainty and incorporating prior knowledge, they also demand significant computational effort and expertise in algorithm design to effectively extract their full potential.

This increased flexibility in the clustering modelling becomes even more powerful when working on spatio-temporal datasets, in which observations are collected over time and across different spatial locations, possibly concealing trends behind both information levels. This type of data, in fact, is inherently complex due to this interaction between spatial and temporal dimensions; a complexity that is further increased if covariates are also available. As a result, model-based methods are fairly more suited to tackle this task, rather than traditional algorithmic methods, since they can combine all these different levels of information. A model-based analysis of such data should also be able to account for the temporal dependency among the partitions, in order to extract possible trends occurring in time, producing clusters which evolve in time in a more gentle and interpretable way, while also granting efficient implementations to be possibly applied on large scale datasets, which are commonly accessible in this context.

Recently, the use of Bayesian models to perform clustering has become more popular, particularly in this field of spatio-temporal datasets. Bayesian clustering, in fact, allows to incorporate prior information into the model enhancing the flexibility and interpretability of the results with respect, for example, to more traditional frequentist approaches. Throughout the years, several models have been proposed in the Bayesian literature, but one of the most relevant is the Dependent Random Partition Model (G. L. Page et al., 2022) which stands out for being able to handle explicitly the temporal dependence of partitions into the model formulation, while also possibly accounting for the spatial information. However, the current DRPM

implementation of the MCMC algorithm, written in C and available through an R interface, lacks some relevant utilities such as the inclusion of covariates, which could further improve the generation and informativity of the clusters, the handling of missing data, and an efficient implementation, which would speed up the model fitting to run multiple chains in parallel, or be more easily applied on large scale datasets.

In this work, we aim to address these three issues by making the original model more flexible. We will show how our updates can indeed be effective and also provide faster execution times. In fact, implementing the model using the Julia language, rather than C, we took advantage of its high-performance capabilities and well-equipped statistical ecosystem. Our comparison will focus on both synthetic and real-world datasets, with the latter case involving air quality measurements from the AgrImOnIA project (Fassò et al., 2023), a comprehensive record of air pollutant levels and other environmental variables measured across the Lombardy region of Italy.

Chapter 1 briefly reviews the literature on Bayesian clustering models for spatio-temporal data, and then dives deeply into the analysis and description of the DRPM and of our generalization.

Chapter 2 provides insights about the computational aspects of the MCMC algorithm, motivating the choice of the Julia language and reporting some optimization possibilities emerged when developing the implementation.

Chapter 3 focuses on testing the original DRPM formulation and our generalized model. We firstly evaluate if they perform similarly at a common testing level, i.e. under the same data, hyperparameters values, and MCMC iterations setup. Then, we assess the performances of our updates by considering fits involving missing data and fits including covariates. A comparative analysis about execution times with respect to the size of the dataset and the type of the fit will also be provided.

Finally, in Chapter 4, we briefly review the strengths and drawbacks this work revealed and suggest possible further improvements.

Chapter 1

Description of the model

> *"Come on, gentlemen, why shouldn't we get rid of all this calm reasonableness with one good kick, just so as to send all these logarithms to the devil and be able to live our own lives at our own sweet will?"*
> — Fëdor Dostoevskij, *Notes from the Underground*

In the Bayesian framework, clustering is possible by employing a random probability measure of discrete type that induces a distribution over random partitions. This discreteness is obtained with the Dirichlet Process (DP), which several clustering models implement either through the stick-breaking representation (Barajas et al., 2012) (Antoniano Villalobos et al., 2015) (Gutiérrez et al., 2016) (Jo et al., 2016) (Kalli et al., 2018) (De Iorio and Kottas, 2018) (De Iorio, Favaro, et al., 2019) or through the Pólya urn scheme (Caron et al., 2017). However, these classical Bayesian methods rely on modelling the dependence in the random partitions by modelling the dependence inside the random probability measures, i.e. on the parameters which underlie those DP representations rather than to the clusters themselves. This approach is therefore kind of a "step back" from the main object of interest, the clusters, which are then only *induced* by the random partition model. As a consequence, there is no guarantee that the correlation that appears in the parameters would subsequently reflect into correlation among the partitions, often producing counterintuitive behaviours in the results. The Dependent Random Partition Model (DRPM) (G. L. Page et al., 2022), on the other hand, models *directly* the sequence of partitions, thus providing a more reasonable, accurate, and interpretable temporal evolution of the clusters.

Before diving into the model description, we define some notation conventions. We setup in a spatio-temporal context with $i = 1, \dots, n$ and $t = 1, \dots, T$ being the indexes for units and time instants. We will denote with $\rho_t = \{S_{1t}, \dots, S_{k_t t}\}$ the partition at time t, of the n experimental units, composed by k_t cluster. Another possible representation of the partition is through cluster membership labels $\boldsymbol{c}_t = \{c_{1t}, \dots, c_{nt}\}$, where $c_{it} = j$ if unit i belongs to cluster S_{jt}. Finally, we will denote with a $\star$ superscript all the variables or quantities which are cluster-specific.

To implement dependence in the partitions one could simply propose a joint probability model for $(\rho_1, \dots, \rho_T)$, denoted as $P(\rho_1, \dots, \rho_T)$, where each ρ_t is set to be possibly affected by all the other partitions. This principle, however, it's far too complex and general to be modelled efficiently; therefore the DRPM authors limited this temporal connection to a first-order Markov-chain structure, where the conditional distribution of ρ_t given all the predecessors $\rho_{t-1}, \rho_{t-2}, \dots, \rho_1$ actually depends only on ρ_{t-1}. This brings the random partition model to the form

$$P(\rho_1, \dots, \rho_T) = P(\rho_T|\rho_{T-1}) \cdots P(\rho_2|\rho_1)P(\rho_1) \tag{1.1}$$

To explicitly manage the relation between ρ_t and ρ_{t-1} some auxiliary variables are introduced. The idea is that if two partitions are highly time-dependent, few changes will occur between them. In turn, partitions which are quite independent will possibly exhibit very different configurations. To express this fixity or flexibility concept, for each unit $i = 1, \dots, n$ the following variable is introduced

$$\gamma_{it} = \begin{cases} 1 & \text{if unit } i \text{ is } \textit{not} \text{ reallocated when moving from time } t-1 \text{ to } t \\ 0 & \text{otherwise (i.e. unit } \textit{is} \text{ reallocated)} \end{cases} \tag{1.2}$$

By construction, we set $\gamma_{i1} = 0$ for all i, meaning that at the first time instant all units will get reallocated since they have no partition to which they could be possibly fixed at. Regarding their modelling, the authors proposed $\gamma_{it} \overset{\text{ind}}{\sim} \text{Ber}(\alpha_t)$ with $\alpha_t \in [0, 1]$ behaving as a temporal dependence parameter. At the two extremes, $\alpha_t = 1$ will denote perfect temporal dependence, with $\rho_t = \rho_{t-1}$, while $\alpha_t = 0$ will imply full independence of ρ_t from ρ_{t-1}. The parameter α_t can actually be global, and we will write simply α without any subscripts, or instead time and/or unit specific, offering the cases of α_t, α_i, or α_{it}. For the sake of clarity, the vector $\boldsymbol{\gamma}_t = (\gamma_{1t}, \dots, \gamma_{nt})$ is created, and the augmented joint model becomes in the form

$$P(\boldsymbol{\gamma}_1, \rho_1, \dots, \boldsymbol{\gamma}_T, \rho_T) = P(\rho_T|\boldsymbol{\gamma}_T, \rho_{T-1})P(\boldsymbol{\gamma}_T) \cdots P(\rho_2|\boldsymbol{\gamma}_2, \rho_1)P(\boldsymbol{\gamma}_2)P(\rho_1) \tag{1.3}$$

The insertion of these additional variables makes the model very powerful in describing the temporal dependence of the partitions but slightly hinders the design of the sampling algorithm. To outline it, we firstly need a

Definition 1.1 (compatibility)**.** Two partitions ρ_t and ρ_{t-1} are *compatible* with respect to $\boldsymbol{\gamma}_t$ if ρ_t can be obtained from ρ_{t-1} by reallocating items as indicated by γ_t; i.e. only moving the units i with $\gamma_{it} = 0$.

To perform this compatibility check, it is enough to ensure that the reduced partitions from ρ_t and ρ_{t-1} are the same, with reduced meaning their restriction to the units which cannot move. Indeed, if those fixed units are clustered in the same ways, then surely the free-movers from ρ_t can be set to match the labels assigned by partition ρ_{t-1}. Denoting as $\mathfrak{R}_t = \{i : \gamma_{it} = 1\}$ the set of fixed units at time t, this check translates into asking that $\rho_t^{\mathfrak{R}_t} = \rho_{t-1}^{\mathfrak{R}_t}$.

The sampling algorithm requires that when we are drawing the new samples for the γ_{it}a, or also for the cluster labels c_{it}, we firstly need to check if those draws can

actually be valid, i.e. if they would keep compatible and coherent all the partitions and parameters involved. For example, when updating γ_{it} during each iteration d of the algorithm, the only case which can raise problems is when we pass from $\gamma_{it}^{(d-1)} = 0$ to $\gamma_{it}^{(d)} = 1$. This step corresponds to the case in which a unit i that was initially (i.e. according to the previous iteration parameters) free to be reassigned is now instead deemed to stay fixed in her cluster. However, this change may not align to the current sampled values of the partitions $\rho_{t-1}^{(d)}$ and $\rho_t^{(d-1)}$. Therefore, compatibility between their reductions to the units in the set $\mathfrak{R}_t \cup \{i\}$ needs to be checked and, if this check fails, the tentative update $\gamma_{it}^{(d-1)} = 0 \to \gamma_{it}^{(d)} = 1$ is not allowed to be performed and we force $\gamma_{it}^{(d)} = 0$ in the sampling algorithm. Similar checks are conducted when ρ_t is updated. In this step, only the units that can actually move, i.e. that have $\gamma_{it} = 0$, are updated, and therefore there are no compatibility problems between ρ_{t-1} and ρ_t. However, since the update of γ_{it} occurs before the one of the partition, compatibility needs to be checked between ρ_t and ρ_{t+1}.

In any case, once the partition model is specified, there is great flexibility in how to setup the rest of the hierarchical model. To allow temporal dependence to propagate through the model, an autoregressive AR(1) component is also added to the formulation of the model (but only optionally in the implementation), both at the data and cluster-specific parameters level. All this led the authors to the following complete model

$$
\begin{aligned}
Y_{it}|Y_{it-1}, \boldsymbol{\mu}_t^\star, \boldsymbol{\sigma}_t^{2\star}, \boldsymbol{\eta}, \boldsymbol{c}_t &\overset{\text{ind}}{\sim} \mathcal{N}(\mu^\star_{c_{it}t} + \eta_{1i} Y_{it-1}, \sigma^{2\star}_{c_{it}t}(1-\eta_{1i}^2)) \\
Y_{i1} &\overset{\text{ind}}{\sim} \mathcal{N}(\mu^\star_{c_{i1}1}, \sigma^{2\star}_{c_{i1}1}) \\
\xi_i = \text{Logit}(\tfrac{1}{2}(\eta_{1i}+1)) &\overset{\text{ind}}{\sim} \text{Laplace}(a, b) \\
(\mu^\star_{jt}, \sigma^\star_{jt}) &\overset{\text{ind}}{\sim} \mathcal{N}(\vartheta_t, \tau_t^2) \times \mathcal{U}(0, A_\sigma) \\
\vartheta_t|\vartheta_{t-1} &\overset{\text{ind}}{\sim} \mathcal{N}((1-\varphi_1)\varphi_0 + \varphi_1\vartheta_{t-1}, \lambda^2(1-\varphi_1^2)) \\
(\vartheta_1, \tau_t) &\overset{\text{iid}}{\sim} \mathcal{N}(\varphi_0, \lambda^2) \times \mathcal{U}(0, A_\tau) \\
(\varphi_0, \varphi_1, \lambda) &\sim \mathcal{N}(m_0, s_0^2) \times \mathcal{U}(-1, 1) \times \mathcal{U}(0, A_\lambda) \\
\{\boldsymbol{c}_t, \dots, \boldsymbol{c}_T\} &\sim \text{tRPM}(\boldsymbol{\alpha}, M) \text{ with } \alpha_t \overset{\text{iid}}{\sim} \text{Beta}(a_\alpha, b_\alpha)
\end{aligned}
\tag{1.4}
$$

where tRPM represents the temporal random partition model (1.3).

Moving towards our update, we decided to refine some parts of that formulation. Regarding the variances $\sigma^{2\star}_{jt}$, τ_t^2, and λ^2, we chose to model them through an inverse gamma distribution rather than the uniform employed originally. This is indeed a more sophisticate choice, since the tuning of the parameters of an invGamma(a, b) is a bit more difficult than simply setting the bounds of a $\mathcal{U}(l, u)$, but should guarantee a better mixing in the chain. In fact, the invGamma distributions recovers conjugacy in the model, thanks to the normal law assigned to the other parameters, allowing the update step of the variances to be performed through the analytically exact Gibbs sampler rather than the acceptance-rejection method of Metropolis algorithm. Finally, to improve the accuracy in fitting the target values, we added a regression parameter $\boldsymbol{\beta}_t$ in the likelihood. We decided to make it only

time-dependent, and not also unit-dependent, to lighten the already quite-heavy formulation.

The final updated model is now proposed, with highlighted in dark red the changes and insertions that we made.

$$
\begin{aligned}
Y_{it}|Y_{it-1}, \boldsymbol{\mu}^\star_t, \boldsymbol{\sigma}^{2\star}_t, \boldsymbol{\eta}, \boldsymbol{c}_t &\overset{\text{ind}}{\sim} \mathcal{N}(\mu^\star_{c_{it}t} + \eta_{1i} Y_{it-1} + \boldsymbol{x}_{it}^T \boldsymbol{\beta}_t, \sigma^{2\star}_{c_{it}t}(1-\eta^2_{1i})) \\
Y_{i1} &\overset{\text{ind}}{\sim} \mathcal{N}(\mu^\star_{c_{i1}1} + \boldsymbol{x}_{i1}^T \boldsymbol{\beta}_1, \sigma^{2\star}_{c_{i1}1}) \\
\boldsymbol{\beta}_t &\overset{\text{ind}}{\sim} \mathcal{N}_p(\boldsymbol{b}, s^2 I) \\
\xi_i = \text{Logit}(\tfrac{1}{2}(\eta_{1i}+1)) &\overset{\text{ind}}{\sim} \text{Laplace}(a, b) \\
(\mu^\star_{jt}, \sigma^{2\star}_{jt}) &\overset{\text{ind}}{\sim} \mathcal{N}(\vartheta_t, \tau^2_t) \times \text{invGamma}(a_\sigma, b_\sigma) \\
\vartheta_t|\vartheta_{t-1} &\overset{\text{ind}}{\sim} \mathcal{N}((1-\varphi_1)\varphi_0 + \varphi_1 \vartheta_{t-1}, \lambda^2(1-\varphi_1^2)) \\
(\vartheta_1, \tau^2_t) &\overset{\text{iid}}{\sim} \mathcal{N}(\varphi_0, \lambda^2) \times \text{invGamma}(a_\tau, b_\tau) \\
(\varphi_0, \varphi_1, \lambda^2) &\sim \mathcal{N}(m_0, s_0^2) \times \mathcal{U}(-1, 1) \times \text{invGamma}(a_\lambda, b_\lambda) \\
\{\boldsymbol{c}_t, \dots, \boldsymbol{c}_T\} \sim \text{tRPM}(\boldsymbol{\alpha}, M) &\text{ with } \alpha_t \overset{\text{iid}}{\sim} \text{Beta}(a_\alpha, b_\alpha)
\end{aligned}
\tag{1.5}
$$

A visual representation of this new version of the DRPM model is also present in Figure 1.1, to more clearly appreciate the hierarchical structure and the relations among the parameters.

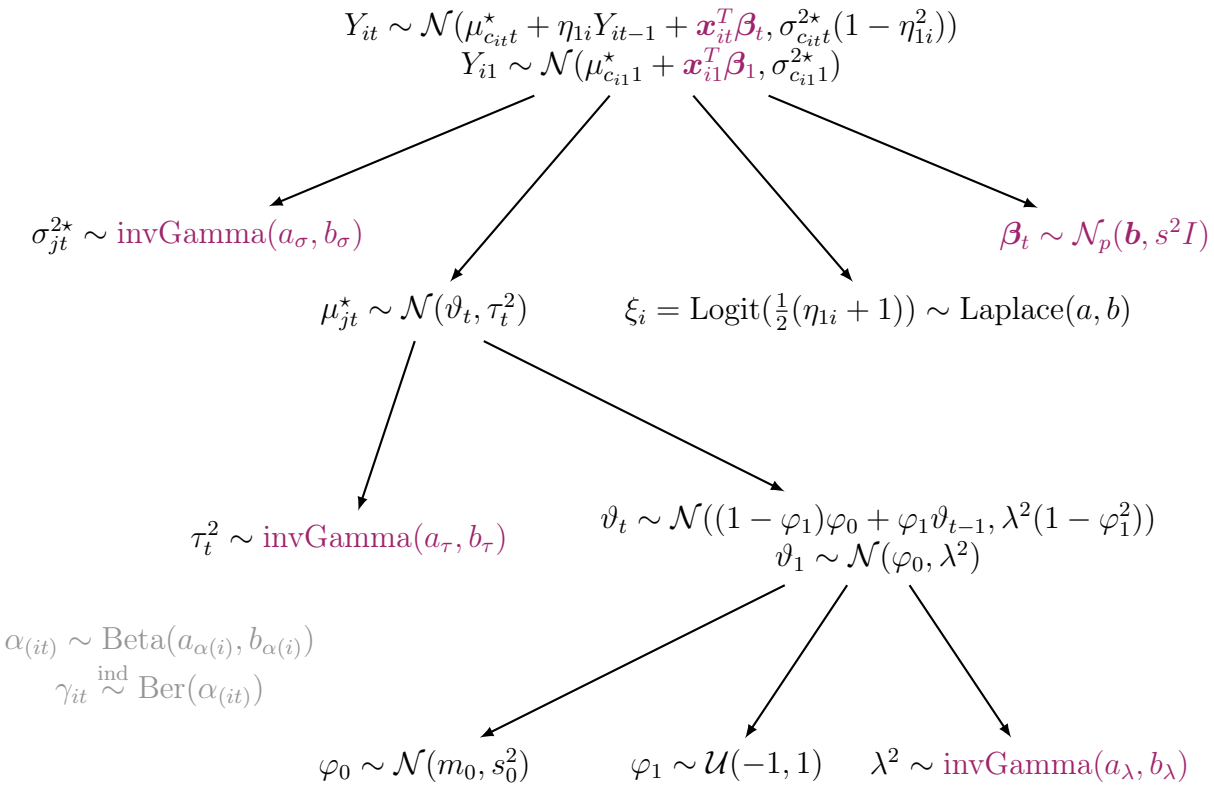

Figure 1.1: Graph visualization of the DRPM model, with highlighted in dark red the changes that we made to the original formulation and in gray the internal variables of the model.

In the course of this work, for the sake of clarity, we will refer to CDRPM for the original model formulation of (G. L. Page et al., 2022), and to JDRPM for our updated version. The starting letters C and J refer to the languages in which their corresponding MCMC algorithm has been implemented: C for the former, Julia for the latter.

We will now dive more deeply into the characteristics of our updated model by outlining the MCMC algorithm and, subsequently, inspecting the behaviours of the spatial cohesions and covariates similarities. This description refers to our generalization, the JDRPM model of (1.5), but we will remark analogies and differences with respect to the original CDRPM of (1.4).

1.1 MCMC sampling algorithm

We now report the full conditionals derivation for the parameters which had a conjugacy in the model (for the complete steps see Appendix A). Their computation is theoretically "simple", where we use the fact that *posterior* $\propto$ *likelihood* $\cdot$ *prior*, but followed useful suggestions and tricks from (Duncan, 2016). The other variables not included here, namely η_{1i} and φ_1, involved instead the classical Metropolis update.

- update $\sigma^{2\star}_{jt}$. This full conditional derivation is characteristic of JDRPM only, since in CDRPM the variance had a uniform law and was therefore updated through a Metropolis step.

$$
\begin{aligned}
&\text{for } t=1\text{: } f(\sigma^{2\star}_{jt}|-) \propto \text{kernel of a invGamma}(a_{\sigma(\text{post})}, b_{\sigma(\text{post})}) \text{ with}\\
&a_{\tau(\text{post})} = a_\sigma + \frac{|S_{jt}|}{2} \quad b_{\tau(\text{post})} = b_\sigma + \frac{1}{2}\sum_{i\in S_{jt}} (Y_{it} - \mu^\star_{jt} - \boldsymbol{x}^T_{it}\boldsymbol{\beta}_t)^2\\
&\text{for } t>1\text{: } f(\sigma^{2\star}_{jt}|-) \propto \text{kernel of a invGamma}(a_{\sigma(\text{post})}, b_{\sigma(\text{post})}) \text{ with}\\
&a_{\tau(\text{post})} = a_\sigma + \frac{|S_{jt}|}{2} \quad b_{\tau(\text{post})} = b_\sigma + \frac{1}{2}\sum_{i\in S_{jt}} (Y_{it} - \mu^\star_{jt} - \eta_{1i}Y_{it-1} - \boldsymbol{x}^T_{it}\boldsymbol{\beta}_t)^2
\end{aligned}
\tag{1.6}
$$

- update $\mu^\star_{jt}$. This update rule is the same for both JDRPM and CDRPM.

$$
\begin{aligned}
&\text{for } t=1\text{: } f(\mu^\star_{jt}|-) \propto \text{kernel of a } \mathcal{N}(\mu_{\mu^\star_{jt}(\text{post})}, \sigma^2_{\mu^\star_{jt}(\text{post})}) \text{ with}\\
&\sigma^2_{\mu^\star_{jt}(\text{post})} = \frac{1}{\frac{1}{\tau^2_t} + \frac{|S_{jt}|}{\sigma^{2\star}_{jt}}} \quad \mu_{\mu^\star_{jt}(\text{post})} = \sigma^2_{\mu^\star_{jt}(\text{post})}\left(\frac{\vartheta_t}{\tau^2_t} + \frac{\sum_{i\in S_{jt}}(Y_{i1} - \boldsymbol{x}^T_{it}\boldsymbol{\beta}_t)}{\sigma^{2\star}_{jt}}\right)\\
&\text{for } t>1\text{: } f(\mu^\star_{jt}|-) \propto \text{kernel of a } \mathcal{N}(\mu_{\mu^\star_{jt}(\text{post})}, \sigma^2_{\mu^\star_{jt}(\text{post})}) \text{ with}\\
&\sigma^2_{\mu^\star_{jt}(\text{post})} = \frac{1}{\frac{1}{\tau^2_t} + \frac{\sum_{i\in S_{jt}}\frac{1}{1-\eta^2_{1i}}}{\sigma^{2\star}_{jt}}} \quad \mu_{\mu^\star_{jt}(\text{post})} = \sigma^2_{\mu^\star_{jt}(\text{post})}\left(\frac{\vartheta_t}{\tau^2_t} + \frac{\sum_{i\in S_{jt}}\frac{Y_{it} - \eta_{1i}Y_{i,t-1} - \boldsymbol{x}^T_{it}\boldsymbol{\beta}_t}{1-\eta^2_{1i}}}{\sigma^{2\star}_{jt}}\right)
\end{aligned}
\tag{1.7}
$$

- update $\boldsymbol{\beta}_t$. This full conditional derivation is characteristic of JDRPM only, since the insertion of a regression term in the likelihood is a feature introduced by our generalized model.

  for $t = 1$: $f(\boldsymbol{\beta}_t|-) \propto$ kernel of a $\mathcal{N}(\boldsymbol{b}_{(\text{post})}, A_{(\text{post})})$ with

  $$A_{(\text{post})} = \left(\frac{1}{s^2}I + \sum_{i=1}^{n} \frac{\boldsymbol{x}_{it}\boldsymbol{x}_{it}^T}{\sigma^{2\star}_{c_{it}t}}\right)^{-1} \quad \boldsymbol{b}_{(\text{post})} = A_{(\text{post})}\left(\frac{\boldsymbol{b}}{s^2} + \sum_{i=1}^{n} \frac{(Y_{it} - \mu^{\star}_{c_{it}t})\boldsymbol{x}_{it}}{\sigma^{2\star}_{c_{it}t}}\right)$$

  i.e. $f(\boldsymbol{\beta}_t|-) \propto$ kernel of a $\mathcal{N}\text{Canon}(\boldsymbol{h}_{(\text{post})}, J_{(\text{post})})$ with

  $$\boldsymbol{h}_{(\text{post})} = \left(\frac{\boldsymbol{b}}{s^2} + \sum_{i=1}^{n} \frac{(Y_{it} - \mu^{\star}_{c_{it}t})\boldsymbol{x}_{it}}{\sigma^{2\star}_{c_{it}t}}\right) \quad J_{(\text{post})} = \left(\frac{1}{s^2}I + \sum_{i=1}^{n} \frac{\boldsymbol{x}_{it}\boldsymbol{x}_{it}^T}{\sigma^{2\star}_{c_{it}t}}\right)$$

  for $t > 1$: $f(\boldsymbol{\beta}_t|-) \propto$ kernel of a $\mathcal{N}(\boldsymbol{b}_{(\text{post})}, A_{(\text{post})})$ with

  $$A_{(\text{post})} = \left(\frac{1}{s^2}I + \sum_{i=1}^{n} \frac{\boldsymbol{x}_{it}\boldsymbol{x}_{it}^T}{\sigma^{2\star}_{c_{it}t}}\right)^{-1} \quad \boldsymbol{b}_{(\text{post})} = A_{(\text{post})}\left(\frac{\boldsymbol{b}}{s^2} + \sum_{i=1}^{n} \frac{(Y_{it} - \mu^{\star}_{c_{it}t} - \eta_{1i}Y_{it-1})\boldsymbol{x}_{it}}{\sigma^{2\star}_{c_{it}t}}\right)$$

  i.e. $f(\boldsymbol{\beta}_t|-) \propto$ kernel of a $\mathcal{N}\text{Canon}(\boldsymbol{h}_{(\text{post})}, J_{(\text{post})})$ with

  $$\boldsymbol{h}_{(\text{post})} = \left(\frac{\boldsymbol{b}}{s^2} + \sum_{i=1}^{n} \frac{(Y_{it} - \mu^{\star}_{c_{it}t} - \eta_{1i}Y_{it-1})\boldsymbol{x}_{it}}{\sigma^{2\star}_{c_{it}t}}\right) \quad J_{(\text{post})} = \left(\frac{1}{s^2}I + \sum_{i=1}^{n} \frac{\boldsymbol{x}_{it}\boldsymbol{x}_{it}^T}{\sigma^{2\star}_{c_{it}t}}\right) \tag{1.8}$$

  Here $\mathcal{N}\text{Canon}(\boldsymbol{h}, J)$ is the canonical formulation of the $\mathcal{N}(\boldsymbol{\mu}, \Sigma)$, with $\boldsymbol{h} = \Sigma^{-1}\boldsymbol{\mu}$ and $J = \Sigma^{-1}$. This other distribution facilitates the sampling, since these full conditional computations allow to derive directly the parameters of the canonical one, e.g. the inverse of the variance matrix rather than the variance matrix itself; and therefore sampling through it does not require any inversion of matrices which would produce more computational load, numerical instabilities, and loss of accuracy. As a consequence, in Julia we can write `rand(MvNormalCanon(h_star, J_star))` rather than the riskier one `rand(MvNormal(inv(J_star)*h_star, inv(J_star)))`; which apart from the previously mentioned disadvantages would be a statistically equivalent form.

- update τ_t^2. This full conditional derivation is characteristic of JDRPM only, since in CDRPM the variance had a uniform law and was therefore updated through a Metropolis step.

  $$\begin{aligned} &f(\tau_t^2|-) \propto \text{kernel of a invGamma}(a_{\tau(\text{post})}, b_{\tau(\text{post})}) \text{ with} \\ &a_{\tau(\text{post})} = \frac{k_t}{2} + a_\tau \quad b_{\tau(\text{post})} = \frac{\sum_{j=1}^{k_t}(\mu^{\star}_{jt} - \vartheta_t)^2}{2} + b_\tau \end{aligned} \tag{1.9}$$

- update ϑ_t. This update rule is the same for both JDRPM and CDRPM.

  for $t = T$: $f(\vartheta_t|-) \propto$ kernel of a $\mathcal{N}(\mu_{\vartheta_t(\text{post})}, \sigma^2_{\vartheta_t(\text{post})})$ with

  $$\sigma^2_{\vartheta_t(\text{post})} = \frac{1}{\frac{1}{\lambda^2(1-\varphi_1^2)} + \frac{k_t}{\tau_t^2}}$$

$$\mu_{\vartheta_t(\text{post})} = \sigma^2_{\vartheta_t(\text{post})} \left(\frac{\sum_{j=1}^{k_t} \mu^\star_{jt}}{\tau_t^2} + \frac{(1-\varphi_1)\varphi_0 + \varphi_1 \vartheta_{t-1}}{\lambda^2(1-\varphi_1^2)} \right)$$

for $1 < t < T$: $f(\vartheta_t|-) \propto$ kernel of a $\mathcal{N}(\mu_{\vartheta_t(\text{post})}, \sigma^2_{\vartheta_t(\text{post})})$ with

$$\sigma^2_{\vartheta_t(\text{post})} = \frac{1}{\frac{1+\varphi_1^2}{\lambda^2(1-\varphi_1^2)} + \frac{k_t}{\tau_t^2}}$$

$$\mu_{\vartheta_t(\text{post})} = \sigma^2_{\vartheta_t(\text{post})} \left(\frac{\sum_{j=1}^{k_t} \mu^\star_{jt}}{\tau_t^2} + \frac{\varphi_1(\vartheta_{t-1} + \vartheta_{t+1}) + \varphi_0(1-\varphi_1)^2}{\lambda^2(1-\varphi_1^2)} \right)$$

for $t = 1$: $f(\vartheta_t|-) \propto$ kernel of a $\mathcal{N}(\mu_{\vartheta_t(\text{post})}, \sigma^2_{\vartheta_t(\text{post})})$ with

$$\sigma^2_{\vartheta_t(\text{post})} = \frac{1}{\frac{1}{\lambda^2} + \frac{\varphi_1^2}{\lambda^2(1-\varphi_1^2)} + \frac{k_t}{\tau_t^2}}$$

$$\mu_{\vartheta_t(\text{post})} = \sigma^2_{\vartheta_t(\text{post})} \left(\frac{\varphi_0}{\lambda^2} + \frac{\varphi_1(\vartheta_{t+1} - (1-\varphi_1)\varphi_0)}{\lambda^2(1-\varphi_1^2)} + \frac{\sum_{j=1}^{k_t} \mu^\star_{jt}}{\tau_t^2} \right) \tag{1.10}$$

- update φ_0. This update rule is also the same for both JDRPM and CDRPM.

$$f(\varphi_0|-) \propto \text{kernel of a } \mathcal{N}(\mu_{\varphi_0(\text{post})}, \sigma^2_{\varphi_0(\text{post})}) \text{ with}$$

$$\sigma^2_{\varphi_0(\text{post})} = \frac{1}{\frac{1}{s_0^2} + \frac{1}{\lambda^2} + \frac{(T-1)(1-\varphi_1)^2}{\lambda^2(1-\varphi_1^2)}}$$

$$\mu_{\varphi_0(\text{post})} = \sigma^2_{\varphi_0(\text{post})} \left(\frac{m_0}{s_0^2} + \frac{\vartheta_1}{\lambda^2} + \frac{1-\varphi_1}{\lambda^2(1-\varphi_1^2)} \sum_{t=2}^{T} (\vartheta_t - \varphi_1 \vartheta_{t-1}) \right) \tag{1.11}$$

- update λ^2. This full conditional derivation is characteristic of JDRPM only, since in CDRPM the variance had a uniform law and was therefore updated through a Metropolis step.

$$f(\lambda^2|-) \propto \text{kernel of a invGamma}(a_{\lambda(\text{post})}, b_{\lambda(\text{post})}) \text{ with}$$

$$a_{\lambda(\text{post})} = \frac{T}{2} + a_\lambda$$

$$b_{\lambda(\text{post})} = \frac{(\vartheta_1 - \varphi_0)^2}{2} + \sum_{t=2}^{T} \frac{(\vartheta_t - (1-\varphi_1)\varphi_0 - \varphi_1 \vartheta_{t-1})^2}{2} + b_\lambda \tag{1.12}$$

- update α. This update rule is the same for both JDRPM and CDRPM.

if global α: $f(\alpha|-) \propto$ kernel of a $\text{Beta}(a_{\alpha(\text{post})}, b_{\alpha(\text{post})})$ with

$$a_{\alpha(\text{post})} = a_\alpha + \sum_{i=1}^{n} \sum_{t=1}^{T} \gamma_{it} \quad b_{\alpha(\text{post})} = b_\alpha + nT - \sum_{i=1}^{n} \sum_{t=1}^{T} \gamma_{it}$$

if time specific α: $f(\alpha_t|-) \propto$ kernel of a $\text{Beta}(a_{\alpha(\text{post})}, b_{\alpha(\text{post})})$ with

$$a_{\alpha(\text{post})} = a_\alpha + \sum_{i=1}^{n} \gamma_{it} \quad b_{\alpha(\text{post})} = b_\alpha + n - \sum_{i=1}^{n} \gamma_{it}$$

if unit specific α: $f(\alpha_i|-) \propto$ kernel of a $\text{Beta}(a_{\alpha(\text{post})}, b_{\alpha(\text{post})})$ with

$$a_{\alpha(\text{post})} = a_{\alpha i} + \sum_{t=1}^{T} \gamma_{it} \quad b_{\alpha(\text{post})} = b_{\alpha i} + T - \sum_{t=1}^{T} \gamma_{it}$$

if time and unit specific α: $f(\alpha_{it}|-) \propto$ kernel of a $\text{Beta}(a_{\alpha(\text{post})}, b_{\alpha(\text{post})})$ with

$$a_{\alpha(\text{post})} = a_{\alpha i} + \gamma_{it} \quad b_{\alpha(\text{post})} = b_{\alpha i} + 1 - \gamma_{it} \tag{1.13}$$

- update a missing observation Y_{it}. This full conditional derivation is characteristic of JDRPM only, since the handling of missing data feature introduced by our generalized model.

for $t = 1$: $f(Y_{it}|-) \propto$ kernel of a $\mathcal{N}(\mu_{Y_{it}(\text{post})}, \sigma^2_{Y_{it}(\text{post})})$ with

$$\sigma^2_{Y_{it}(\text{post})} = \frac{1}{\frac{1}{\sigma^{2\star}_{c_{it}t}} + \frac{\eta^2_{1i}}{2\sigma^{2\star}_{c_{it+1}t+1}(1-\eta^2_{1i})}}$$

$$\mu_{Y_{it}(\text{post})} = \sigma^2_{Y_{it}(\text{post})} \left(\frac{\mu^{\star}_{c_{it}t} + \boldsymbol{x}^T_{it}\boldsymbol{\beta}_t}{\sigma^{2\star}_{c_{it}t}} + \frac{\eta_{1i}(Y_{it+1} - \mu^{\star}_{c_{it+1}t+1} - \boldsymbol{x}^T_{it+1}\boldsymbol{\beta}_{t+1})}{\sigma^{2\star}_{c_{it+1}t+1}(1-\eta^2_{1i})} \right)$$

for $1 < t < T$: $f(Y_{it}|-) \propto$ kernel of a $\mathcal{N}(\mu_{Y_{it}(\text{post})}, \sigma^2_{Y_{it}(\text{post})})$ with

$$\sigma^2_{Y_{it}(\text{post})} = \frac{1-\eta^2_{1i}}{\frac{1}{\sigma^{2\star}_{c_{it}t}} + \frac{\eta^2_{1i}}{\sigma^{2\star}_{c_{it+1}t+1}}}$$

$$\mu_{Y_{it}(\text{post})} = \sigma^2_{Y_{it}(\text{post})} \left(\frac{\mu^{\star}_{c_{it}t} + \eta_{1i}Y_{it-1} + \boldsymbol{x}^T_{it}\boldsymbol{\beta}_t}{\sigma^{2\star}_{c_{it}t}(1-\eta^2_{1i})} + \frac{\eta_{1i}(Y_{it+1} - \mu^{\star}_{c_{it+1}t+1} - \boldsymbol{x}^T_{it+1}\boldsymbol{\beta}_{t+1})}{\sigma^{2\star}_{c_{it+1}t+1}(1-\eta^2_{1i})} \right)$$

for $t = T$: $f(Y_{it}|-)$ is just the likelihood of Y_{it} (1.14)

Finally, we briefly highlight in Algorithm 1 the steps which compose the MCMC sampling algorithm. Regarding the computation of the LPML and WAIC metrics, they follow classic ideas from (Christensen et al., 2010) and (Gelman et al., 2013).

The core of the clustering process happens in the updating steps of γ_{it} and ρ_t. Their update step is indeed quite complex, and as we said before involves the check of compatibility issues. In any case, the general idea is that, for each unit i currently belonging to cluster j, we simulate to assign her to one of the existing clusters, plus to a new singleton cluster, and compute for each case the likelihood of this to happen, deriving probability weights to finally sample the decision for the next iteration. The key elements participating into the definition of such weights are the spatial cohesions and, with the JDRPM update, also the covariate similarities, which we will now both investigate.

1.2 Spatial cohesions analysis

The clustering relies on the Product Partition Model (PPM) (Hartigan, 1990) (Barry et al., 1993) (Crowley, 1997). At its core, this model assigns a prior for ρ_t in the form $P(\rho_t) \propto \prod_{j=1}^{k_t} C(S_{jt})$, with the function $C(S_{jt})$ that measures how likely

Algorithm 1: Pseudocode for the MCMC fitting algorithm of the JDRPM model (1.5).

for $d = 1, \ldots,$ *draws* **do**
  if *target variable has missing values* **then**
    update the missing Y_{it}'s using (1.14)
  end
  for $t = 1, \ldots, T$ **do**
    for $i = 1, \ldots, n$ **do**
      if $t = 1$ **then**
        $\gamma_{it} = 0$
      else
        update γ_{it}
      end
    end
    for $i \in \{l : \gamma_{lt} = 0\}$ **do**
      update c_{it} (i.e. update ρ_t)
    end
    update $\mu^{\star}_{jt}$ using (1.7)
    update $\sigma^{2\star}_{jt}$ using (1.6)
    if *are there covariates in the likelihood* **then**
      update $\boldsymbol{\beta}_t$
    end
    update ϑ_t using (1.10)
    update τ^2_t using (1.9)
  end
  if *update_eta = true* **then**
    update η_{1i} using Metropolis sampling
  end
  if *update_alpha = true* **then**
    update α using (1.13)
  end
  update φ_0 using (1.11)
  if *update_phi1 = true* **then**
    update φ_1 using Metropolis sampling
  end
  update λ^2 using (1.12)
  if $d >$ *burnin and* $d \,\%\, thin = 0$ **then**
    save MCMC current iterate
  end
end
compute LPML and WAIC metrics
if *perform diagnostics* **then**
  print diagnostics (ESS and $\hat{R}$) on parameters λ^2, φ_0, τ^2_t, ϑ_t, η_{1i}, α
end

elements of S_{jt} would be grouped in the same cluster a priori. To enhance this model by incorporating spatial information, the PPM can be extend from being a function of just $C(S_{jt})$ to the more informed one $C(S_{jt}, \boldsymbol{s}^{\star}_{jt})$, where $\boldsymbol{s}^{\star}_{jt}$ is the subset of spatial coordinates of the units inside S_{jt}. For the sake of clarity, in this section where we are just interested in analysing the cohesions we employ the notation S_h to indicate a general h-th cluster, rather than the more precise S_{jt}. For the same reason, the temporal dependence that linked ρ_t with on $\boldsymbol{\gamma}_t$ and ρ_{t-1}

Regarding the computation of spatial cohesion, several choices are available (G. Page et al., 2015). The main common idea of the following formulas is to favour few spatially connected clusters rather than a lot of singleton ones, to derive more interpretable and meaningful results.

We will now describe briefly all the cohesions which are implemented in the JDRPM model, and were implemented as well in the CDRPM model, and conduct tests on each of them, to see how the tuning of their parameters reflects on the computed values.

All the tests of Figures **??** and **??** refer to the partition of Figure 1.2, taken as test case here from a general fit on the same spatio-temporal dataset of Chapter 3. The following results, as well as the ones of the next section, are presented with the logarithm applied to better highlight the differences among them, otherwise for example all values could be really close together and make the analysis less understandable, and moreover because this is the actual perspective in which the implementation works. In fact, the fitting algorithm firstly saves the log-transformed values generated by the cohesions, in order to avoid numerical problems and instabilities, and secondly exponentiates and normalizes them into proper scaled probabilities, from which finally draw the cluster assignments.

The first cohesion uses a tessellation idea from (Denison et al., 2001) that considers $\mathcal{D}_h = \sum_{i \in S_h} \|\boldsymbol{s}_i - \bar{\boldsymbol{s}}_h\|$ as the total distance from the units to the cluster centroid $\bar{\boldsymbol{s}}_h$. The computation is then an adjustment of a decreasing function in terms of $\mathcal{D}_h$, to give an higher weight on clusters which are denser, i.e. that have lower $\mathcal{D}_h$, with an additional parameter α to provide more control on the penalization.

$$C_1(S_h, \boldsymbol{s}^{\star}_h) = \begin{cases} \dfrac{M \cdot \Gamma(|S_h|)}{\Gamma(\alpha \mathcal{D}_h)\mathbb{1}_{[\mathcal{D}_h \geq 1]} + \mathcal{D}_h \mathbb{1}_{[\mathcal{D}_h < 1]}} & \text{if } |S_h| > 1 \\ M & \text{if } |S_h| = 1 \end{cases} \tag{1.15}$$

The second function provides, instead, a hard cluster boundary where the weight is set to 1 (i.e. 0 with the logarithm view) only if all the distances between all possible pairs of points inside the cluster are below the threshold parameter, i.e. if all units are "close enough" to each other. If this does not happen, even for a single pair of points, the returned value is 0, which corresponds to the maximum penalization since it would be $-\infty$ in the logarithm perspective. The strictness of this requirement can be adjusted through the parameter a.

$$C_2(S_h, \boldsymbol{s}^{\star}_h) = M \cdot \Gamma(|S_h|) \cdot \prod_{i,j \in S_h} \mathbb{1}_{[\|\boldsymbol{s}_i - \boldsymbol{s}_j\| \leq a]} \tag{1.16}$$

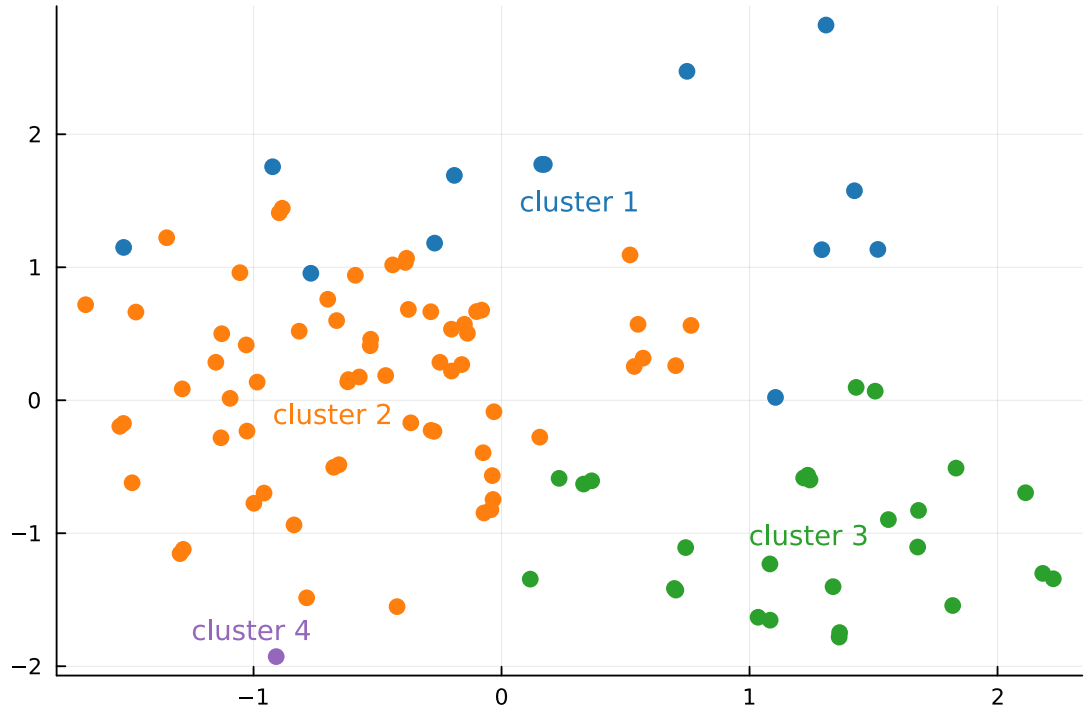

Figure 1.2: Partition and data considered to analyse the spatial cohesions. The points refer to the spatial coordinates of the dataset that will be used in Chapter 3.

According to this function, from Figure **??** we can see how the purple cluster is considered the one with the highest cohesion, being a singleton. The runner-up is the green cluster, because it's the first among all the non-singletons which activates cohesion 2 when we increase the parameter a. The orange and blue clusters, in contrast, appear to be less dense since they require an higher value of a to "pass" the distance check.

However, cohesions C_1 and C_2 do not preserve the exchangeability property, meaning that if we would marginalize the random partition model over the last of m units we would not get to the same model as if we only had $m-1$ units. This coherence property, known as sample size consistency or addition rule (De Blasi et al., 2015), is instead often desirable, for theoretical or computational purposes, and the following two cohesions are able to provide it (Müller et al., 2011).

Cohesion 3, called auxiliary similarity, treats the spatial coordinates $\boldsymbol{s}$ as if they were random, applying on them a model such as the Normal/Normal-Inverse-Wishart with $\boldsymbol{\xi} = (\boldsymbol{m}, V)$, $\boldsymbol{s}|\boldsymbol{\xi} \sim \mathcal{N}(\boldsymbol{m}, V)$ and $\boldsymbol{\xi} \sim \mathcal{NIW}(\boldsymbol{\mu}_0, \kappa_0, \nu_0, \Lambda_0)$. The idea is to assign a larger weight on clusters which produce large marginal likelihood values, i.e. which according to the modelling are more probable to appear.

$$C_3(S_h, \boldsymbol{s}_h^\star) = M \cdot \Gamma(|S_h|) \cdot \int \prod_{i \in S_h} q(\boldsymbol{s}_i|\boldsymbol{\xi}_h) q(\boldsymbol{\xi}_h)\, d\boldsymbol{\xi}_h \tag{1.17}$$

On the same line there is cohesion 4, the double dipper cohesion (F. Quintana et al., 2015), which now employs the posterior predictive distribution rather than

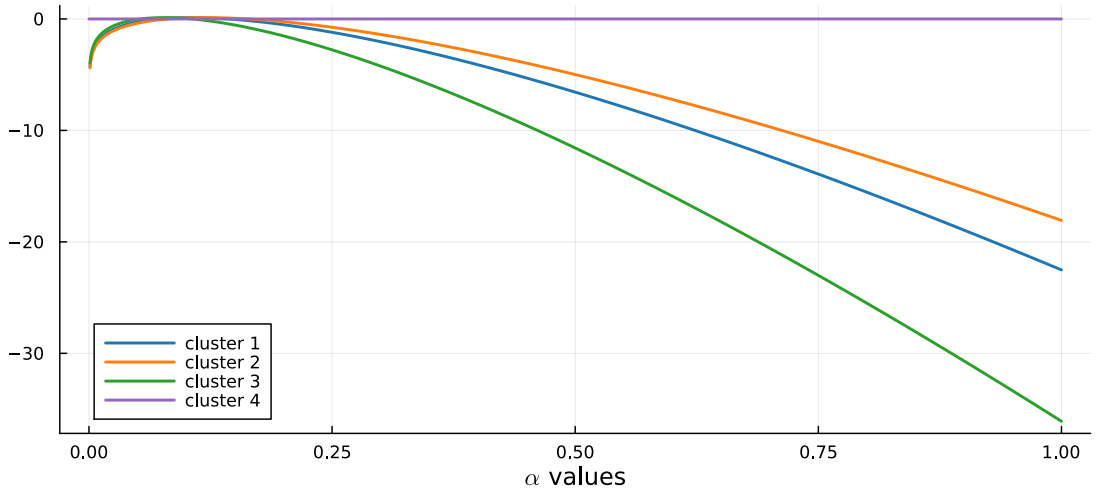

Figure 1.3: Cohesions 1 log-transformed values computed on the test case partition of Figure 1.2, with respect to different values of its tuning parameter α.

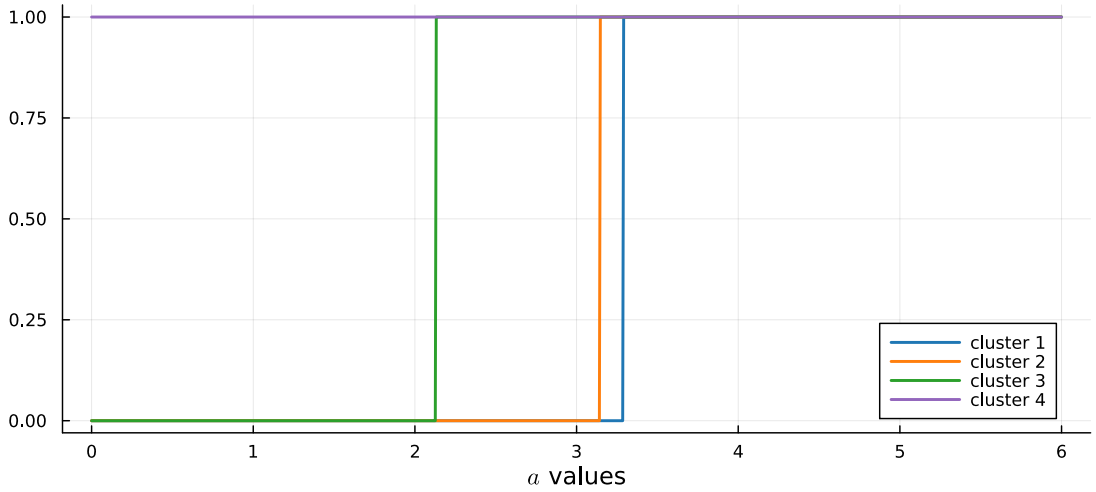

Figure 1.4: Cohesions 2 computed on the test case partition of Figure 1.2, with respect to different values of its tuning parameter a. The values here are without not log-transformed for plotting purposes since otherwise the values would have been $-\infty$ and 0.

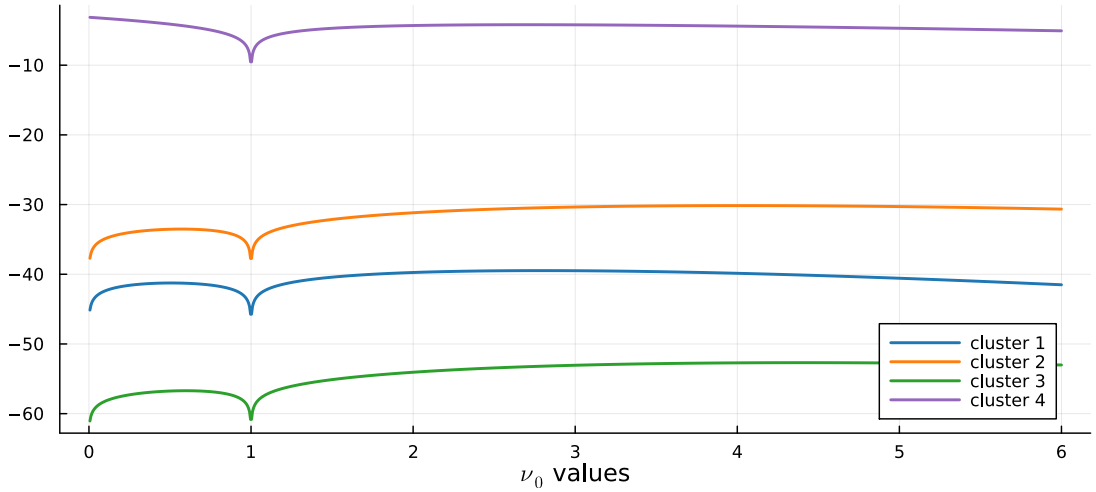

Figure 1.5: Cohesions 3 log-transformed values computed on the test case partition of Figure 1.2, with respect to different values of its tuning parameter ν_0.

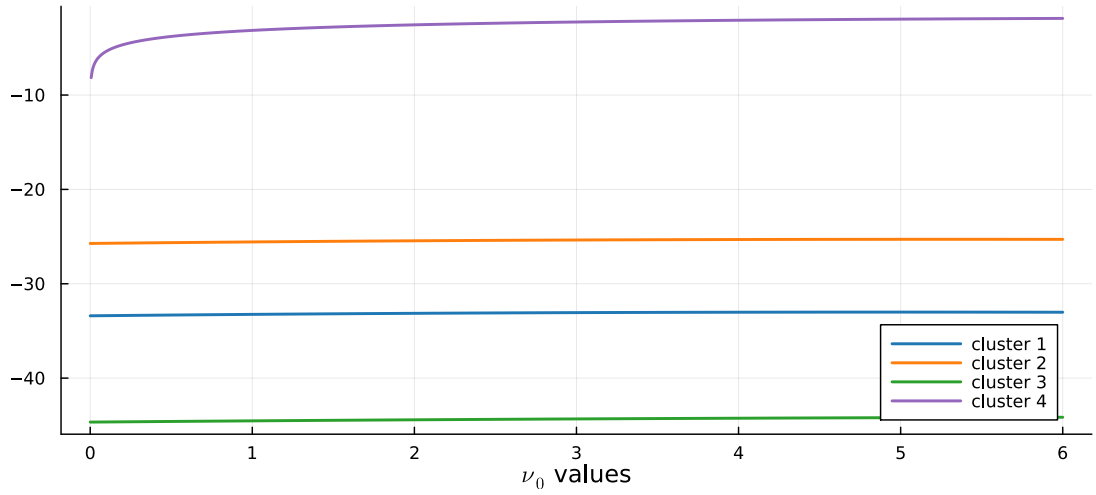

Figure 1.6: Cohesions 4 log-transformed values computed on the test case partition of Figure 1.2, with respect to different values of its tuning parameter ν_0.

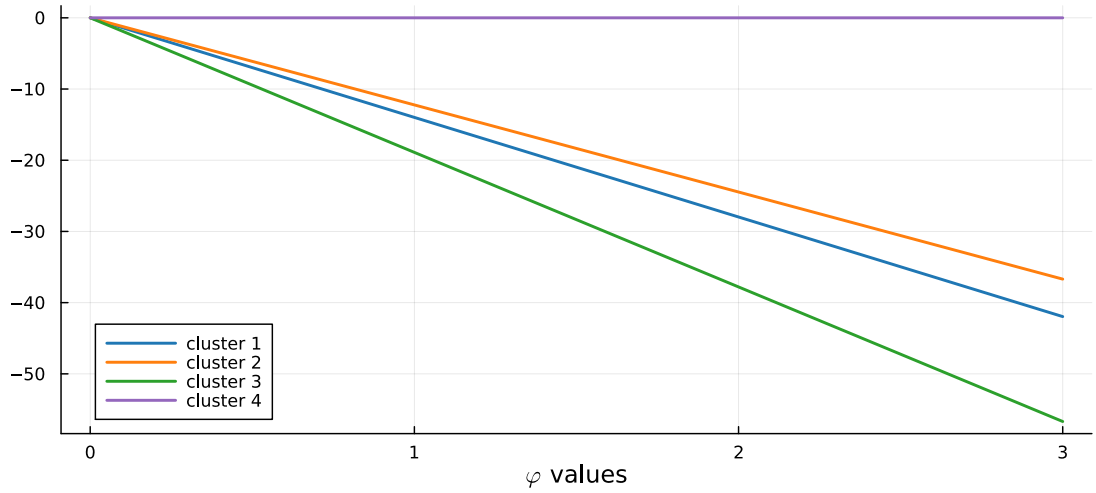

Figure 1.7: Cohesions 5 log-transformed values computed on the test case partition of Figure 1.2, with respect to different values of its tuning parameter φ.

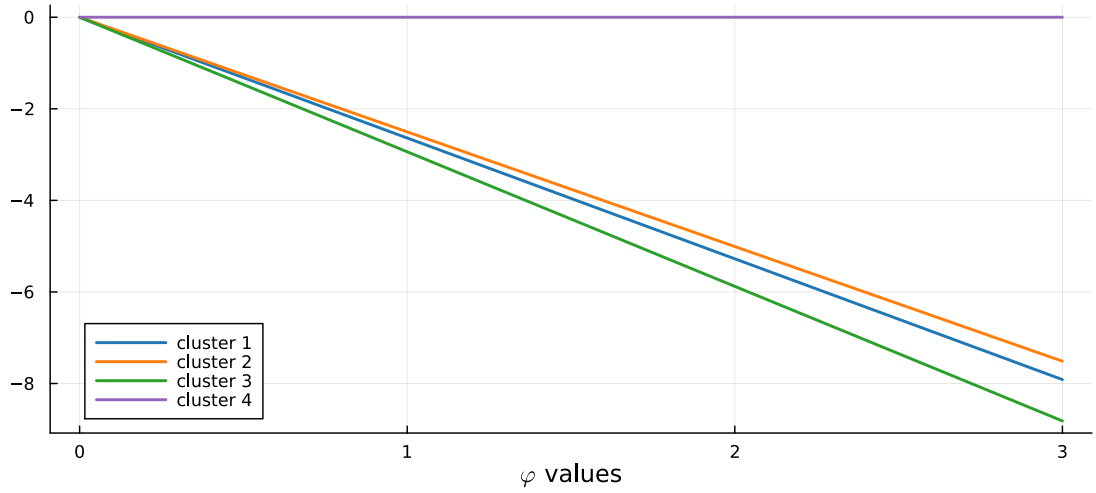

Figure 1.8: Cohesions 3 log-transformed values computed on the test case partition of Figure 1.2, with respect to different values of its tuning parameter φ.

the prior predictive distribution of cohesion C_3.

$$C_4(S_h, \boldsymbol{s}_h^\star) = M \cdot \Gamma(|S_h|) \cdot \int \prod_{i \in S_h} q(\boldsymbol{s}_i|\boldsymbol{\xi}_h) q(\boldsymbol{\xi}_h|\boldsymbol{s}_h^\star)\, d\boldsymbol{\xi}_h \tag{1.18}$$

Another final idea comes from the cluster variance/entropy similarity function, a very general methodology to measure the closeness of a set of values which in fact will be used also for the covariates case. As in cohesion C_1, the idea is to derive a summary of the closeness of the units, summing the distances of the units from the cluster centroid, and then adjust the parameter φ to control how much penalize dissimilar values. In this way we arrive to the final two cohesions (G. Page et al., 2018).

$$C_5(S_h, \boldsymbol{s}_h^\star) = \exp\left\{-\varphi \sum_{i \in S_h} \|\boldsymbol{s}_i - \bar{\boldsymbol{s}}_h\|\right\} \tag{1.19}$$

$$C_6(S_h, \boldsymbol{s}_h^\star) = \exp\left\{-\varphi \log\left(\sum_{i \in S_h} \|\boldsymbol{s}_i - \bar{\boldsymbol{s}}_h\|\right)\right\} \tag{1.20}$$

1.3 Covariates similarities analysis

A wide spectrum of choice is also available for covariates similarities (G. Page et al., 2018). To account for them, the idea consists in extending the PPM to make it function of S_{jt}, $\boldsymbol{s}_{jt}^\star$, and now also of $X_{jt}^\star$, being this the $p \times |S_{jt}|$ matrix storing the covariates of the units belonging to cluster j at time t, i.e. $X_{jt}^\star = \{\boldsymbol{x}_{it}^\star = (x_{it1}, \ldots, x_{itp})^T : i \in S_{jt}\}$.

For the current implementation of JDRPM we decided to treat each covariate individually, therefore the PPM will actually be function of the set of unidimensional vectors which record the different p covariates of the units inside cluster S_{jt}, meaning $\boldsymbol{x}_{jt1}^\star, \ldots, \boldsymbol{x}_{jtp}^\star$, of which all contributions will be considered independently one to each other. In this way, the final PPM form will be

$$P(\rho) \propto \prod_{h=1}^{k_t} C(S_{jt}, \boldsymbol{s}_{jt}^\star) \left(\prod_{r=1}^{p} g(S_{jt}, \boldsymbol{x}_{jtr}^\star)\right) \tag{1.21}$$

where $\boldsymbol{x}_{jtr}^\star$ represents the vector recording the r-th covariate values for all the units inside cluster S_{jt}, i.e. row r of matrix $X_{jt}^\star$. This choice is lighter from the theoretical and computational perspectives, and allows a mixture of numerical and categorical covariates without any problem. A unified and multidimensional consideration of the covariates is nonetheless possible, with proper adjustments on the similarities functions, and would have lead to a PPM of the form

$$P(\rho) \propto \prod_{h=1}^{k_t} C(S_{jt}, \boldsymbol{s}_{jt}^\star) g(S_{jt}, X_{jt}^\star) \tag{1.22}$$

As in the previous section, we will now discuss all the similarities implemented in the JDRPM model and perform tests on each of them. All the tests will be

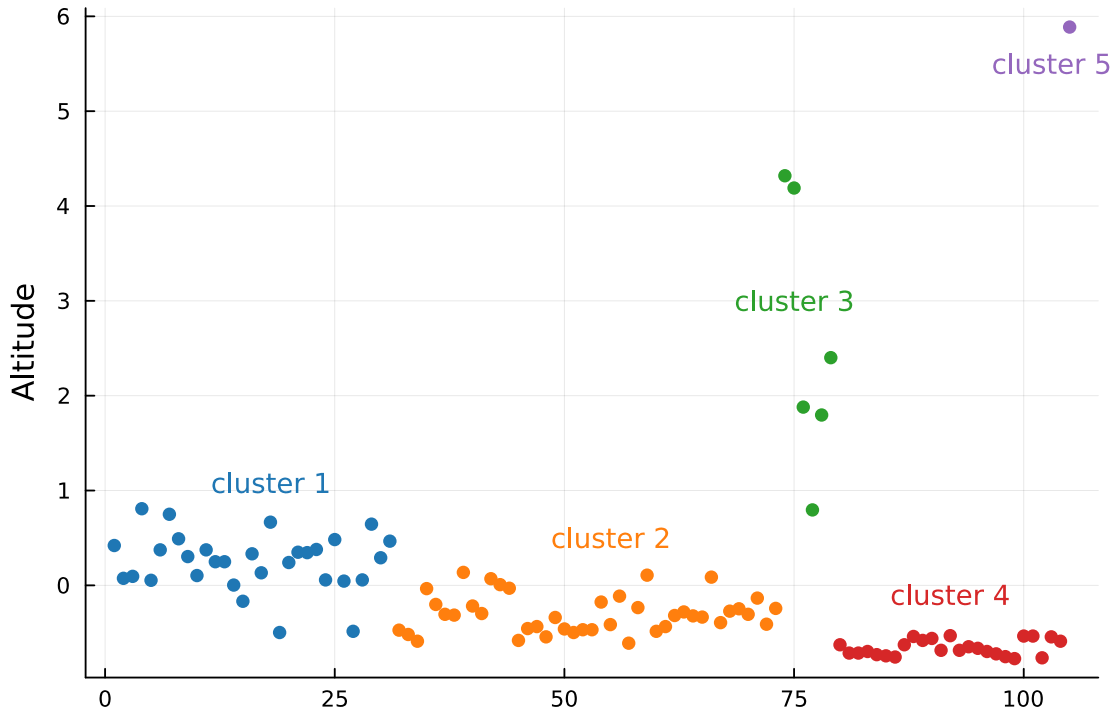

Figure 1.9: Partition considered to analyse the covariate similarities. The order of the units has been modified to plot together all units belonging to the same cluster.

referred to the test case partition displayed in Figure 1.9 which is about the `Altitude` covariate from the spatio-temporal dataset that will be used in Chapter 3. Regarding the notation, we will again employ the simpler and general one dropping the spatio-temporal context.

The first similarity is the cluster variance/entropy similarity function (G. Page et al., 2018), which as the name suggest can work with both numerical and categorical variables. The general form is

$$g_1(S_h, \boldsymbol{x}_h^\star) = \exp\left\{-\varphi H(S_h, \boldsymbol{x}_h^\star)\right\} \tag{1.23}$$

with $H(S_h, \boldsymbol{x}_h^\star) = \sum_{i \in S_h} (x_i - \bar{x}_h)^2$ for numerical covariates, being $\bar{x}_h$ the mean value of the $\boldsymbol{x}_h^\star$ vector, and $H(S_h, \boldsymbol{x}_h^\star) = -\sum_{c=1}^{C} \hat{p}_c \log(\hat{p}_c)$ for categorical covariates, with $\hat{p}_c$ indicating the relative frequency at which each factor appears. The parameter φ controls the amount of penalization to apply. This function can be extended quite easily to the multidimensional case, at least for the case of numerical covariates only, where the H function becomes $H(S_h, X_h^\star) = \sum_{r=1}^{p} \|\boldsymbol{x}_r - \bar{\boldsymbol{x}}_h\|$.

Another popular choice is the Gower similarity function (Gower, 1971), which was originally designed for a multivariate context, where vectors of covariates are compared to each other. As a consequence, some work was required to adapt it to the univariate case. The simple idea of comparing all cluster-specific pair-wise similarities leads to the total Gower similarity.

$$g_2(S_h, \boldsymbol{x}_h^\star) = \exp\left\{-\alpha \sum_{i,j \in S_h, i \neq j} d(x_i, x_j)\right\} \tag{1.24}$$

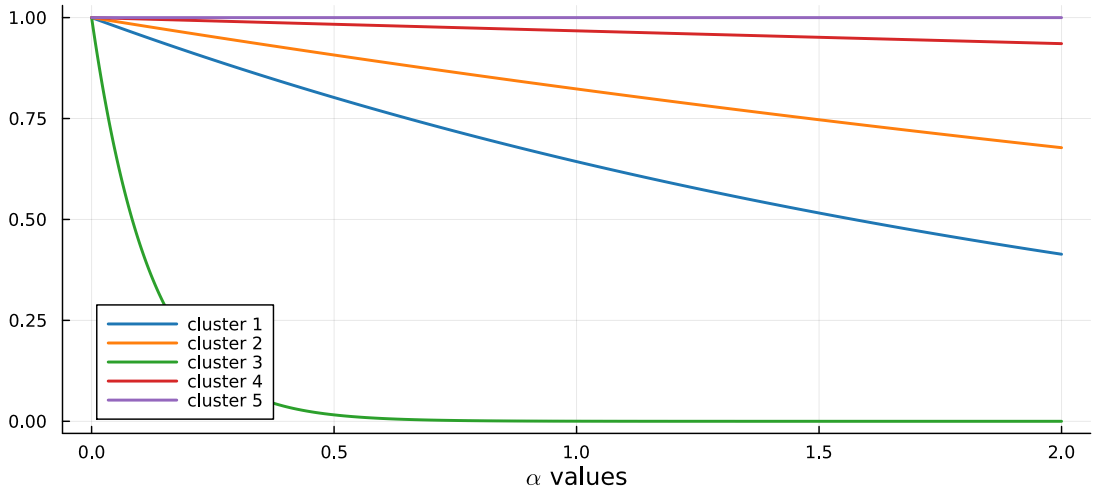

Figure 1.10: Similarity 1 values, computed on the test case partition of Figure 1.9, with respect to different values of its tuning parameter α. The values here are without not log-transformed to better highlight the difference of the computed values among the clusters.

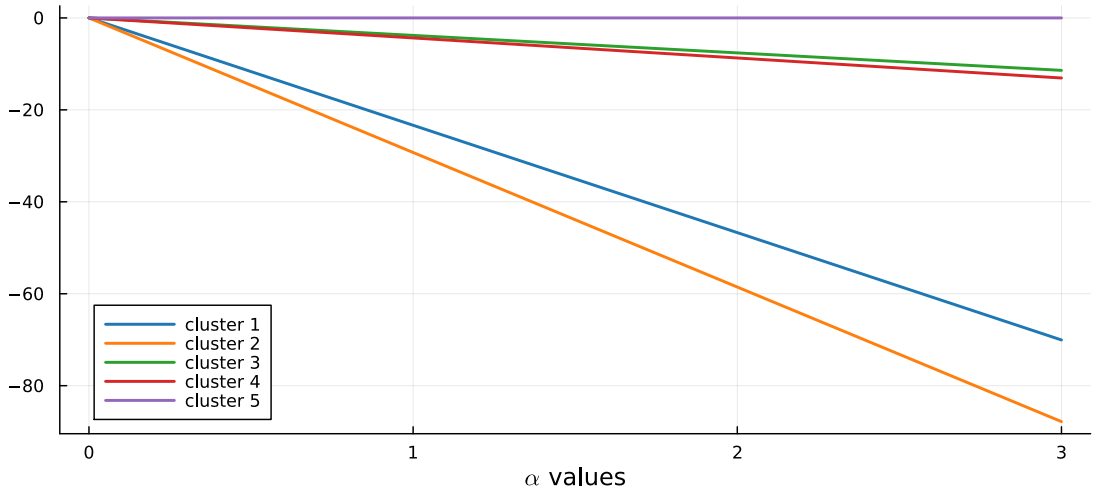

Figure 1.11: Similarity 5 log-transformed values computed on the test case partition of Figure 1.9, with respect to different values of its tuning parameter α.

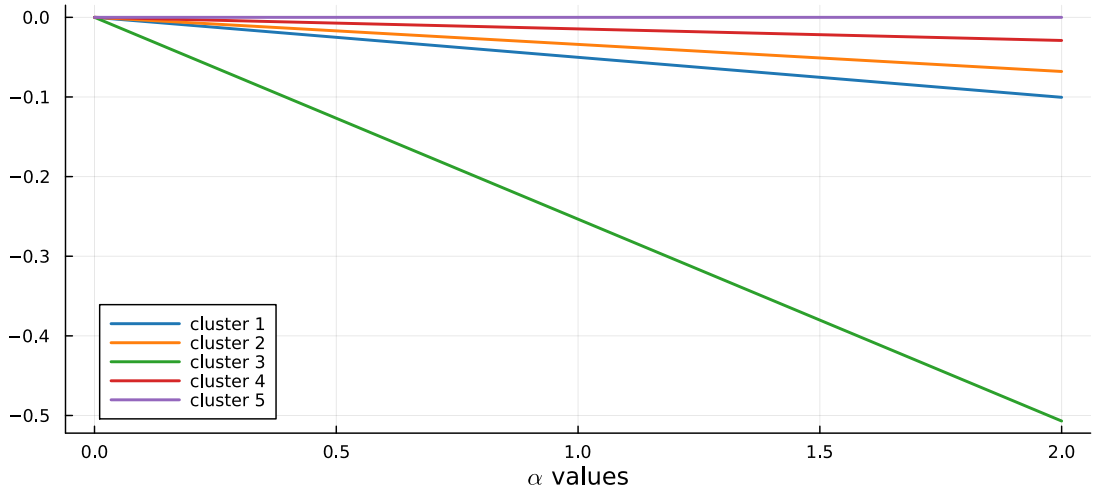

Figure 1.12: Similarity 3 log-transformed values computed on the test case partition of Figure 1.9, with respect to different values of its tuning parameter α.

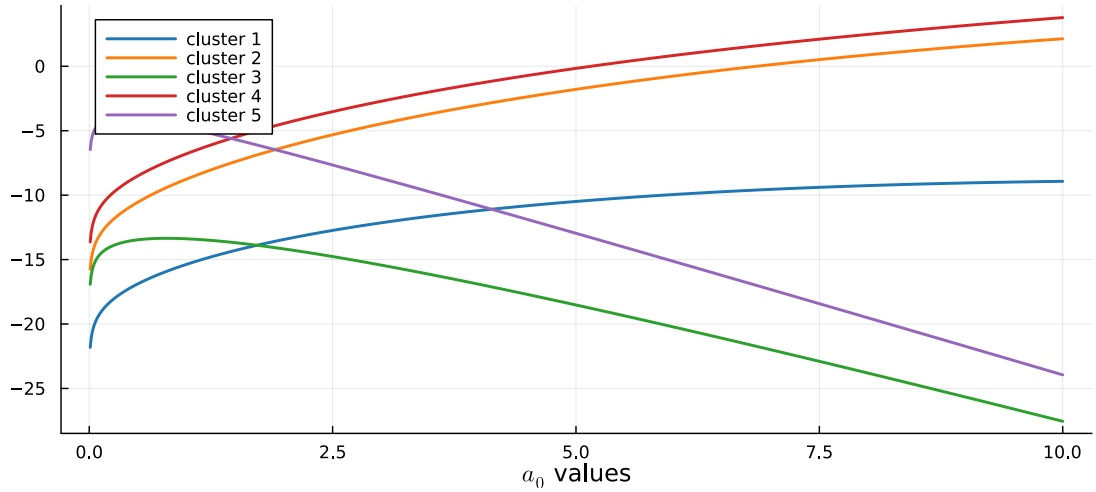

Figure 1.13: Similarity 4 log-transformed values values, computed on the test case partition of Figure 1.9, with respect to different values of its tuning parameter a_0. The other parameters has been set to $\mu_0 = 0$, $\lambda_0 = 1$, $b_0 = 1$.

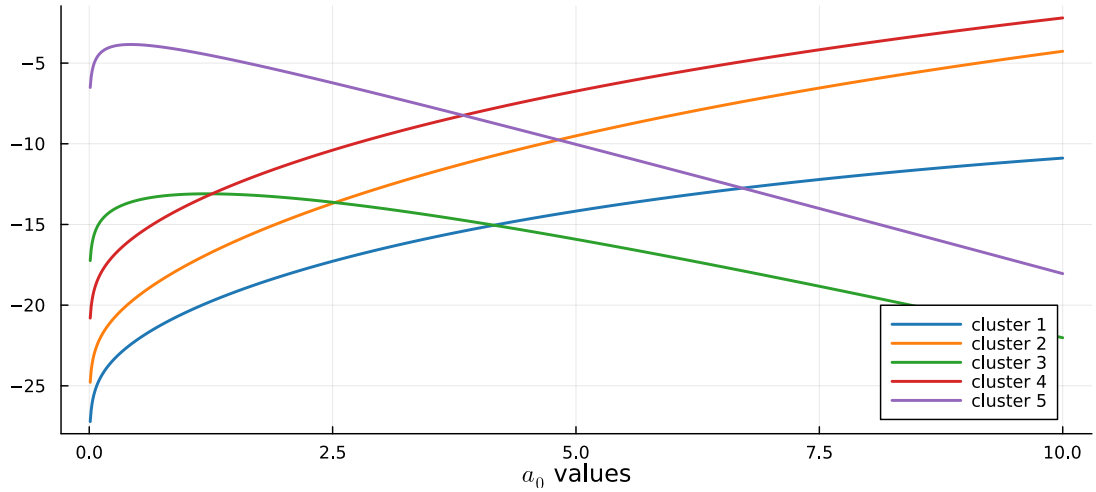

Figure 1.14: Similarity 4 log-transformed values computed on the test case partition of Figure 1.9, with respect to different values of its tuning parameter a_0. The other parameters has been set to $\mu_0 = 0$, $\lambda_0 = 1$, $b_0 = 2$.

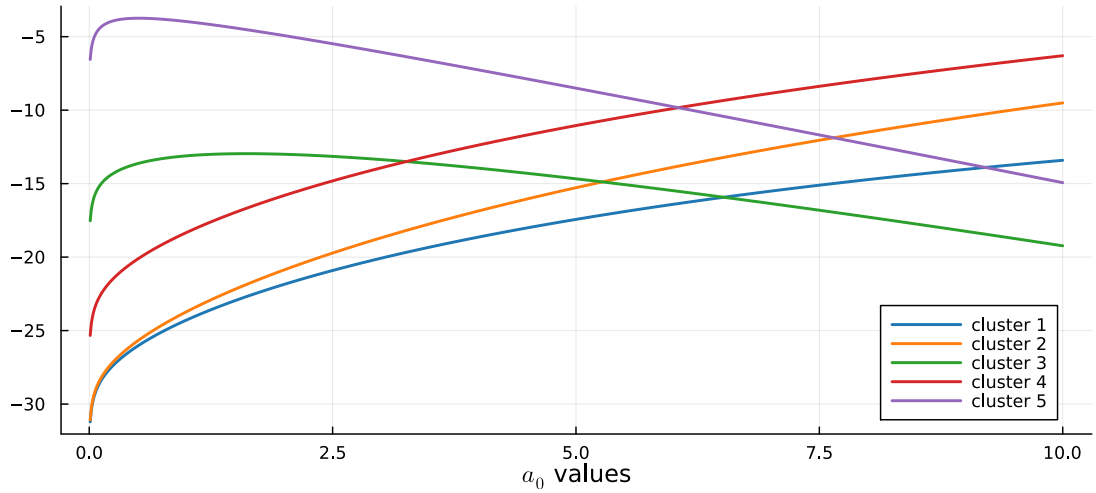

Figure 1.15: Similarity 4 log-transformed values computed on the test case partition of Figure 1.9, with respect to different values of its tuning parameter a_0. The other parameters has been set to $\mu_0 = 0$, $\lambda_0 = 1$, $b_0 = 3$.

This function, however, is strictly increasing with respect to the cluster size, meaning that it will naturally tend to propose a large number of small clusters. For that reason, a correction can be applied, accounting for the size of the cluster S_h, leading to the average Gower similarity.

$$g_3(S_h, \boldsymbol{x}_h^\star) = \exp\left\{-\frac{2\alpha}{|S_h|(|S_h|-1)} \sum_{i,j \in S_h,\, i \neq j} d(x_i, x_j)\right\} \tag{1.25}$$

In both functions, $d(x_i, x_j)$ is the Gower dissimilarity between x_i and x_j, with $d(x_i, x_j) = |x_i - x_j|/R$ in the case of numerical covariates, being $R = \max(\boldsymbol{x}) - \min(\boldsymbol{x})$ the range of the covariate values, considering all the units independently from their cluster, while $d(x_i, x_j) = \mathbb{1}_{[x_i \neq x_j]}$ in the case of categorical covariates. This is a dissimilarity since values closer to 0 refer to similar data, while values closer to 1 to dissimilar data; therefore the minus sign inside g_2 and g_3 exponents converts the function to a similarity. For the multidimensional design there are natural extensions of the $d(\boldsymbol{x}_i, \boldsymbol{x}_j)$ function.

The last similarity (G. Page et al., 2015) recalls the structure of the spatial cohesion C_3, where now are the covariates to be treated as if they were random variables. However, since we chose to deal with each covariate individually, in this unidimensional setting a Normal/Normal-Inverse-Gamma model is employed, with $\boldsymbol{\xi} = (\mu, \sigma^2)$, $x|\boldsymbol{\xi} \sim \mathcal{N}(\mu_0, \sigma^2)$, and $\mu \sim \mathcal{N}(\mu_0, \sigma^2/\lambda_0)$, $\sigma^2 \sim \text{invGamma}(a_0, b_0)$, i.e. $\boldsymbol{\xi} \sim \mathcal{N}\text{invGamma}(\mu_0, \lambda_0, a_0, b_0)$. A multivariate extension is thus possible through the same modelling style of the spatial coordinates case.

$$g_4(S_h, \boldsymbol{x}_h^\star) = \int \prod_{i \in S_h} q(x_i|\boldsymbol{\xi}_h) q(\boldsymbol{\xi}_h)\, d\boldsymbol{\xi}_h \tag{1.26}$$

All the similarities, except for g_2, agree to classify the non-singleton clusters with the red being the one with the highest similarity, followed by the orange, blue, and green, as we can see from Figures **??** and **??**. Intuitively, Figure 1.9 seems to confirm this ranking, by visually reasoning about the sparsity of each cluster. Similarities g_4 and g_2 seems to be the only ones which are able to give a considerable weight also to the green partition, which is indeed sparser but collects all the large, sort of outliers, values of the covariate at test.

Regarding their flexibility, we tested their behaviour changing the testing covariate. Similarity g_1 appeared to be the most adaptive one, working well (i.e. returning very reasonable orders in the clusters) in every covariate we tested. However, it tends to penalize a lot sparse clusters, as we saw in the previous test case. This could suggest that maybe other distance metrics rather than the L^2 norm could be used in the computation of $H(S_h, \boldsymbol{x}_h^\star)$. On the other hand, similarity g_4 appeared to be quite sensitive to the parameters regulating the invGamma distribution for σ^2. This suggests that covariates should be standardized prior to their usage, in order to simplify the research and uniform the choice of the most appropriate set of parameters. In any case, the JDRPM implementation can provide some flexibility in this regard by possibly assigning separately the pair of a_0 and b_0 for each covariate that we wish to include in the clustering process.

Chapter 2

Implementation and optimizations

To implement our updated model, and to do it efficiently, we decided to opt for the Julia language (Bezanson et al., 2017).

Julia is a relatively new programming language that combines the ease and expressiveness of high-level languages to the efficiency and performance of low-level ones. Such balance is largely achieved through the just-in-time (JIT) compilation, implemented using the LLVM framework, together with many nice features like dynamic multiple dispatch and heavy code specialization against multiple run-time types. This design choice allows Julia to be used interactively, in the same fashion to the R, Matlab, or Python consoles, while also supporting the more traditional program execution style of statically compiled languages such as C, C++ and Fortran. This solution provides faster development phases, since for examples code sections can be evaluated and tested line by line, but at the same time guarantees efficient implementations. Performances are further enhanced by the native integration of the optimized BLAS (Lawson et al., 1979) and LAPACK libraries for linear algebra operations, which are often at the core of all scientific applications. Moreover, Julia provides an extensive ecosystem, currently comprised by more than ten thousand packages, spanning over almost all branches of science and engineering. Most of those packages are already highly tested and optimized, and can therefore reduce the implementation time required to the users. As an example, in this work we employed the `Distributions` (Besançon et al., 2021) (Lin et al., 2019) and `Statistics` packages, while the original C implementation had to write all the statistical functionalities from scratch. Considering all this, the Julia choice was deemed very natural.

As we will see in Chapter 3, even despite the higher complexity of the model we managed to get better performance in Julia compared to the original C implementation, at the reasonable cost of a smaller increase in the memory requirements, which nowadays should not be a big deal. Anyway, this improvement was possible through several refinements and optimizations, which we will now briefly discuss.

2.1 Optimizations

One of the major issues encountered during the design of the fitting function in Julia was controlling the amount of memory and allocations that some functions, structures, or algorithms would require. At the beginning of the development and testing, where the correctness of the algorithm was the only priority, we saw in fact that most of the execution time was actually spent by the garbage collector of Julia, which had the burden of track all the allocated memory and reclaim the unused one in order to make it available again for new computations.

Together with avoiding useless allocations, or in general managing more precisely the memory, another important aspect to focus on to get better performance is ensuring type stability of the function. Luckily, Julia disposes of several tools to inspect and address both problems.

Regarding the second point, there are several packages such as `Cthulhu` or even the simple `@code_warntype` macro which allow to ensure that a function is type-stable, i.e. that the types of all variables can be correctly predicted by the compiler and stay consistent throughout the execution. Type stability is crucial for performance as it enables the compiler to generate optimized machine code, removing the load derived from dynamic type checks. In fact, Julia is dynamically typed, which means that variables do not have necessarily to be declared with their type, in contrast to fully statically typed languages such as C, and they could change it during execution. For example, a variable initialized as an integer could later become a float, or even a string. However, for performance purposes, these dynamicisms should be avoided, and those tools help to ensure that this happens. We managed to reduce all the useless type instabilities, but some are instead still present to guarantee some flexibility to the users, e.g. to select at run time which cohesion and similarity functions use in the fit.

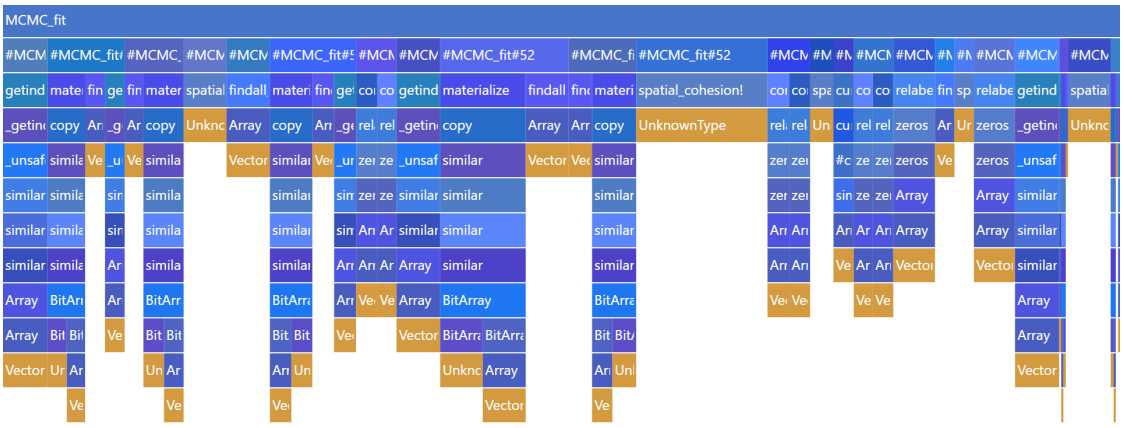

Figure 2.1: Flame graph derived from a simple fit with $n = 20$, $T = 50$, ran for 10000 iterates. Each section, identified with a colored box, represents a function call with its stack trace below, i.e. all the other subsequent function calls generated from the initial top one. The widths are proportional to allocation counts, i.e. to how many times a memory allocation was required for their corresponding box. The plot should be read from top to bottom with respect to function calls, and from left to right with respect to the fitting steps.

Regarding the first point, the memory issues, we heavily inspected it through the `ProfileCanvas` package. This profiler generates a plot, the flame graph, represented in Figure 2.1, which illustrates the different sections of code with regions whose size is proportional to a certain metric, e.g. the time spent on them during execution or, in this case of memory investigation, the number or size of allocations that was required for that section. This allows to see if the running time is spent on actual useful operations or instead on "bad" ones, such as garbage collection and run-time evaluations; therefore highlighting the sections of code which could possibly be optimized. All the modelling and working variables were of course preallocated, but the key idea has been to refactor the code to make it work more *in-place*, passing as arguments the variables which would be modified by a function and applying those changes directly inside the function, rather than returning some values and then use them to modify the initial variables. On top of that, some other easier improvements were possible through various features of the Julia language, such as the `@view` macro which allowed to remove unnecessary copies by just passing a reference to the portion of vectors or matrices which was needed to perform a certain computation, rather than passing the whole structure.

Also the `BenchmarkTools` (Chen et al., 2016) package has been in general a great tool to quickly analyse and compare entire fits or just small sections of code. For example, that package allows to simply test different versions of equivalent instructions to see which one could be the most efficient, as in this case

```
using BenchmarkTools
nh_tmp = rand(100)
@btime nclus_temp = sum($nh_tmp .> 0)
# 168.956 ns (2 allocations: 112 bytes)
@btime nclus_temp = count(x->(x>0), $nh_tmp)
# 11.612 ns (0 allocations: 0 bytes)
```

or this other one

```
n = 100; rho_tmp = rand((1:5),n); k = 1
@btime findall(j -> ($rho_tmp)[j]==$k, 1:n) # with anonymous function
# 272.302 ns (5 allocations: 384 bytes)
@btime findall_faster(j -> ($rho_tmp)[j]==$k, 1:n) # custom implementation
# 214.259 ns (3 allocations: 960 bytes)
@btime findall($rho_tmp .== $k) # with element-wise comparison
# 184.112 ns (3 allocations: 320 bytes)
```

where the $ symbol is used for interpolating a variable, ensuring to treat it as a local variable inside the benchmark and therefore avoiding any performance bias caused by accessing a global variable. This was a quick and simple comparison, yet very precise and effective, which would be instead more complex to replicate in C.

During the finer and final refinements of the code we also used more low-levels analysis tools such as the `--track-allocation` option which asks Julia to execute the code and annotate, line by line, the source file to see where and of which amount allocations occurred.

2.1.1 Optimizing spatial cohesions

The memory allocation problem was especially visible in the spatial cohesion computation. In fact, such computation appears in both sections of updating γ_{it} and updating ρ_t, which are inside of outer loops on draws, time, and units, and involve themselves some other loops on clusters. All this implied that those cohesion computations will be executed possibly millions of times during each fit. A simple and quick inspection suggests a value between dTn and dTn^2, being d the number of iterations, T the time horizon and n the number of units. We can't provide more precise estimate due to the variability and randomicity of the inside loops, which depend on the distribution of the clusters. With all that in mind, it was crucial to optimize the performance of the cohesion functions.

The only optimizing task consisted in carefully designing the cohesion function implementations. Cohesions 1, 2, 5 and 6 didn't exhibit any complication or need for optimization: the natural conversion in code from their mathematical models proved to be already optimally performing. The main problem was instead with cohesions 3 and 4, the auxiliary and double dippery, which by nature would involve some linear algebra computations with vectors and matrices.

The first implementation of those cohesions turned out to be really slow, due to the overhead generated by allocating and then freeing, at each call, the memory devoted to all vectors and matrices. This in the end meant that most of the execution time was actually spent by the garbage collector, rather than in the real and useful operations. A first solution was then to resort to a scalar implementation, which would remove the overhead of the more complex memory structures. In the end, we managed to combine the readability of the first idea with the performance of the second one into a final version, as we can see from Listing 1.

Listing 1: Sections of the Julia code for the three implementation cases of the spatial cohesions 3 and 4. The first one has the first-thought vector implementation derived from the mathematical formulation, the second one is the conversion to only have scalar variables, while the third one is the final version, keeping the vector form but improved using static structures.

```
# original vector version
sbar = [mean(s1), mean(s2)]
vtmp = sbar - mu_0
Mtmp = vtmp * vtmp'
Psi_n = Psi + S + (k0*sdim) / (k0+sdim) * Mtmp

# scalar-only version
sbar1 = mean(s1); sbar2 = mean(s2)
vtmp_1 = sbar1 - mu_0[1]
vtmp_2 = sbar2 - mu_0[2]
Mtmp_1 = vtmp_1^2
Mtmp_2 = vtmp_1 * vtmp_2
Mtmp_3 = copy(Mtmp_2)
Mtmp_4 = vtmp_2^2
aux1 = k0 * sdim; aux2 = k0 + sdim
Psi_n_1 = Psi[1] + S1 + aux1 / (aux2) * Mtmp_1
Psi_n_2 = Psi[2] + S2 + aux1 / (aux2) * Mtmp_2
Psi_n_3 = Psi[3] + S3 + aux1 / (aux2) * Mtmp_3
Psi_n_4 = Psi[4] + S4 + aux1 / (aux2) * Mtmp_4
```

```
# static improved version
sbar1 = mean(s1); sbar2 = mean(s2)
sbar = SVector((sbar1, sbar2))
vtmp = sbar .- mu_0
Mtmp = vtmp * vtmp'
aux1 = k0 * sdim; aux2 = k0 + sdim
Psi_n = Psi .+ S .+ aux1 / (aux2) .* Mtmp
```

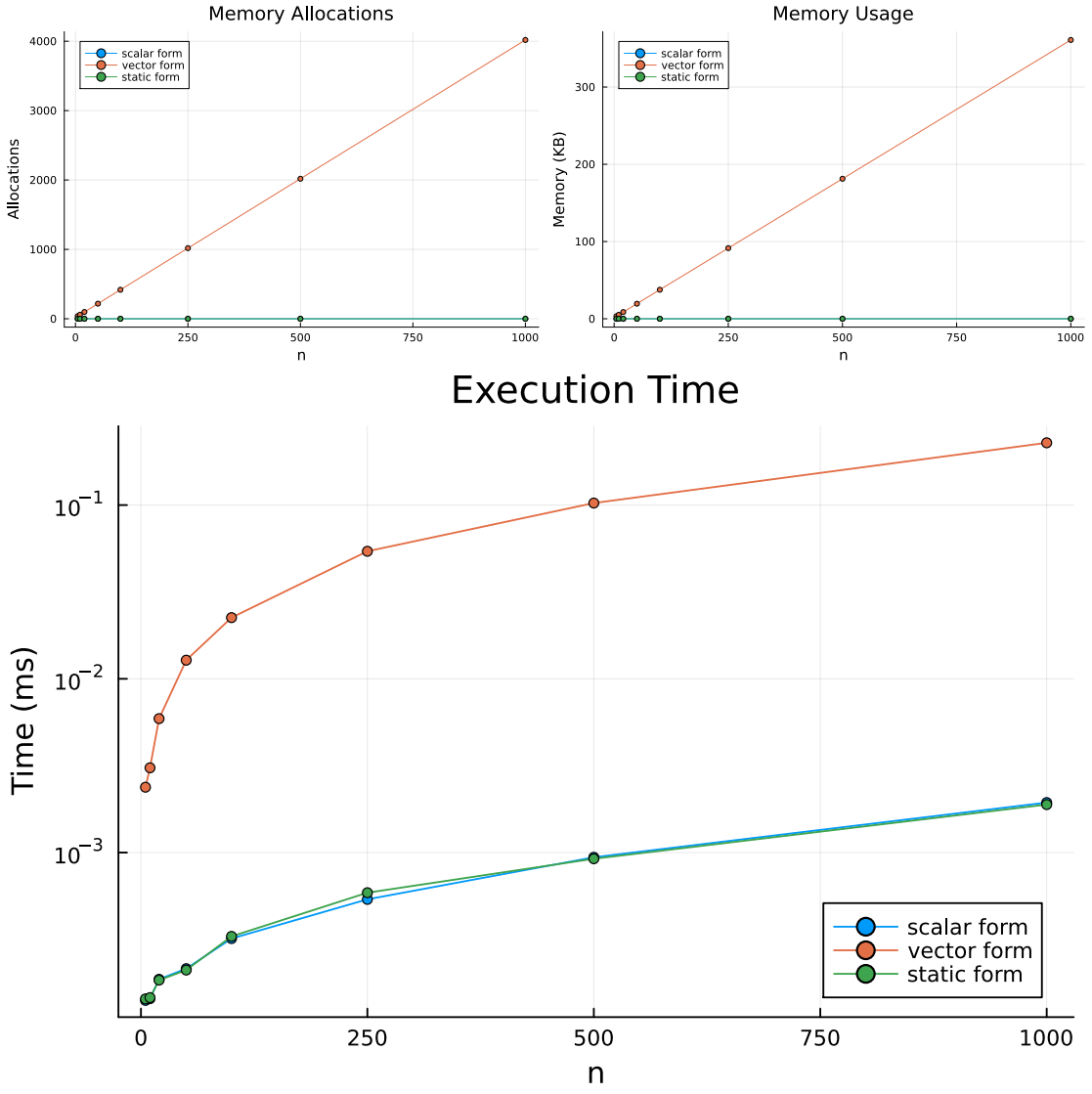

Figure 2.2: Performance comparison between the three versions of the cohesion 4 function. Tests ran through the `BenchmarkTools` package of Julia by randomly generating the spatial coordinates of the various test sizes n, with similar results standing for cohesion 3. The memory allocation and usage plots are constant at zero for both the scalar and vector static cases.

This final version exploits the `StaticArrays` package of Julia, which allows to use vectors and matrices more efficiently if their size is known at compile time; which is the case of the spatial cohesions computation since working with planar spatial coordinates we will always have 2×1 vectors and 2×2 matrices. The

benefits of this final version are that we maintain the natural mathematical form of the first one, improving the clearness of the code, together with the efficiency of the second one, since now with static structures the compiler is able to optimize all memory allocations as it was doing with the simple scalar variables.

Figure 2.2 shows the comparison of their performances, where we can see how the scalar and static versions indeed perform very similarly to each other, and more quickly with respect to the first version.

Noticeably, the C implementation of the model didn't have to worry about all this reasoning, since C can't natively, nor gracefully, work with vectors and matrices and was therefore forced to the scalar implementation.

2.1.2 Optimizing covariates similarities

Another problem has been understanding how to speed up the computation of the similarity functions, since those would also be called possibly millions of times as the cohesion ones or even more, considering that we can incorporate more than one covariate into the clustering process, and this would add an additional loop based on p, the number of covariates decided to be included.

As in the previous case, some of the functions didn't show any special need or room for relevant optimizations. The fourth one instead, the auxiliary similarity function, was essential to be optimized not only because it is one the most common choice among the similarities, but also because it involves a computationally heavy sum of the squares of the covariate values, as we can see in Listing 2.

Listing 2: Version of the similarity 4 function with all the possible optimizing macros. The performance analysis will focus just on that inside loop, since the rest is not negotiable.

```
function similarity4(X_jt::AbstractVector{<:Real}, mu_c::Real, lambda_c::Real,
↪  a_c::Real, b_c::Real, lg::Bool)
    n = length(X_jt)
    nm = n/2
    xbar = mean(X_jt)
    aux2 = 0.
    @inbounds @fastmath @simd for i in eachindex(X_jt)
        aux2 += X_jt[i]^2
    end
    aux1 = b_c + 0.5 * (aux2 - (n*xbar + lambda_c*mu_c)^2/(n+lambda_c) +
    ↪  lambda_c*mu_c^2 )
    out = -nm*log2pi + 0.5*log(lambda_c/(lambda_c+n)) + lgamma(a_c+nm) -
    ↪  lgamma(a_c) + a_c*log(b_c) + (-a_c-nm)*log(aux1)
    return lg ? out : exp(out)
end
```

The idea to optimize it has been to annotate the loop with some macros provided by Julia. They are the following:

- `@inbounds` eliminates the array bounds checking within expressions. This allows to skip those checks to save some execution time. This insertion is harmless as long as we are sure that in our code design no out-of-bounds

or wrong accesses will occur. Otherwise some undefined behaviour will take place. The above loop is indeed very simple and safe, so this assumption is clearly satisfied.

- `@fastmath` executes a transformed version of the expression which calls functions that may violate strict IEEE semantics[1]. For example, its use could make $(a+b)+c \neq a+(b+c)$, but just in very pathological cases. Again, this is not a problem in our function, where we are just computing $\sum X_i^2$, since it does not have an intrinsically "right order" in which it has to be done.
- `@simd` (single instruction multiple data) annotate a for loop to allow the compiler to take extra liberties to allow loop re-ordering. This is a sort of parallelism technique, but rather than distributing the computational load on more processors we just *vectorize* the loop, i.e. we enable the CPU to perform that single instruction (summing the square of the i-th component to a reduction variable) on multiple data chunks at once, using vector registers, rather than working on each element of the vector individually.

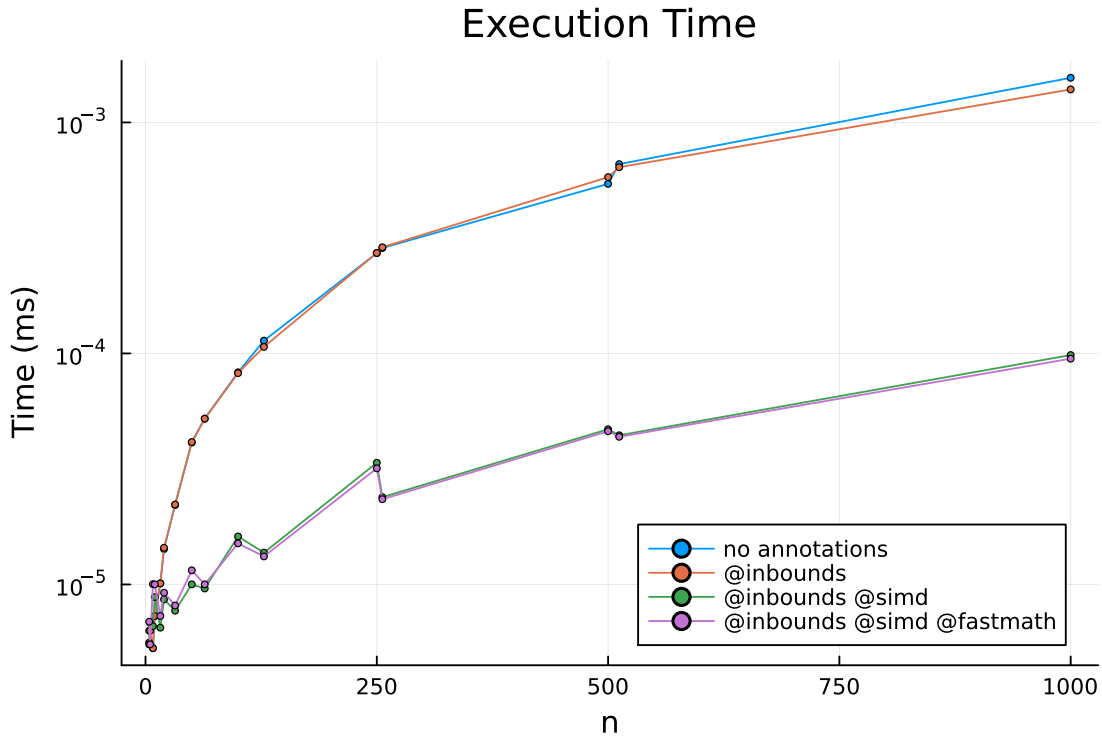

Figure 2.3: Comparison of the performances of the different possible loop annotations in the similarity 4 implementation. Their numerical output results are indeed the same for all cases. There are no memory allocation and usage plots since the analysis has been conducted only to evaluate the performances of the inside loop, which has no memory issues.

As we can see from Figure 2.3, the actual performance difference basically derives just from the use of `@simd`, with the other two annotations making not

[1]Institute of Electrical and Electronics Engineers. The IEEE-754 standard defines floating-point formats, i.e. the ways to represent real numbers in hardware, and the expected behaviour of arithmetic operations on them, including precision, rounding, and handling of special values (e.g. NaN (Not a Number) and infinity).

much of a difference. For that reason, and to reassure all pure mathematicians, we decided to remove the `@fastmath` annotation, leaving just `@inbounds` and `@simd`.

We can also notice interestingly how the tests with `@simd` annotation run quicker in the case of n being a power of two, compared to their closest rounded integers (e.g. 256 against 250 or 512 against 500), despite having relatively some more data. This is a proof of the effectiveness of the SIMD paradigm: according to the different architectures, the CPUs can provide different register sizes (e.g. 64, 128, 256 or 512 bits) and therefore the data subdivision can fit perfectly in them when the total memory occupied by the elements is a multiple of that register size (i.e. the number of data values is a power of two). Otherwise there will be some "leftovers chunks", which will of course be processed, but will also cause, as a consequence of the imperfect fit, a bit of overhead.

Chapter 3

Comparative analysis of CDRPM and JDRPM

In the following analyses, we will make use of the Adjusted Rand Index (ARI) (Hubert et al., 1985) to compare the partitions generated by the models. The ARI index serves as a correlation metric that quantifies the similarity between two clusterings. Specifically, for two partitions ρ_1 and ρ_2, the function $\text{ARI}(\rho_1, \rho_2)$ produces a value within the range $[-1, 1]$ where higher values indicating greater agreement between the partitions. A perfect match $\rho_1 = \rho_2$ is represented with the limit case $\text{ARI}(\rho_1, \rho_2) = 1$.

We will employ this index to study both the temporal evolution of clusterings, examining whether ρ_{t+k} correlates with ρ_t, and to assess the level of agreement between the two models, by comparing clusters estimates produced by CDRPM and JDRPM.

All analyses of this Chapter were conducted on a laptop equipped with 8 GB of RAM and a 1.80 GHz CPU base clock speed. The software used was R (R Core Team, 2024), interfaced with Julia through the `JuliaConnectoR` library (Lenz et al., 2022). This library handled all the communication between R and Julia, where the JDRPM algorithm is implemented. The CDRPM model is also accessible from R via a dedicated package, `drpm`, which similarly employs a wrapper to invoke the C code where the algorithm is implemented.

3.1 Assessing the equivalence of the models

Our model, along with its corresponding Julia implementation, represents an enhancement over the original DRPM and its associated C implementation. The improvements, as outlined in previous chapters, include the ability to incorporate covariates into both the prior and likelihood levels of the Bayesian model, the possibility of allowing for missing data in the response variable, and the guarantee of greater computational efficiency. In this regard, our updates serve as extensions to the original model. Therefore, when tested under equivalent hyperparameters and MCMC configurations, both models are expected to perform similarly and

produce comparable clusters estimates for a given dataset.

To evaluate the numerical performance of both algorithms, we will analyse posterior samples and cluster estimates in two scenarios: firstly using a synthetic dataset that includes only the response variable, and secondly employing a real-world spatio-temporal dataset. The latter also provides covariates; however, their effects will be extensively examined in the dedicated Section 3.3.

3.1.1 On a synthetic dataset

For the initial comparison we generated a dataset of $n = 10$ units and $T = 12$ time instants. The data generating function was the same employed in (G. L. Page et al., 2022) for their analyses and it allows for the creation of data points with temporal dependence, which could be adjusted through specific parameters. Regarding the MCMC setup, both algorithms were executed deriving 2000 iterates from a total of 50000 iterations, by discarding the first 40000 as burnin and then thinning by 5. Both models were fitted using a time specific α and using their full formulations, i.e. including and updating also the optional autoregression parameters η_{1i} and φ_1.

Table 3.1: Comparison between CDRPM and JDRPM fits and their associated algorithms in the simulated data scenario.

	MSE mean	MSE median	execution time
CDRPM	1.6221	1.5823	19s
JDRPM	**1.2634**	**1.2034**	**13s**

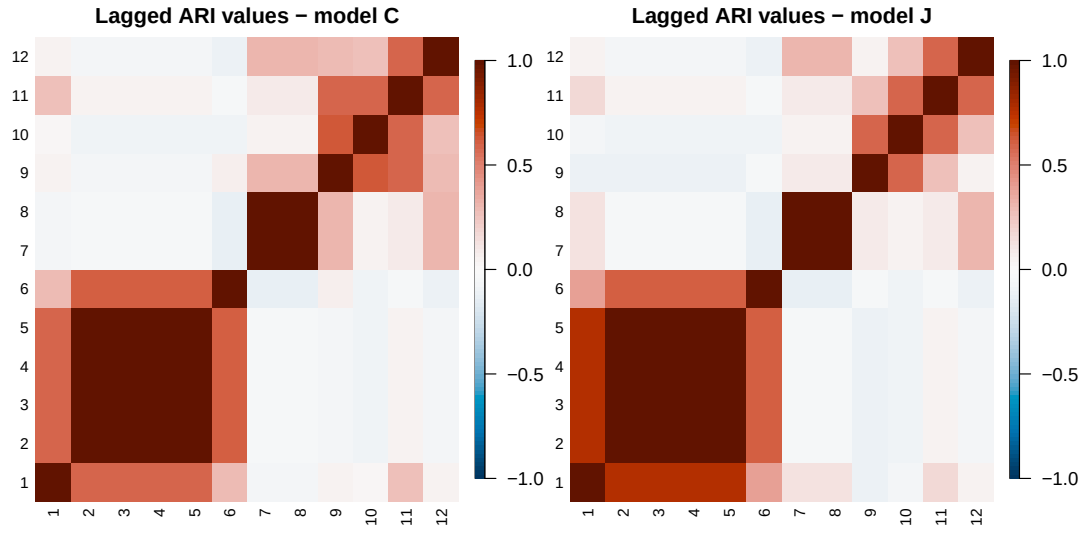

Figure 3.1: Lagged ARI values of CDRPM and JDRPM fits in the simulated data scenario.

During this testing phase, the clusters were defined solely by the target values from Y_{it}, and both models achieved satisfactory results. Fitted values are presented in Figure 3.4 alongside the original data. From Table 3.1 we can see how JDRPM

exhibited greater accuracy, as proven by the lower mean squared error (MSE), and a faster execution time. In the table, the MSEs were computed by comparing the fitted values generated by the models, estimated by taking the the mean and median of the 2000 iterations, with the true values of the target variable. We do not report fitting metrics for WAIC and LPML since both models were conceptually equivalent and tested under identical hyperparameters and MCMC configurations. Consequently, any observed differences in these metrics would be likely attributable to chance.

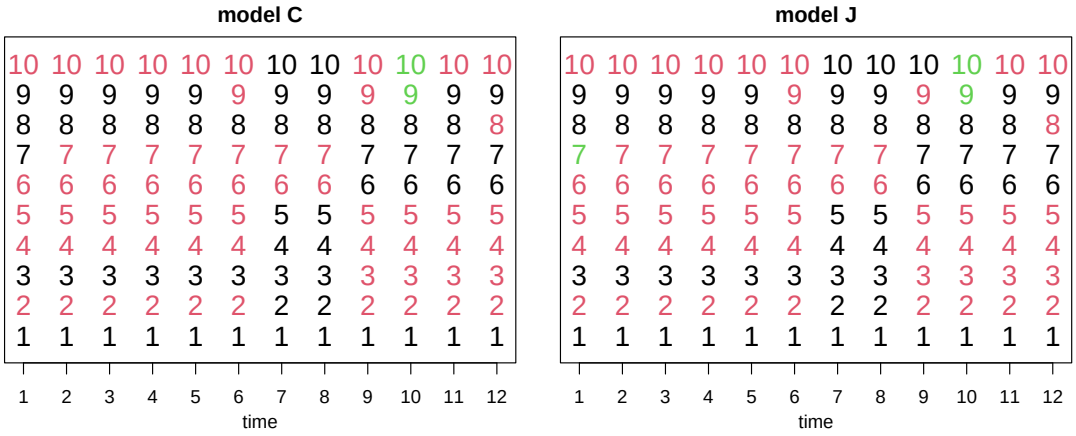

Figure 3.2: Clusters estimates produced by CDRPM and JDRPM fits in the simulated data scenario. Time instants are on the x axis, units are indicated vertically by their number, and colors represent the cluster label.

The resulting partitions, estimated using the `salso` function from the corresponding R library (David B. Dahl et al., 2022), were remarkably similar. As illustrated in Figure 3.1, both models effectively captured the temporal dynamics of the response variable. Moreover, Figure 3.2 confirms the agreement in the cluster estimates; however, it also reveals two minor differences which we will now discuss.

A closer examination of the clusters presented in Figure 3.3 reveals interesting distinctions at times $t = 1$ and $t = 9$. At $t = 1$, JDRPM classified unit 7 as a singleton within the green cluster, whereas CDRPM assigned unit 7 to the black cluster. Both classifications are reasonable: the data point is indeed closer to the black cluster, but it later aligns more distinctly to the red cluster; suggesting the classification given by JDRPM as a detection of its initial anomalous behaviour. At $t = 10$, both models successfully identified a small, temporary third cluster resulting from the transition of units 9 and 10. The JDRPM interprets this transition as a label swap: between times $t = 9$ and $t = 11$, unit 9 shifts from the red cluster to the black cluster, while unit 10 from the black cluster to red cluster. In contrast, at $t = 9$ CDRPM assigns both units to the red cluster, potentially reflecting a misclassification considering the temporal trend of unit 10 which, until $t = 10$, indicated a closer alignment with the black cluster.

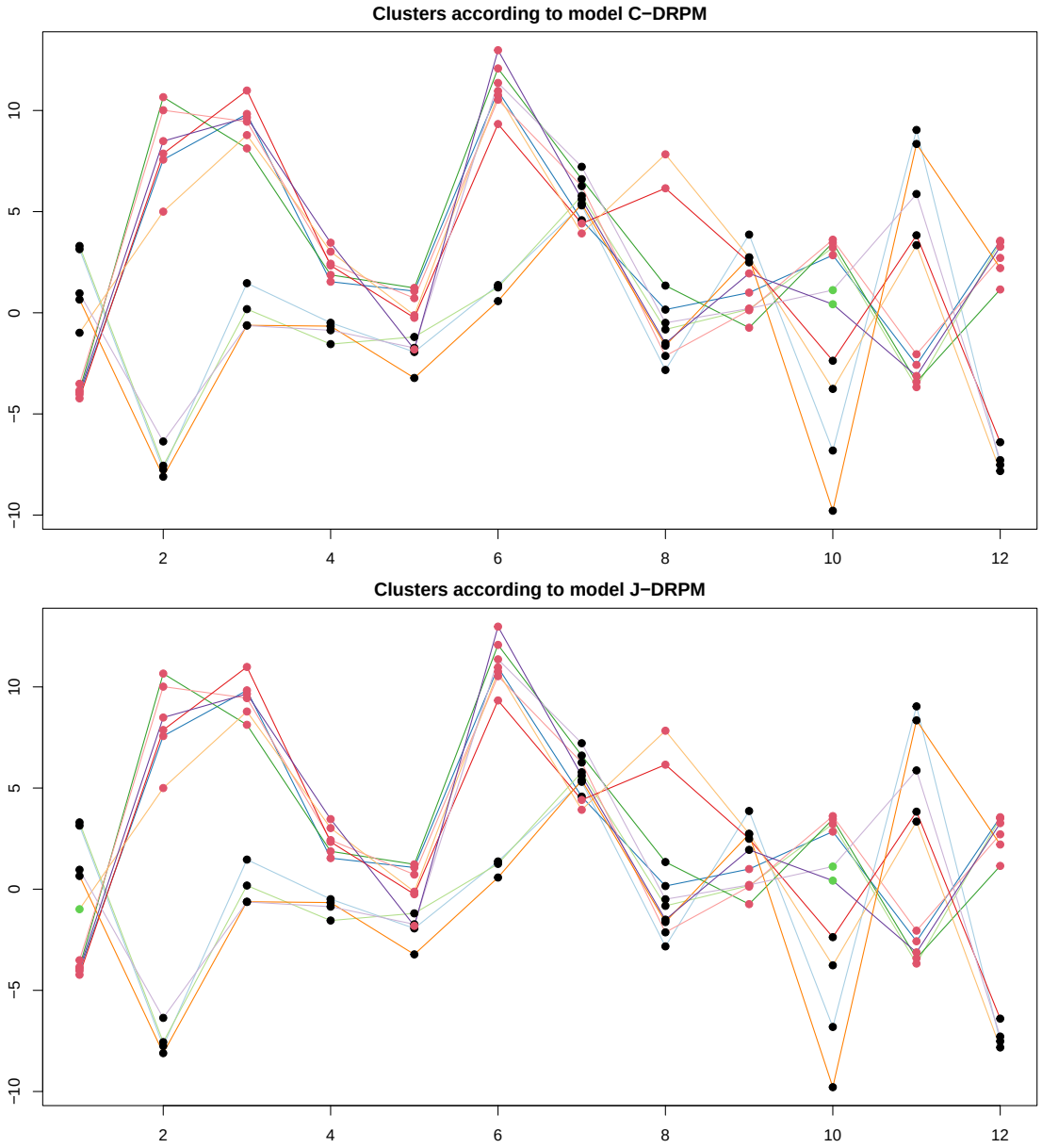

Figure 3.3: Visual representation of the clusters estimates produced by CDRPM and JDRPM fits in the simulated data scenario. Cluster labels are represented as colored dots overlaid to the trend of the target variable.

3.1.2 On spatio-temporal data

In this section we examine a more real-world application by fitting the models on a spatio-temporal dataset. Specifically, we used the AgrImOnIA dataset (Fassò et al., 2023) which encompasses measurements of air pollutants, together with many environmental and livestock variables, in the Lombardy region of Italy from 2016 to 2021.

For our subsequent analyses, we employed a dataset comprising weekly averages from the year 2018. The target variable selected for this studies was PM_{10} which underwent log-transformation, to recover a normal distribution, and was centered

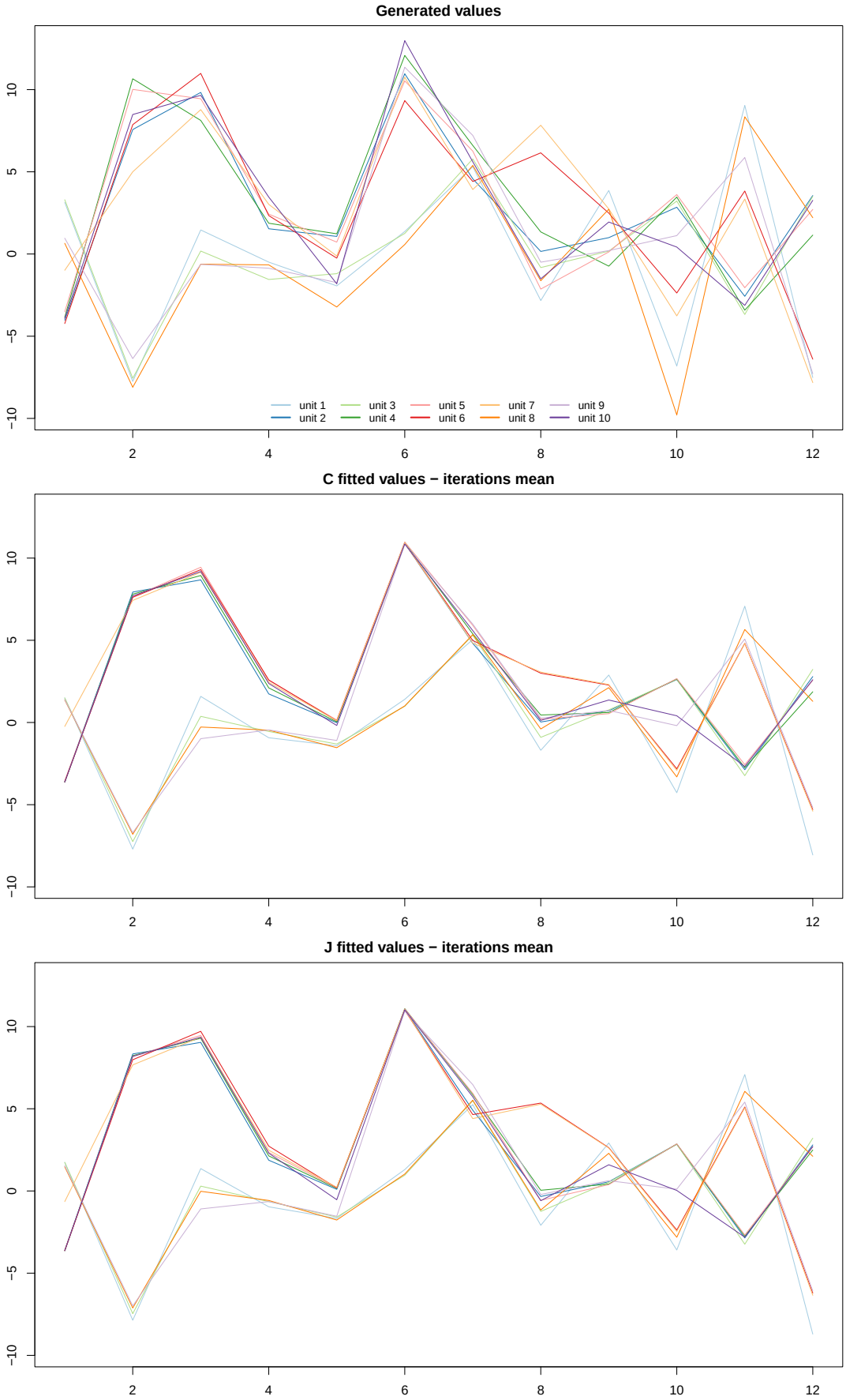

Figure 3.4: Fitted values of CDRPM (middle) and JDRPM (bottom) fits in the simulated data scenario, alongside the generated target values (top).

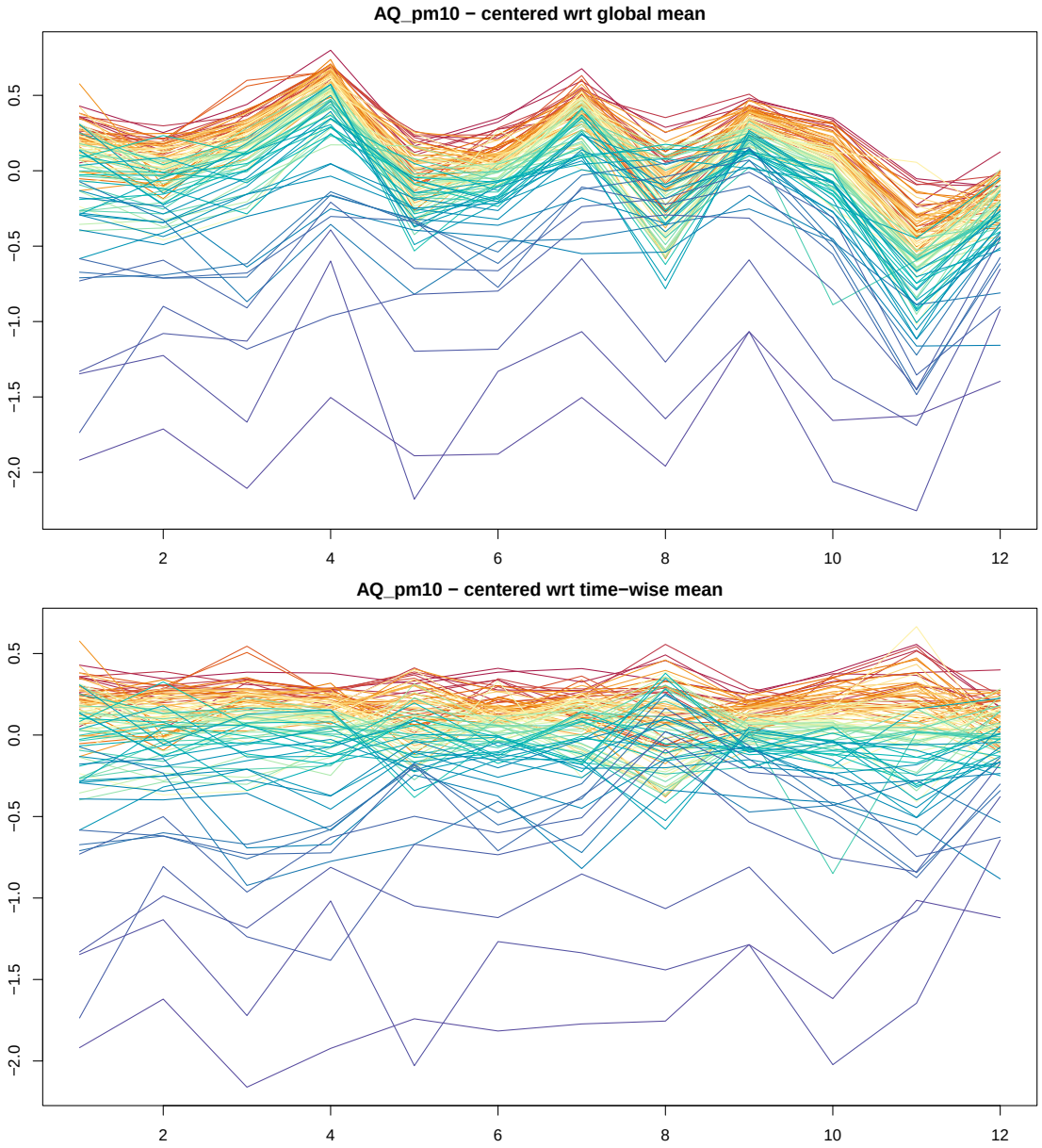

Figure 3.5: Values of the target variable `AQ_pm10` adjusted using the global mean (top) and the time-wise mean (bottom). Coloring is based on the ranking of PM_{10} values of the units according to their median, from highest (red) to lowest (blue).

with respect to time-wise means. More precisely, each observation Y_{it} was adjusted by subtracting the mean $\bar{Y}_t$ of all observations at that time instant t. This approach, consistent with the methodology employed by (G. L. Page et al., 2022) during their analyses, helps to emphasize variations within each time point rather than across the entire dataset. This approach is particularly beneficial for understanding how individual units deviate from their typical behavior at specific times, thereby highlighting temporal trends and anomalies. Moreover, this method effectively mitigates any temporal bias that may arise from periods in which all target values are disproportionately high or low due to external anomalous factors. In contrast, the traditional approach of centering the data around their global mean $\bar{Y}$ would

primarily facilitate the detection of overall trends, without providing an elaborate examination of each time step. For instance, preliminary analyses using global centering revealed only three clusters across all time points. While this result is indeed valid in light of the trend illustrated in Figure 3.5, our alternative approach produced multiple clusters, thereby enhancing the specialization of the clusters and also their interpretability.

To perform the fit, we used all the available stations in the dataset, amounting to $n = 105$, but restricted the time horizon to $T = 12$, corresponding to a three-month monitoring period. This limitation was implemented solely to reduce the computational time required to conduct the analyses. As in the previous section, both CDRPM and JDRPM algorithms were fitted with a time-specific parameter α and using their complete model formulations including the optional parameters η_{1i} and φ_1. To ensure convergence, we inspected the trace plots of both model and, in the case of JDRPM, we checked numerical diagnostics as the Effective Sample Size (ESS) and $\hat{R}$. In fact, JDRPM is able to provide such statistical assessments directly from the fitting function. Regarding the MCMC setup, we derived 4000 iterates from 110000 total iterations, by discarding the first 90000 as burnin and then thinning by 5.

Table 3.2: Comparison between CDRPM and JDRPM fits and their associated algorithms in the real-world scenario.

	MSE mean	MSE median	execution time
CDRPM	0.0142	0.0149	1h38m
JDRPM	**0.0131**	**0.0138**	**48m**

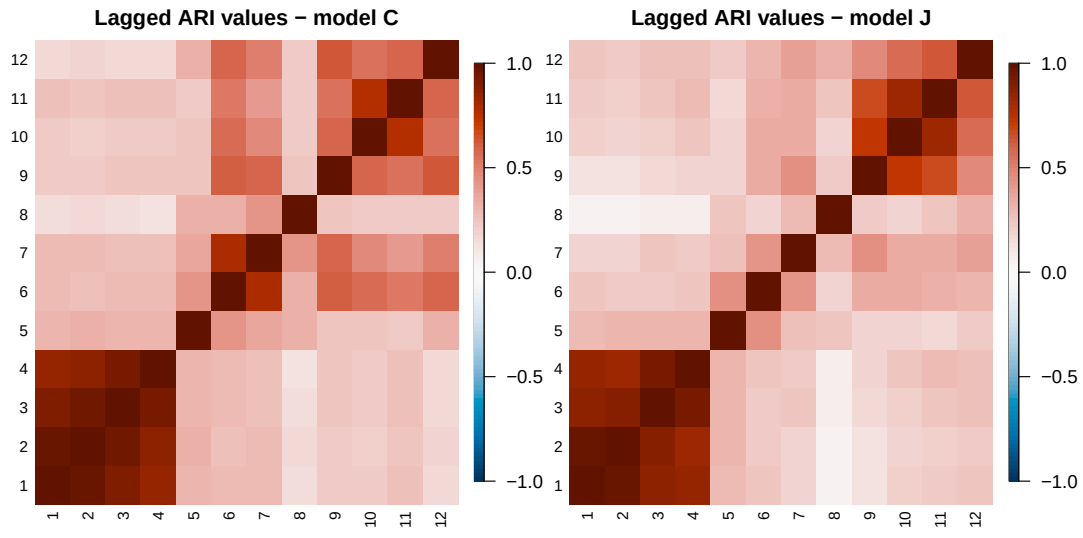

Figure 3.6: Lagged ARI values of CDRPM and JDRPM fits in the real-world scenario.

Table 3.2 shows how both model managed to be accurate in terms of the fitted values, with JDRPM again performing better in terms of MSEs. As in the previous section, we do not report the fitting metrics of WAIC and LPML because of the

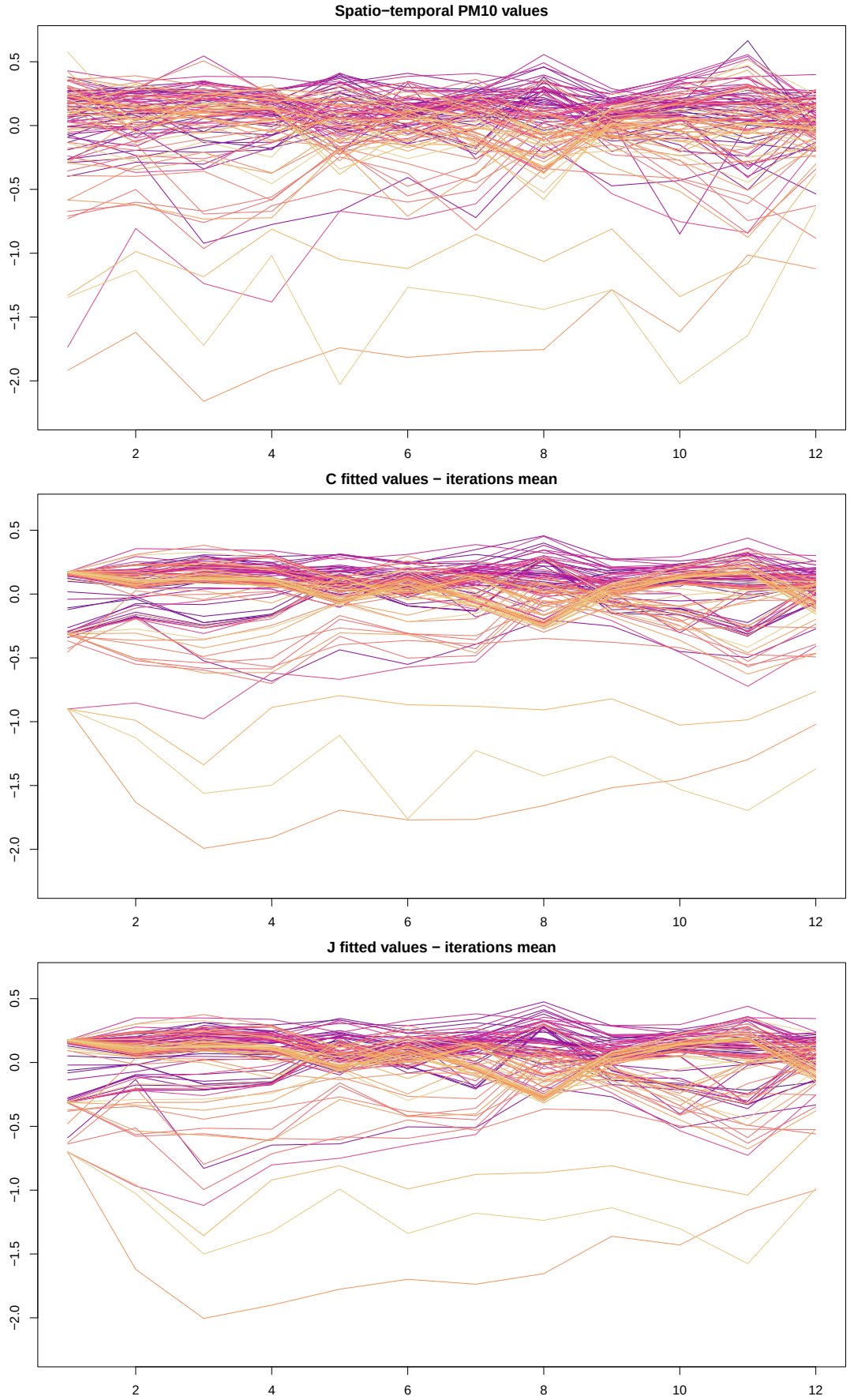

Figure 3.7: Fitted values of CDRPM (middle) and JDRPM (bottom) fits in the real-world scenario, alongside the generated target values (top).

theoretical equivalence of the models. Execution times are also reported, but they are somewhat inaccurate since during the fitting I was busy in writing this thesis, meaning that not all the computational resources of my laptop were devoted to the fitting task. In any case, more precise performance evaluations on the timings will be conducted in Section 3.4.

From Figure 3.6 we can see how the temporal trend was very similar, confirming again the correctness of the JDRPM implementation. Regarding the similarity of the produced clusters, the partition plot as the one of Figure 3.2 would now be more crowded due to the high number of units. For this reason, in order to still convey that information, we computed $\text{ARI}(\rho_{\text{JDRPM}}(t), \rho_{\text{CDRPM}}(t))$ for all time instants $t = 1, \dots, 12$, and we obtained a mean of 0.80 and a median of 0.86, denoting high levels of agreement in the clusters produced.

A visual representation of the clusters is provided in Figure 3.8, but will be further detailed and commented in Section 3.3.2 together with the fits including covariates in the clustering.

3.2 Performance with missing values

In this section, we replicate the analyses and evaluations from Section 3.1, this time focusing on scenarios involving missing values. Our objective is to investigate how the JDRPM performs in the absence of complete datasets and to determine whether it maintains effective performance under such conditions.

Given the extent of missing values in the AgrImOnIA dataset (Fassò et al., 2023), which was used for the spatio-temporal analysis, we opted to set 10% of the values as missing (NAs). To implement this, we randomly selected $nT/10$ indexes from the sets $[1, \dots, n]$ and $[1, \dots, T]$ to identify all the pairs (i, t) that would be designated as missing in the target variable Y_{it}. The ability to handle missing data is an enhancement introduced by the JDRPM; therefore these studies cannot be repeated with the original CDRPM model, which does not accept incomplete datasets.

All the following fits were conducted under the same conditions of their full-dataset counterpart, i.e. using the same models formulation, parameters, and MCMC setup.

3.2.1 No spatial information

The JDRPM model demonstrates remarkable performance even in the presence of missing values. As shown in Table 3.3, the model's performance is understandably lower compared to the full dataset scenario; however, it clearly remains satisfactory. The MSE has naturally increased due to the partial absence of data points which led to less accurate fitted values for the corresponding missing entries. Nevertheless, the fitted values, illustrated in Figure 3.9, remain closely aligned with the ones derived from the full dataset analysis.

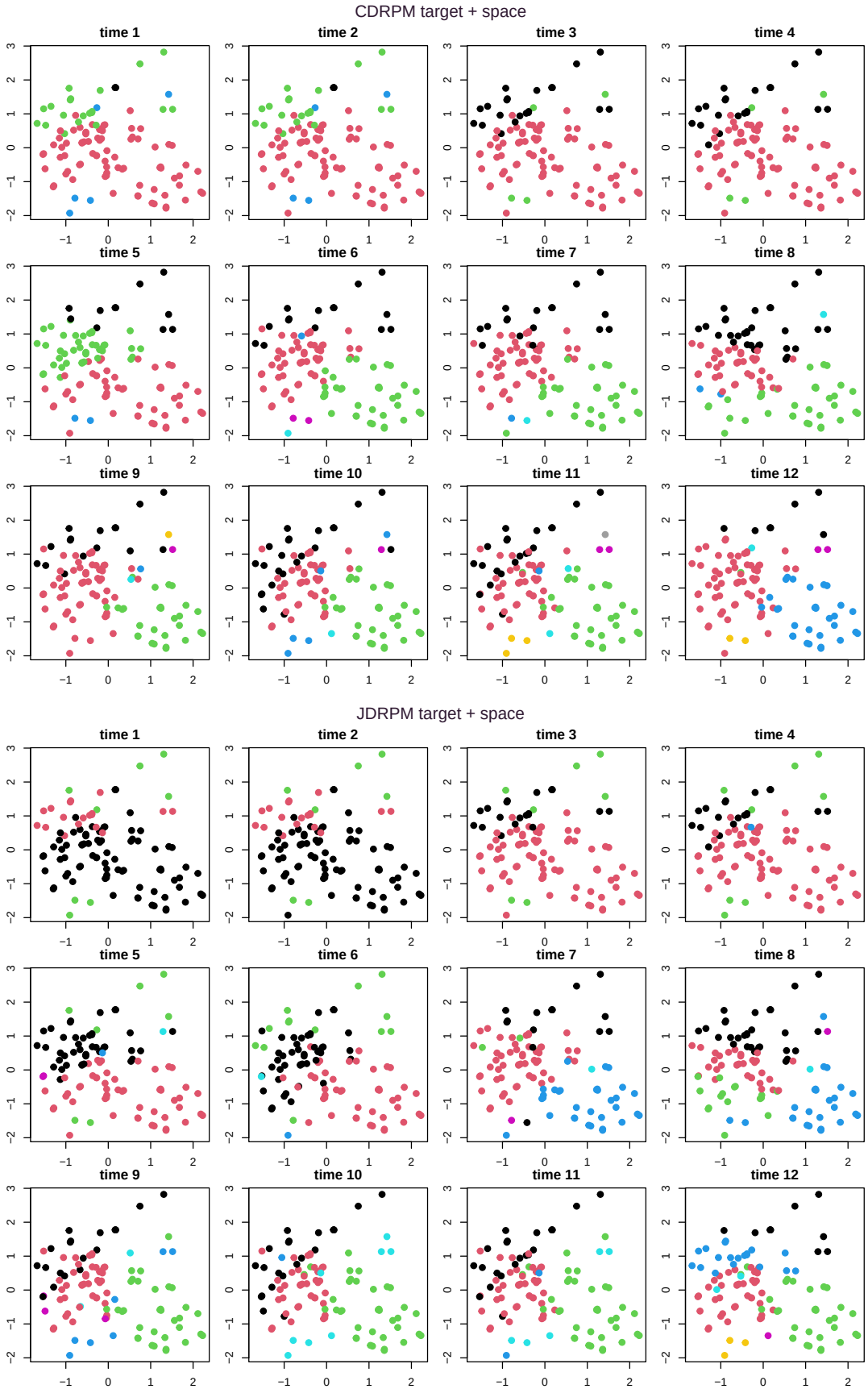

Figure 3.8: Visual representation of the clusters estimates produced by CDRPM and JDRPM fits in the real-world scenario.

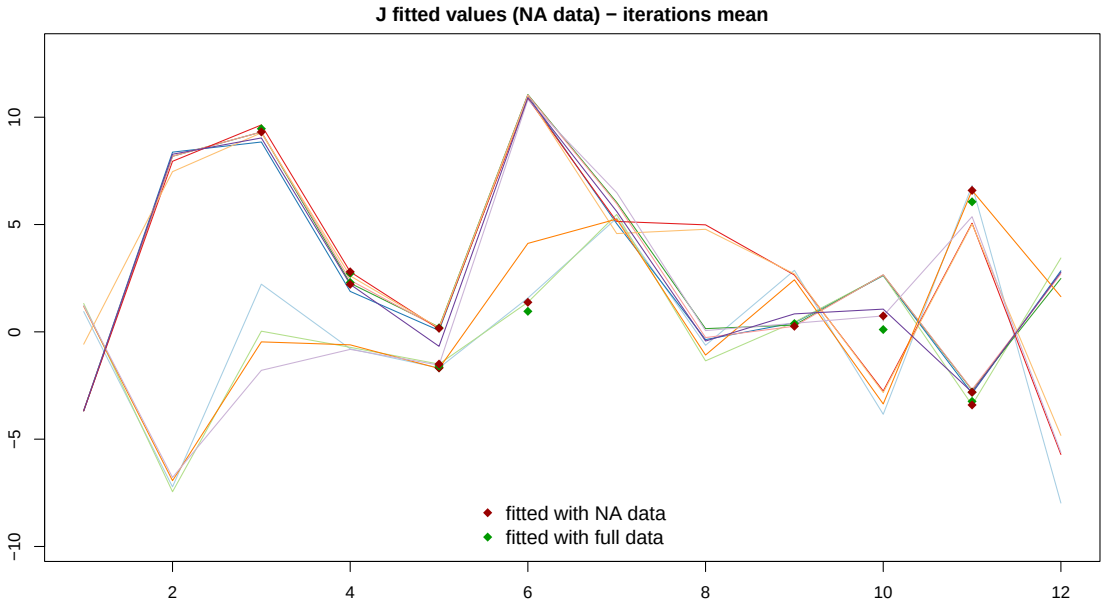

Figure 3.9: Fitted values estimate through the mean of the 1000 iterates generated by model JDRPM. Special point markers are used for the data points which were missing, to highlight the gaps between the fitted values on the full dataset (green squares) and the fitted ones on the NA dataset (red squares).

Table 3.3: Comparison of the JDRPM with no spatial information on a dataset with missing values.

JDRPM	MSE mean	MSE median	LPML	WAIC	exec. time
NA data	1.4721	1.2101	-236.93	401.44	13s
full data	1.2634	1.2034	-223.36	393.97	13s

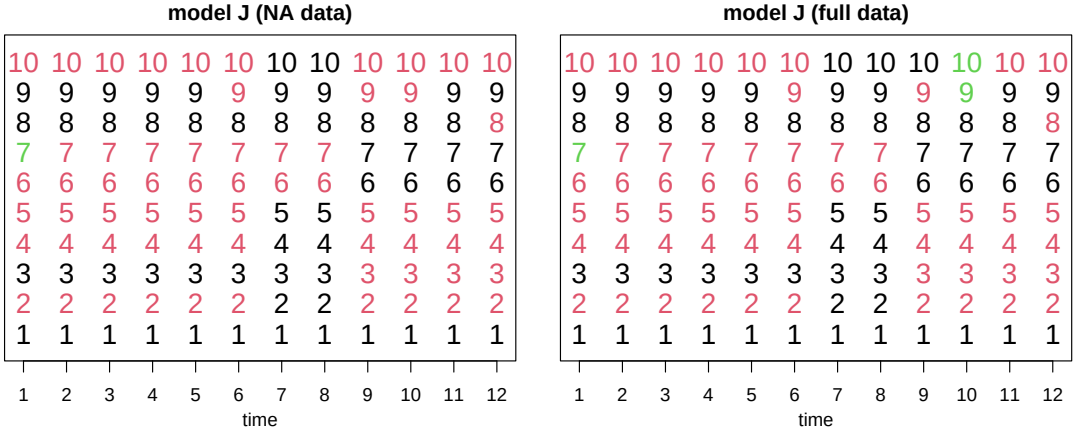

Figure 3.10: Clustering produced by the two tests on the JDRPM model, with time points on the x axis, units indicated vertically by their number, and colors representing the cluster label.

From Figures 3.11 we can see how we get almost the same temporal trend which we saw in the case without missing data, meaning that the JDRPM is able to recover a good temporal dependency structure even if some data are missing. Also the generated clusters, represented in Figure 3.12, appeared to be really similar.

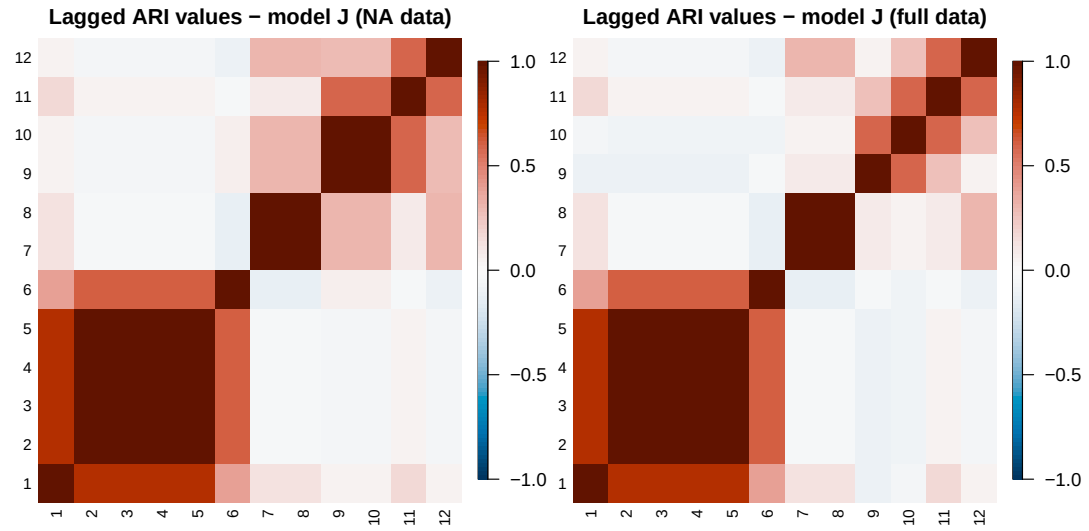

Figure 3.11: Lagged ARI values for the two fits on the JDRPM model with target values only. The partitions were estimated using the `salso` function from the corresponding R library.

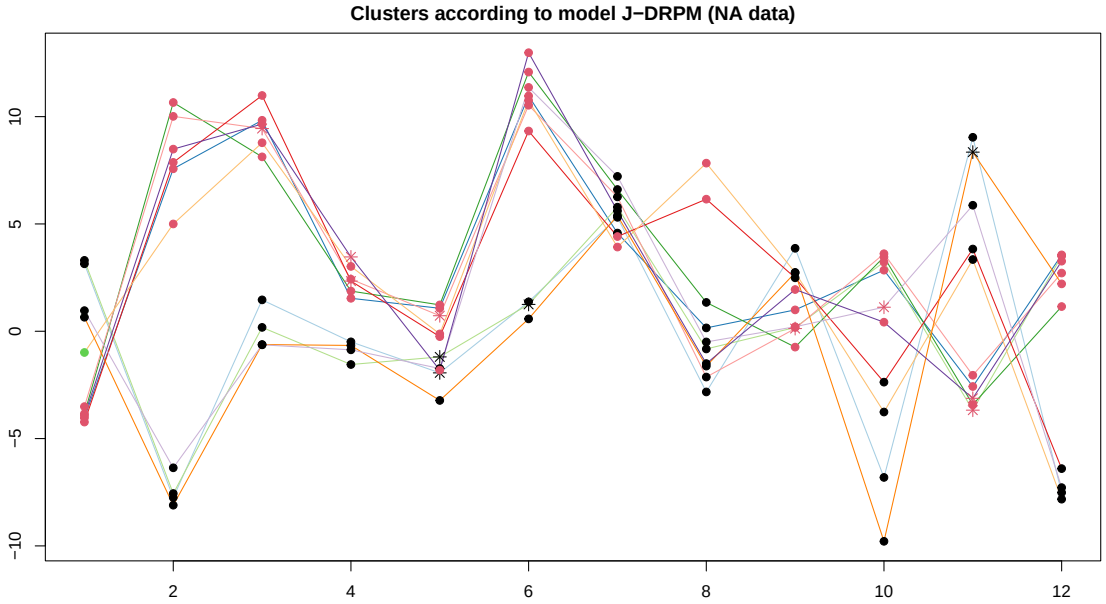

Figure 3.12: Visual representation of the clusters produced by the model, with units' labels represented as colored dots overlaid to the trend of the original generated target variables. Special point markers are used for the data points corresponding to missing values.

The only relevant different occurred at time $t = 10$, where now the model was not able to identify the green cluster which characterized the final transition phase of units 9 and 10. This is possibly due to the fact that the random creation of the NA data set unit 9 at time 10 to be missing, therefore removing important information for the retrieving of that special third cluster.

Finally, Figure 3.3.1 shows the 95% credible intervals for the fitted values corresponding to the missing data points. We can see how in almost all cases, except for one, the true value lies inside the credible interval, denoting the accuracy

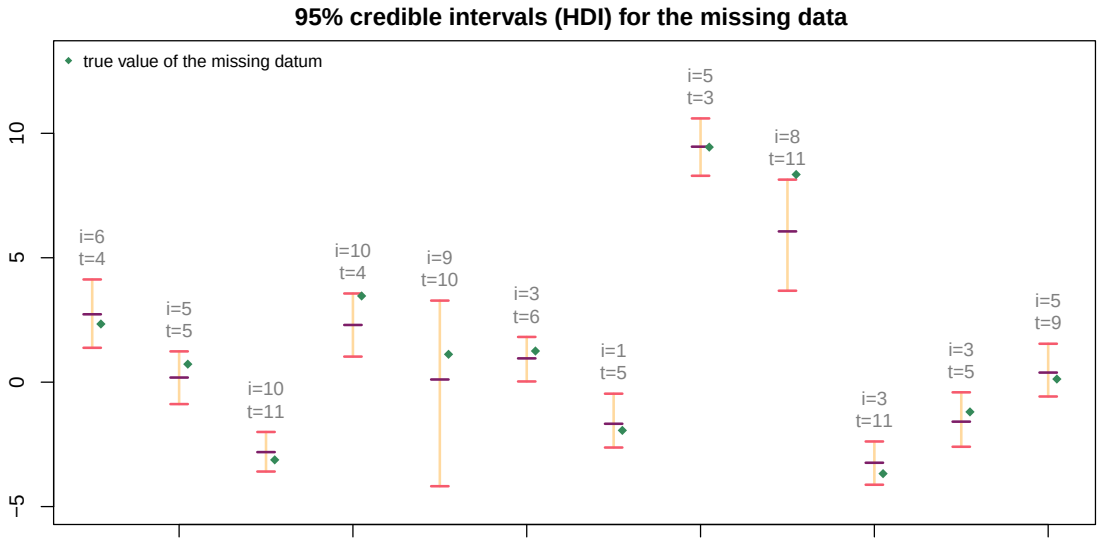

Figure 3.13: Credible intervals, computed with the highest posterior density method and at a 95% level, for the fitted values of the missing units in the JDRPM fit with NA data. In gray are reported the indexes of the units i and time instants t which where missing, while green dots refer to the true values of those missing data.

of JDPRM in retrieving good estimates of the target values, even in this case where no additional information was available either through space or covariates.

3.2.2 With spatial information

Table 3.4: Summary of the comparison between the two Julia fits on target plus space values. The MSE columns refer to the accuracy between the fitted values generated by the models (estimated by taking the mean and the median of the returned 4000 iterates) and the true values of the target variable. Higher LPML and lower WAIC indicate a better fit.

JDRPM	MSE mean	MSE median	LPML	WAIC	exec. time
NA data	0.0160	0.0170	502.86	-1793.64	43m
full data	0.0131	0.0138	624.91	-1898.05	48m

The JDRPM model seems able to perform well also in the case of fits including spatial information. Table 3.4 shows how the accuracy reduces, which again is inevitable since we are fitting with missing data, but not drastically. In fact, the drops in LPML and WAIC metrics are just of 3.16% and 0.95% respectively. Fitted values are reported in Figure 3.15. Regarding the reported execution times, they are not completely truthful, as already said before, due to the not-full commitment of my laptop resources to the fitting task. In fact, the fit with NA data appeared to be faster than the one with full data, which is somewhat implausible since in the presence of NA data there is the additional load of updating the missing Y_{it} values. Again, more accurate results will be provided in Section 3.4.

The temporal trend managed as well to remain similar to the trend we saw in Section 3.1.2, as proved by Figure 3.14. Noticeably, the ARI plot of the fit with NA

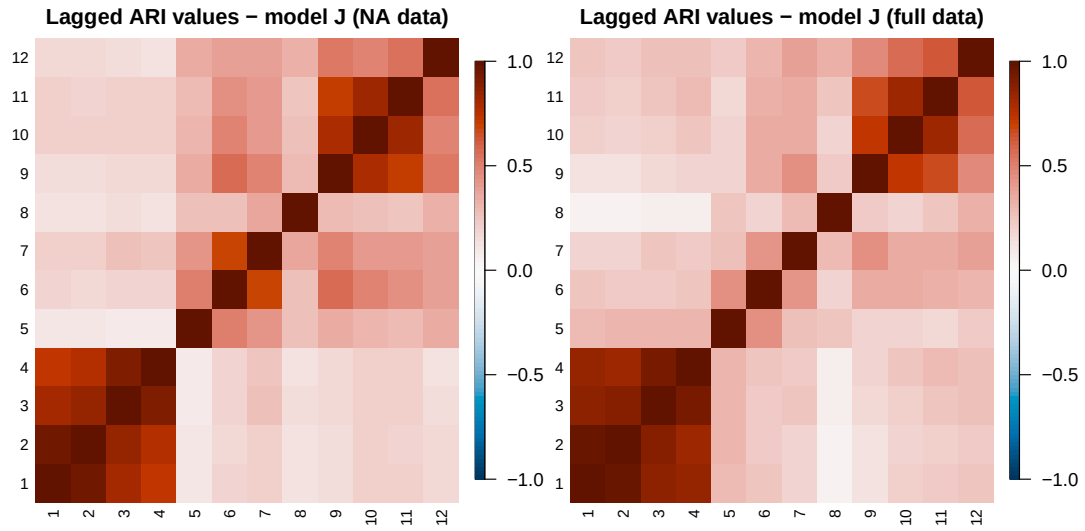

Figure 3.14: Lagged ARI values for the two fits on the JDRPM model with target plus space values. The partitions were estimated using the `salso` function from the corresponding R library.

data managed to resemble more the original trend displayed by the CDRPM fit on the full data; this same fact happened also in the previous section on fits without the additional spatial information. Regarding the similarity of the produced clusters, we computed the values $\mathrm{ARI}(\rho_{\mathrm{JDRPM\_NA}}(t), \rho_{\mathrm{JDRPM\_full}}(t))$ for all time instants $t = 1, \ldots, 12$, and we obtained a mean of 0.82 and a median of 0.86, denoting still a relatively high level of agreement in the partitions despite the loss of quite some data (121 points out of the 1260 of the full dataset).

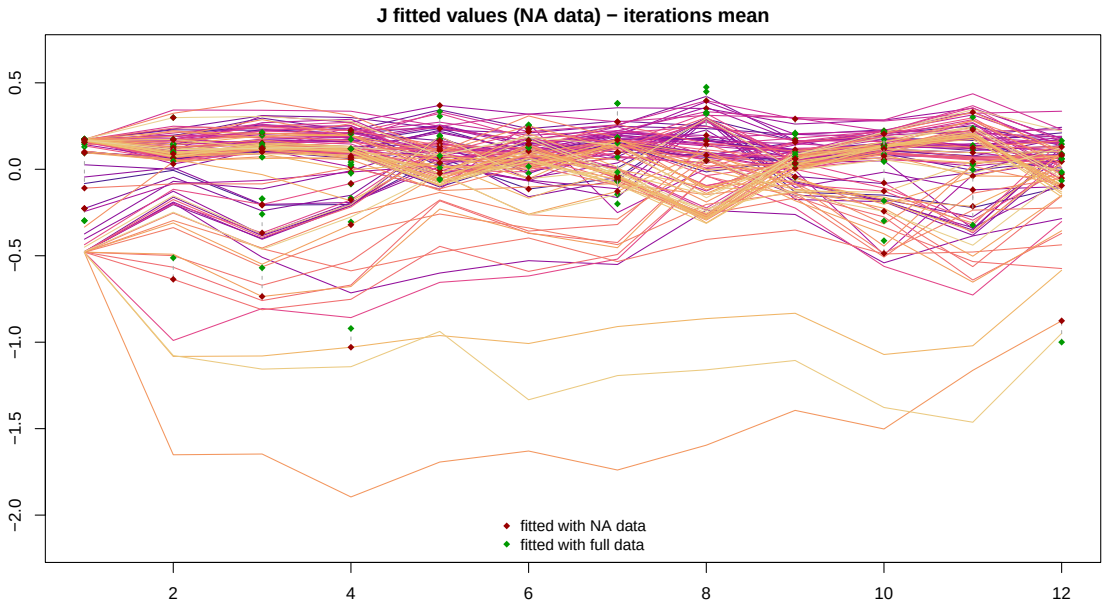

Figure 3.15: Fitted values estimate through the mean of the 4000 iterates generated by model JDRPM. The generated target values were the same of Figure 3.7. Special point markers are used for the data points which were missing, to highlight the gaps between the fitted values on the full dataset (green squares) and the fitted ones on the NA dataset (red squares).

3.3 Effects of the covariates

To perform the fits that will now follow, all the included covariates were treated in the same way as the target value, with the time-wise centering procedure and reasoning described in Section 3.1.2. Again, this was performed in order to remove any trend or bias on the covariates and to equalize their contribution at each time instant.

We will now see some testing fits which employ the core advancement of the JDRPM update, i.e. the inclusion of covariates. Being with radically different purposes, we will distinguish the cases of covariates in the likelihood and covariates in the clustering.

3.3.1 Covariates in the likelihood

Continuing on the line of the previous section, we can test if the insertion of covariates in the likelihood can help to recover some accuracy in the case of fits with missing data. In fact, the addition of the regression parameter $\boldsymbol{\beta}_t$ had the main goal of improving the accuracy of the model when estimating the target values Y_{it}, without affecting too much the cluster generation. With that in mind, the most natural use case of such parameter would be when fitting with missing values.

Table 3.5: Summary of the comparison between the JDRPM fits, on target plus space values, plus the fits including also covariates in the likelihood. The MSE columns refer to the accuracy between the fitted values generated by the models (estimated by taking the mean and the median of the returned 4000 iterates) and the true values of the target variable. Higher LPML and lower WAIC indicate a better fit.

JDRPM	MSE mean	MSE median	LPML	WAIC	exec. time
full data	0.0131	0.0138	624.91	-1898.05	**48m**
full data + Xlk	**0.0112**	**0.0113**	**778.96**	**-2029.84**	56m
NA data	0.0160	0.0170	502.86	-1793.64	**43m**
NA data + Xlk	**0.0127**	**0.0130**	**625.81**	**1902.74**	58m

Indeed, after including one or multiple covariates in the likelihood, and repeating the fit on the NA dataset under the same conditions, apart from this addition, we saw some improvements. To better illustrate them, we also ran the corresponding fit using the same covariates set in the likelihood, but this time on the full dataset. Results are summarized in Table 3.5 which also includes, as a reference, the results of the previous fits without the regressor component. Again, the execution times have to be taken with a pinch of salt.

We can see how clearly the insertion of covariates in the likelihood managed to improve all fitting metrics with, as expected, a decrease in the MSEs, especially in the fits with NA data, proving how that insertion can indeed recover some performance in the case of missing values. The regression vectors $\boldsymbol{\beta}_t$ displayed good trace plots, represented in Figures 3.17 and 3.18, proving the correctness and effectiveness of the implementation. Moreover the values at which the regressors

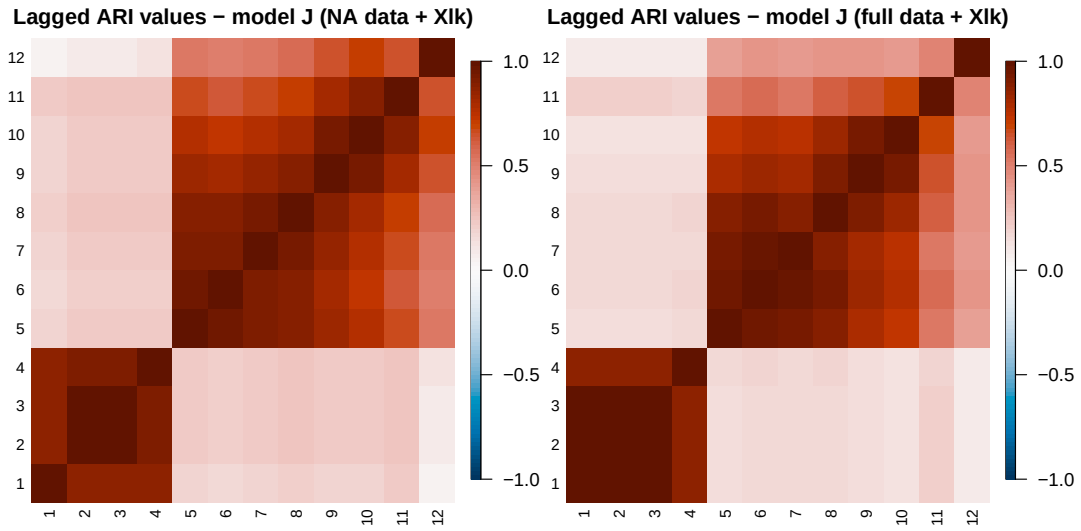

Figure 3.16: Lagged ARI values of the two JDRPM fits with target plus space values on the full and NA datasets, with covariates in the likelihood.

settled seems to be reasonable and interpretable. For example, it is known that higher altitudes implies lower air pollution, due to the nearly absence of emission sources like industries and vehicles, the more intense winds, the lower atmospheric pressure which facilitates the mixing of the air, and so on; and in fact the $\boldsymbol{\beta}_t$ component referring to `Altitude` wanders around negative values, indicating a reduction impact on PM_{10} concentrations. On the other hand, the `LI_bovine` covariate, which refers to the density of bovines per km^2 in the the area of the measuring station, tends to stay around positive values, since indeed the presence of livestock industries contributes to the emission of air pollutants.

Regarding the generated partitions, they remained substantially unchanged, as briefly depicted in Figure 3.19. The spatio-temporal trend was as well preserved, displayed in Figure 3.16, except for a generally higher dependence in the second part of the time interval, after the same identified "change point" at $t = 4$.

The JDRPM fitting function also includes a `beta_update_threshold` argument, defaulted to zero, to set after which iteration the algorithm should start to update the $\boldsymbol{\beta}_t$ parameter. This was an harmless and simple addition, which was considered useful to firstly let the model update and improve the more delicate and relevant parameters for the clustering, such as $\mu^{\star}_{jt}$ and $\sigma^{2\star}_{jt}$, and secondly tune also the less impactful $\boldsymbol{\beta}_t$. Otherwise, maybe, the initial development of the model parameters and clusterings could be biased by early inaccurate samples of the likelihood regressor.

Finally, Figure 3.20 encloses the fitted values of NA run with covariates in the likelihood. We can see how indeed, visually but also as proved by the better MSEs, these fitted values resemble more the ones of the original target variable, especially if compared to the case of Figure 3.7, in which both fits were without any "external suggestion" of covariates in the likelihood. A further proof of this insertion is given by Figure 3.21, representing the trace plot of the fitted values for a problematic unit

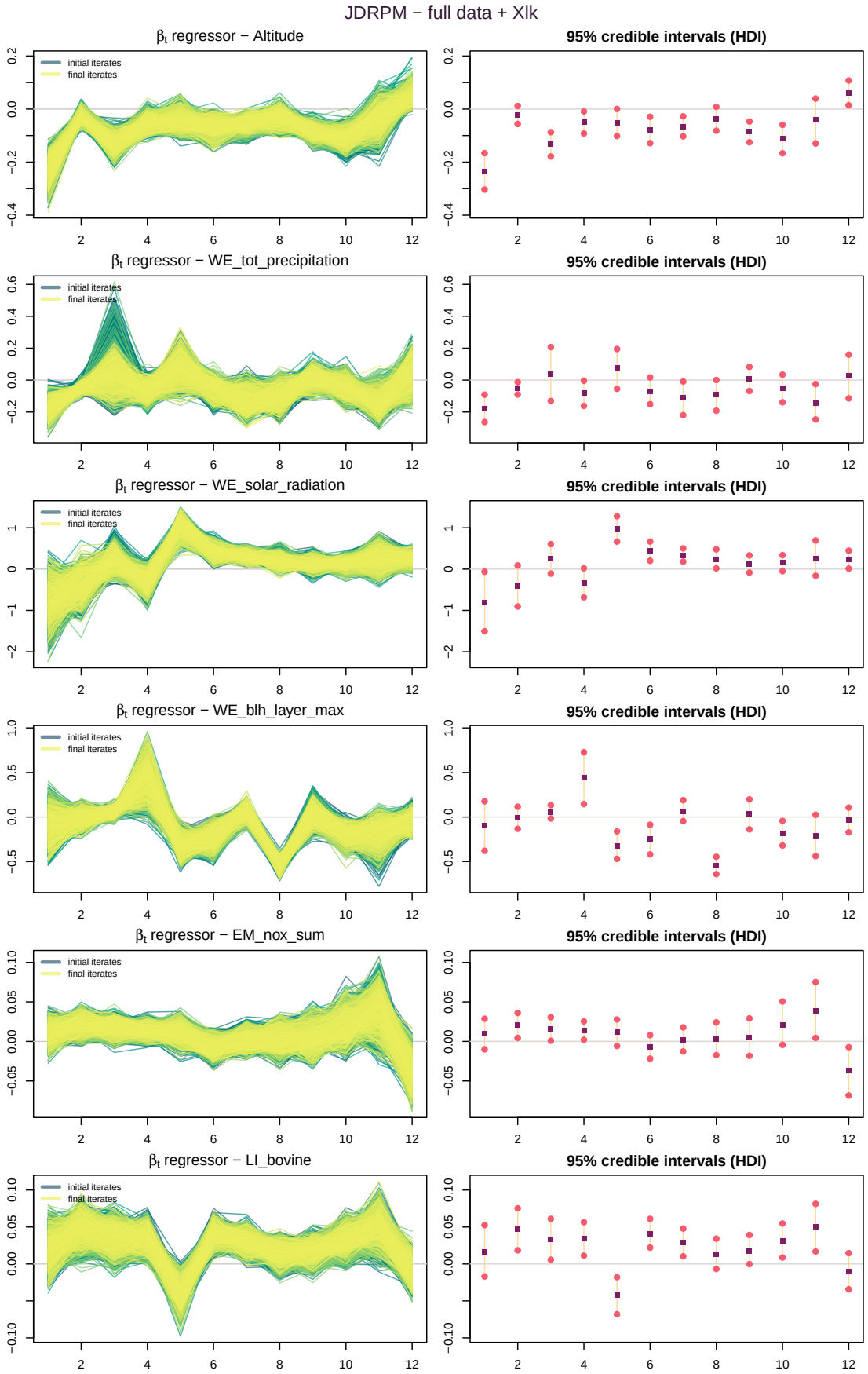

Figure 3.17: Regression vector $\boldsymbol{\beta}_t$ for the $p = 6$ covariates inserted in the likelihood in the full data spatio-temporal fit test, with trace plots (left) and 95% credible intervals computed with the highest density interval (HDI) method.

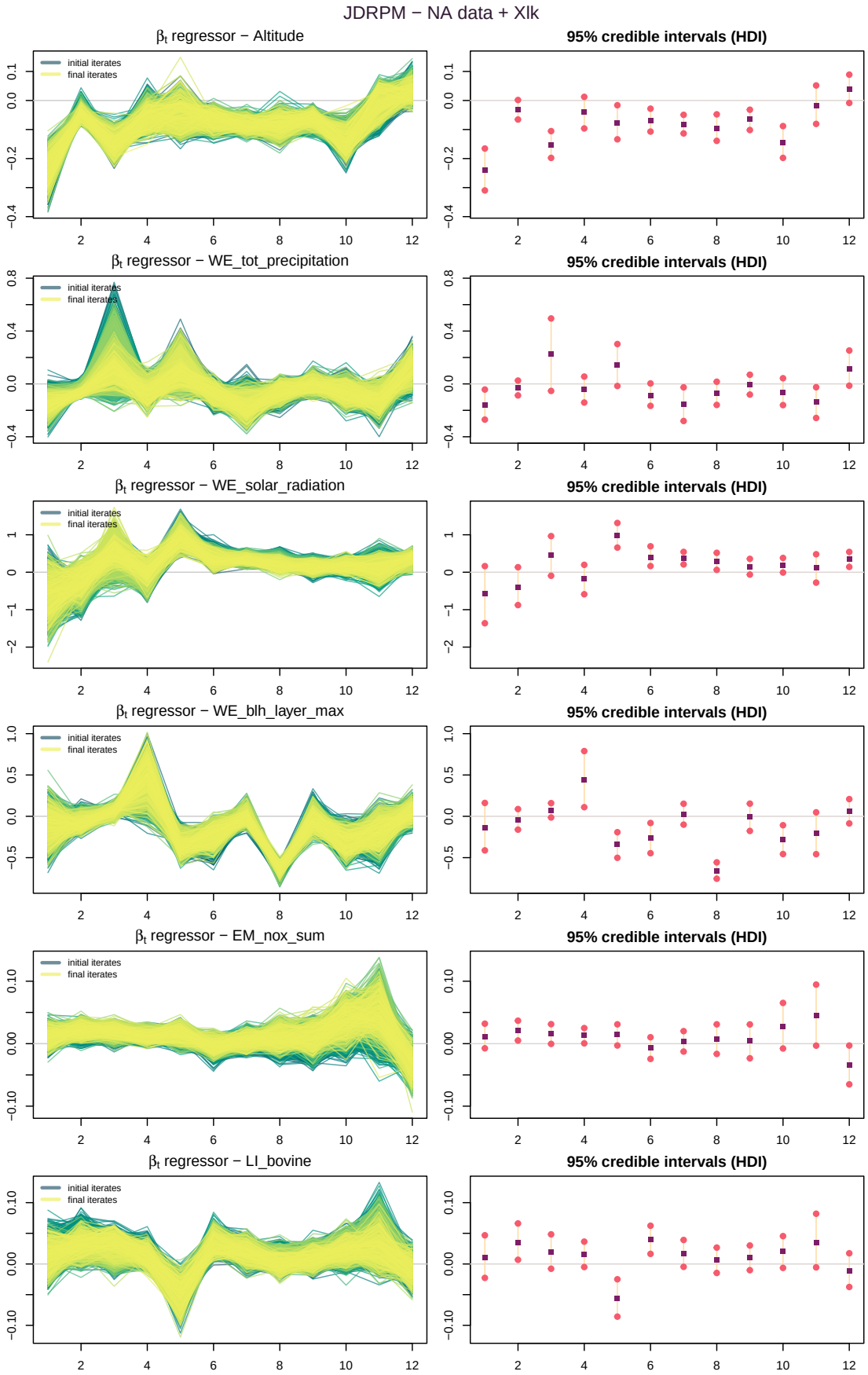

Figure 3.18: Regression vector $\boldsymbol{\beta}_t$ for the $p = 6$ covariates inserted in the likelihood in the NA data spatio-temporal fit test, with trace plots (left) and 95% credible intervals computed with the highest density interval (HDI) method.

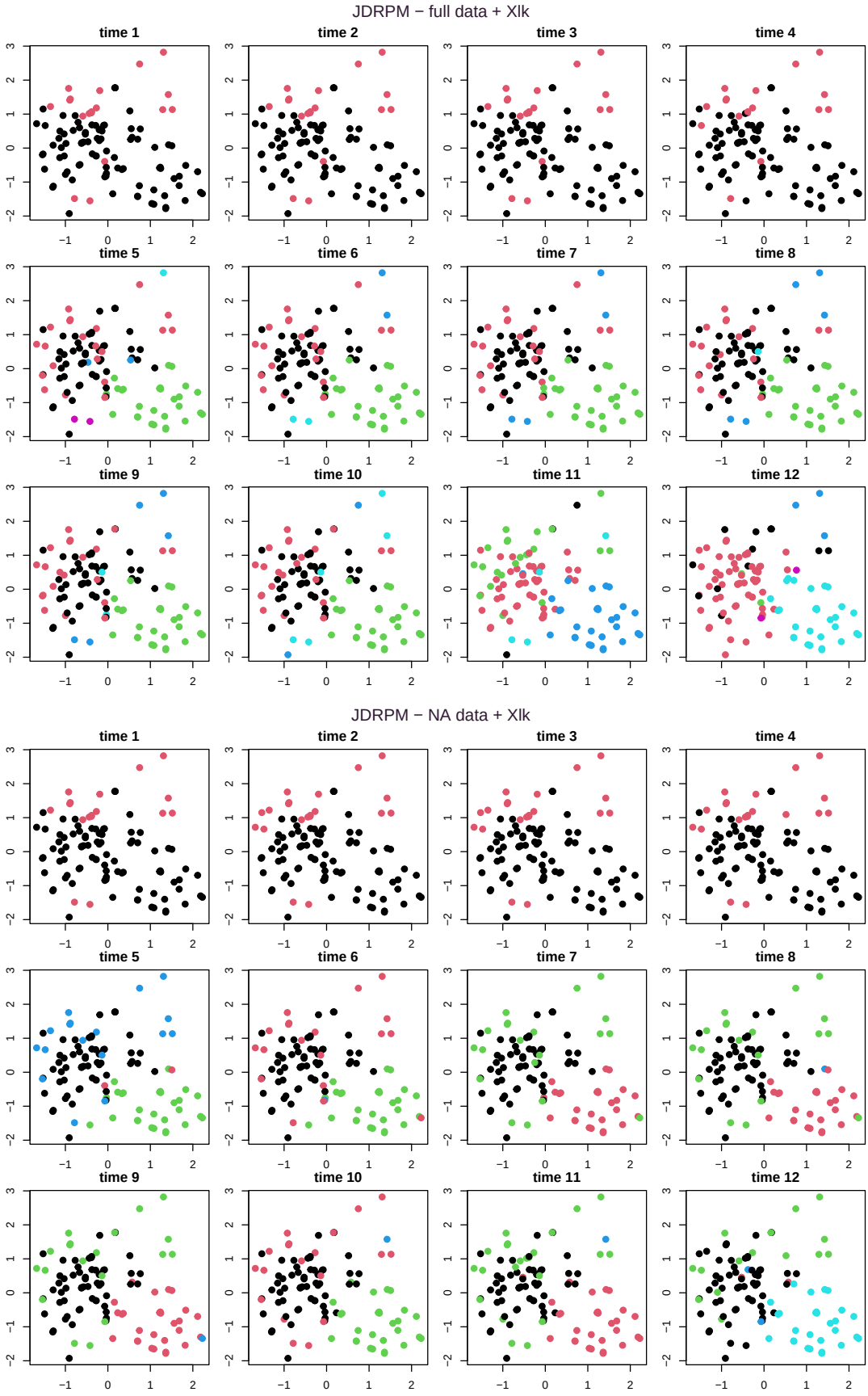

Figure 3.19: Clusters generated by the two JDRPM fits, with target plus space values, on the full and NA datasets, with covariates in the likelihood.

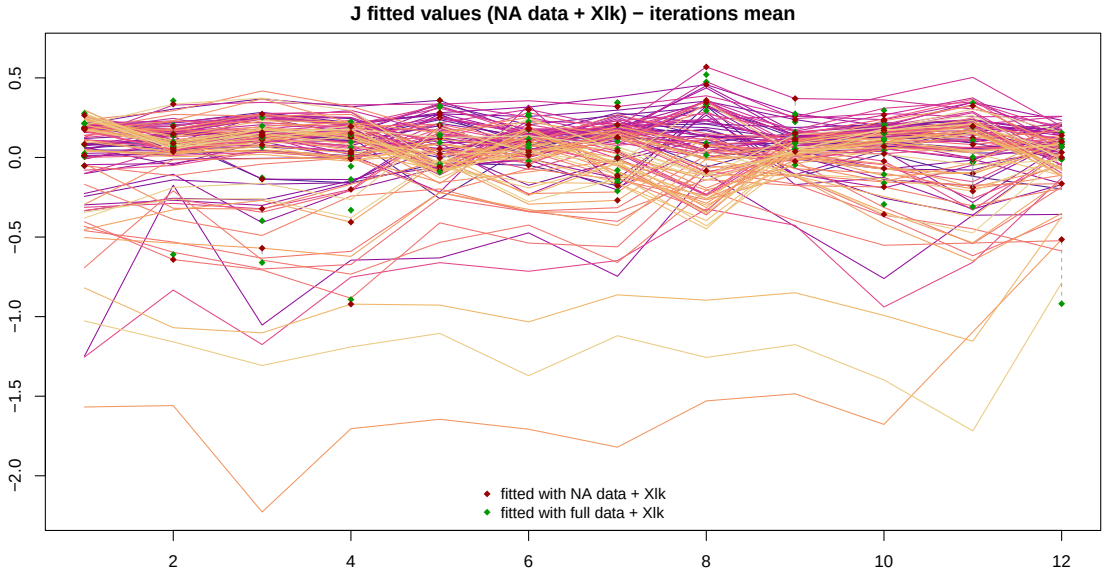

Figure 3.20: Target and fitted values of the JDRPM fits with target plus space values, on the NA and full dataset, to see the effects of the insertion of covariates in the likelihood.

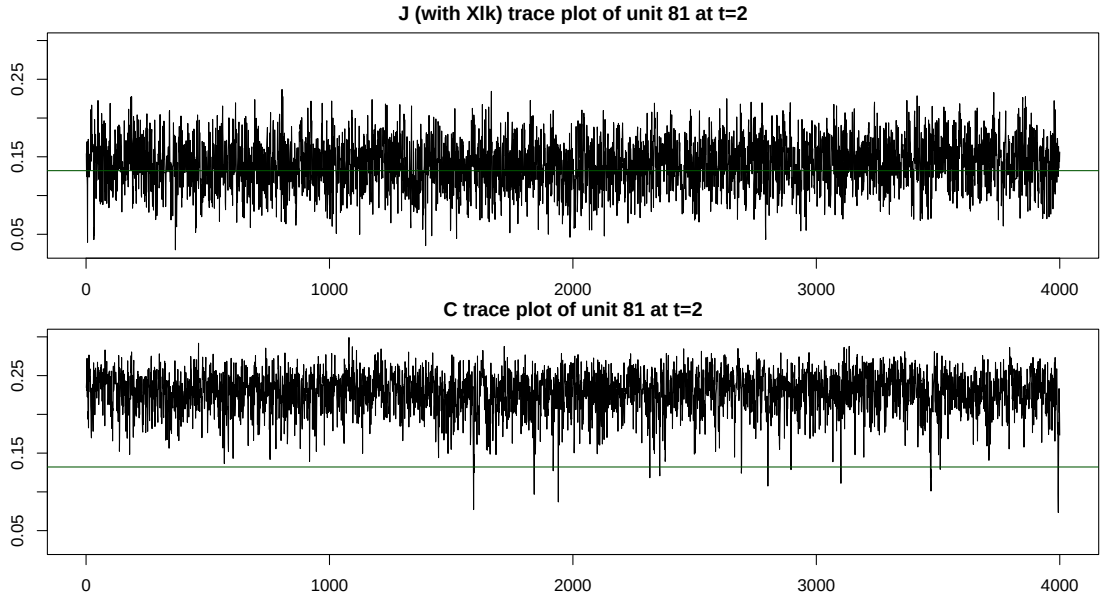

Figure 3.21: Example of a trace plot of the fitted values, on a problematic unit i and time instant t, comparing the JDRPM fit with covariates in the likelihood to the base (target plus space) CDRPM fit. The green line represents the true value of Y_{it}.

and time instant, with problematic in the sense that both the standard JDRPM and CDRPM fits didn't manage to provide precise estimates, which now became more accurate. In the end, this analysis denotes how the addition of this regression parameter $\boldsymbol{\beta}_t$ could be beneficial to recover more accuracy in the results, and also help the clustering process since the regressor contribution manifests when using variables computed from the target values inside the update steps of the parameters.

3.3.2 Covariates in the prior

Now we consider the more theoretically effective and impactful inclusion of covariates in the prior for $(\rho_1, \dots, \rho_T)$. For the choice of which covariates to include, we reasoned about which where the aspects that could affect more the PM_{10} concentrations, and we ended up selecting the following three covariates:

- `WE_wind_speed_10m_max`. Wind speed plays a significant role in the concentration levels of air pollutants. Its effect is of dual: wind can disperse the pollutants away from their source, spreading them to different areas and thus locally reducing the levels, but it can also have an opposite effect, increasing the amount of contaminants in the air by resuspending the particles which were settled down on the earth surface, such as roads, soils, or buildings. This latter effect is particularly visible in dry and windy rural areas, of which Lombardy is a suitable example. The dataset offered also the wind speed at 100m, but this would be relevant for a wider analysis, where e.g. the trend of PM_{10} concentrations are followed over multiple regions or countries. Our setup, as with the time-wise mean adjustment, was instead more focused on local and particular behaviours, on the more the ground-level perspective about Lombardy cities.

- `WE_tot_precipitation`. It is well known how rainwater can improve the air quality thanks to water droplets that attract aerosol particles, taking them away from the air, and bringing them to the ground. This process, known as wet deposition, precipitation, scavenging, or washout is indeed very effective in reducing the concentrations of air pollutants.

- `WE_blh_layer_max`. The boundary layer height (BLH) is another relevant variable in terms of the dispersion of air contaminants. This layer defines the height at which air mixing occurs. Usually air gets colder when rising in the atmosphere; however, there could be some warm air regions on top of colder ones. At this boundary, air is not more able to mix, with the warm layer causing a sort of lid, a covering, which traps the lower cold air, with all the contaminants, below it. This reduces the quality of the air since the pollution builds up and accumulates since it has no way to disperse. This covariate, therefore, records the maximum height at which this problematic layer occurs: the lower the values, the higher we should expect the pollutants concentrations to be.

To perform this terminal fit with also covariates in the clustering we used the same parameters setup of the previous fits, meaning the same prior coefficients and MCMC configuration. For the covariates we employed similarity g_4, the one with the Normal/Normal-Inverse-Gamma model, where we set $\mu_0 = 0$, $\lambda_0 = 1$, $a_0 = 7.5$ and $b_0 = 2$. These choices were motivated both by experimental tunings and by the standardization of the covariates, whose trend, as effectively illustrated by Figure 3.22, rarely moves outside the $[-1, 1]$ interval.

The results are indeed encouraging, as we can see from Table 3.6 where all metrics appeared to have improved in this ultimate fit. Even with the inclusion of

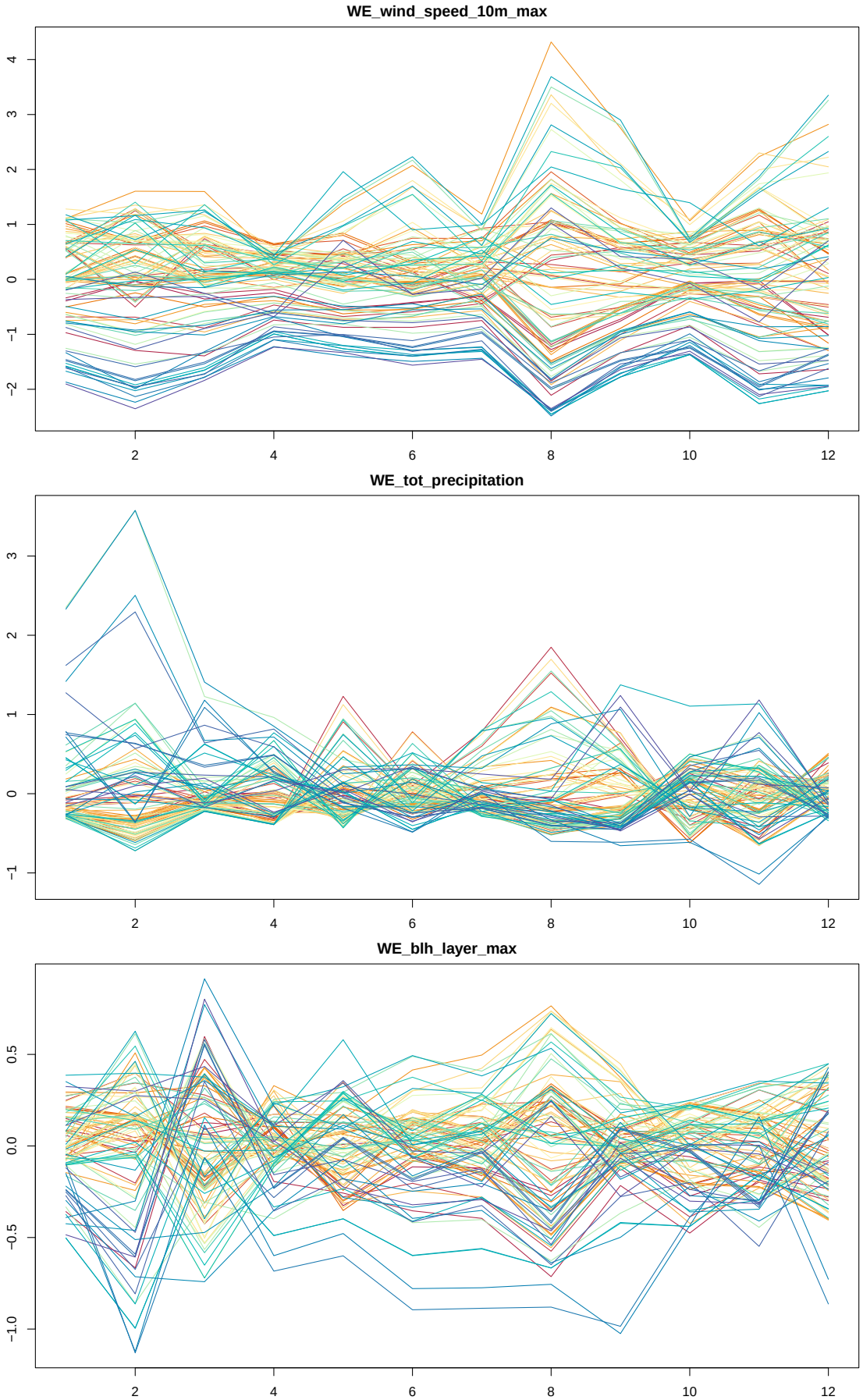

Figure 3.22: The three variables used to perform the test fit with covariates in the clustering. Colors are based on the ranking of PM_{10} values of the units according to their median, from highest (red) to lowest (blue).

Table 3.6: Summary of the comparison between the two fits, on target plus space values, plus also the JDRPM fits including covariates in the clustering process. The MSE columns refer to the accuracy between the fitted values generated by the models (estimated by taking the mean and the median of the returned 4000 iterates) and the true values of the target variable. Higher LPML and lower WAIC indicate a better fit.

	MSE mean	MSE median	LPML	WAIC	exec. time
CDRPM	0.0142	0.0149	694.81	-1768.42	1h38m
JDRPM	0.0131	0.0138	624.91	-1898.05	**48m**
JDRPM + Xcl	**0.0126**	**0.0135**	**677.71**	**-1969.76**	1h20m

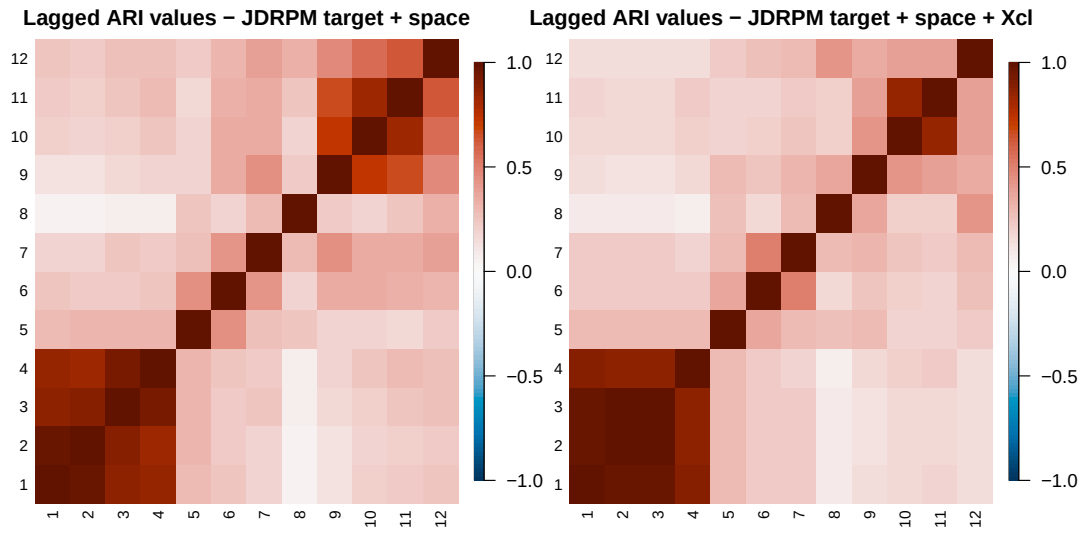

Figure 3.23: Comparison of the lagged ARI values of the JDRPM fits with covariates in the clustering and the standard fit on target plus space values.

multiple covariates, i.e. with the risk of their "clustering suggestions" to differ, their contribution can still be appreciated by complementing the partition representation to cluster-specific boxplots of the relevant variables, i.e. the target PM_{10} plus and three included covariates, in this case. Such a comparison is presented in Figure 3.24, where we can see how the JDRPM fit with also covariates seemed to have captured a slightly better clustering structure than the two competitors.

Regarding the highest polluted clusters, CDRPM did not manage to characterize better the stations in the right side of the map, while correctly identifying, as the other models did, the big cluster on the right side mostly spanning on Mantova and Brescia areas. The middle-level polluted cluster, which encloses the mountain area was also accurately recovered, similarly to what the JDRPM plus covariates fit did. This cluster seems in fact to be characterized by the lowest level of `WE_wind_speed_10m_max`. In contrast, the corresponding covariate boxplot in the JDRPM standard fit seems to be more oriented towards higher values. This improvement of a a more reasonable cluster could have been ascribed to the contribute of covariates into the clustering.

Regarding the lowest polluted cluster, CDRPM decided to separate it into a

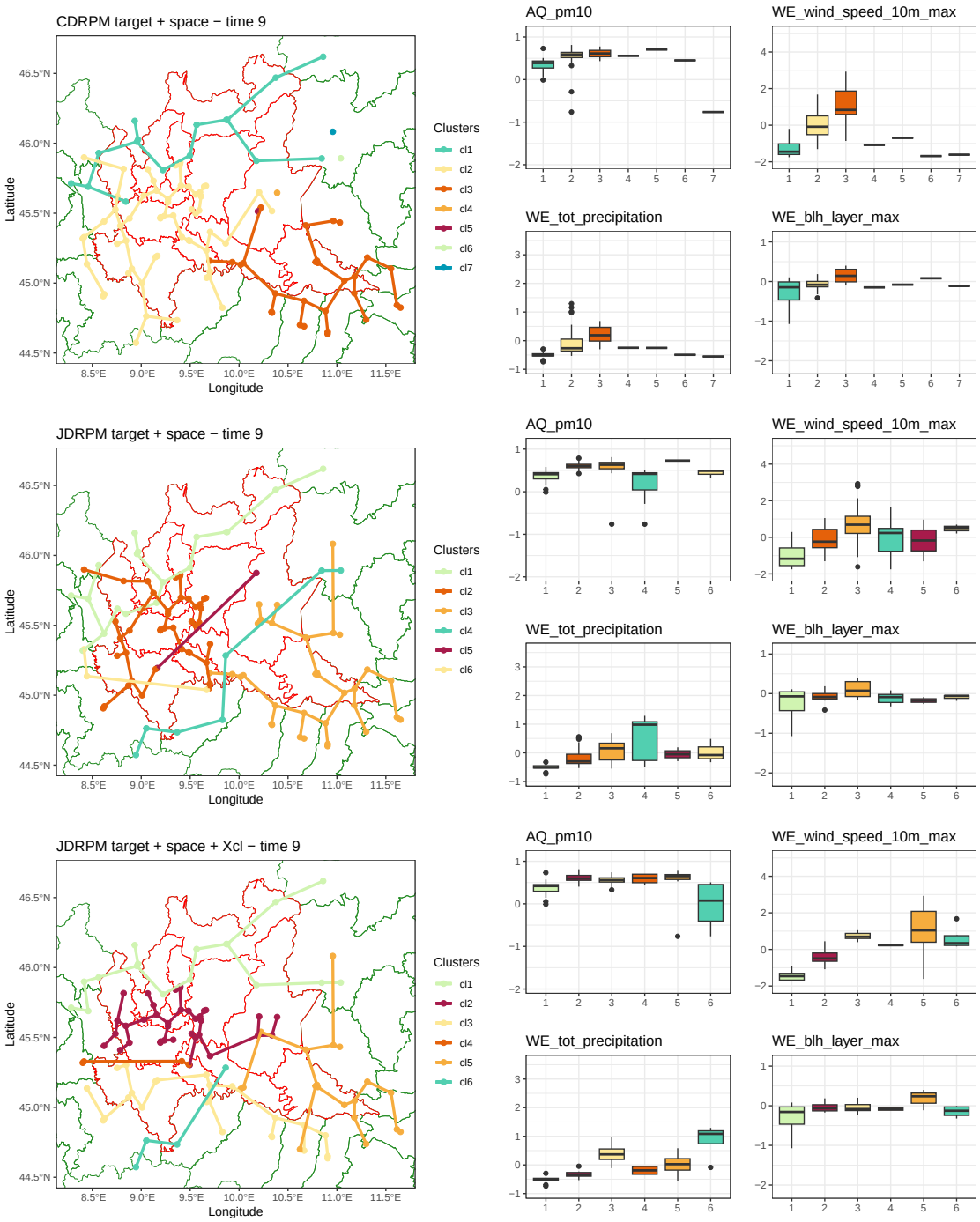

Figure 3.24: Comparison of the clusterings provided by the three main models under our analysis: CDRPM and JDRPM with target plus space values, and JDRPM plus with also covariates included in the clustering.

singleton, while both JDRPM fits decided to keep it into another cluster, therefore causing the appearance of an outlier in the boxplots. As this unit belongs to a mountain region, the inclusion of the `Altitude` covariate could have possibly helped to improve her cluster assignment. Nonetheless, this testing fit seems to provide a confirmation of the potential effectiveness and functionality of the insertion of covariates. The summary representation of the clusters of the JDRPM plus

covariates fit is also available in Figure 3.25, and the temporal trend in Figure 3.23.

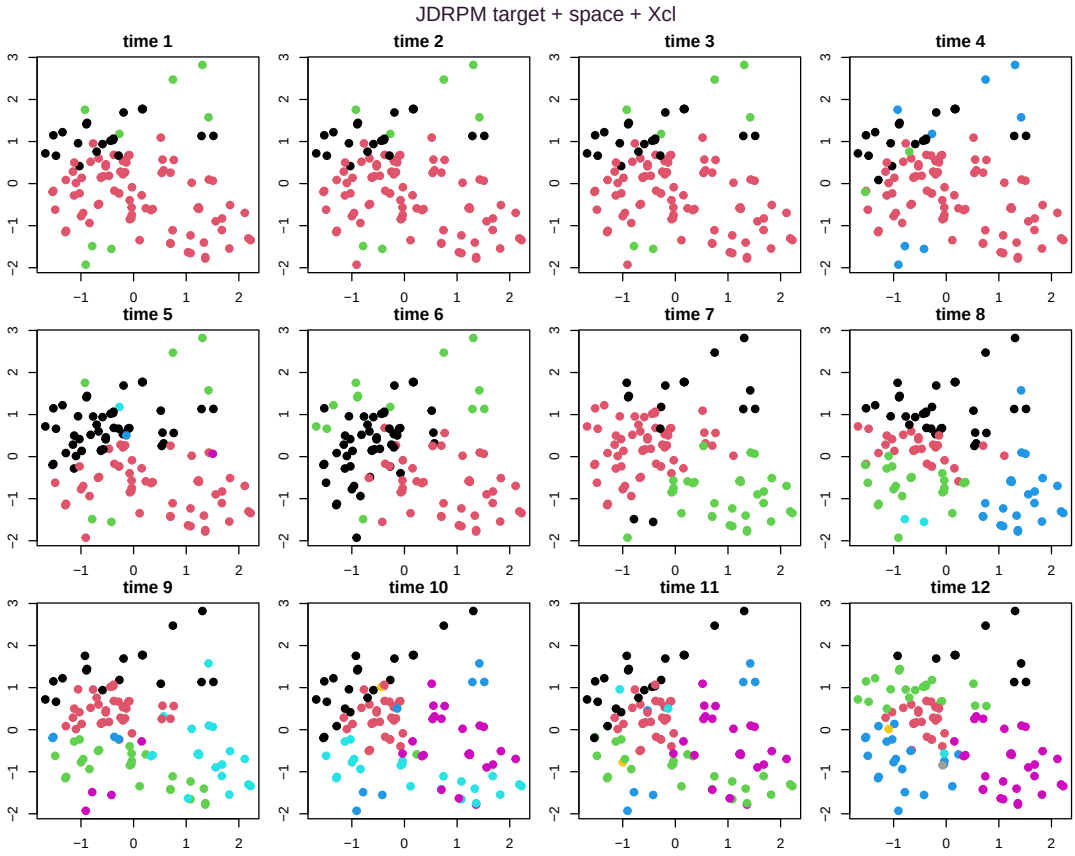

Figure 3.25: Clusters generated by the JDRPM fit, on target plus space values, with covariates in the prior.

The effect of the insertion of covariates is also proved by Figures 3.26 and 3.27, where we compare the distribution of the clusters with respect to one of the covariate, `WE_wind_speed_10m_max` in the case of the proposed figure. All the fits had of course the usual PM_{10} variable as target, meaning that the highest separation should appear there, but we could expect that, with the insertion of covariates, a clustering pattern should also emerge slightly in the auxiliary covariates included. Indeed, the distribution of the clusters in the JDRPM fit with covariates shows a sharper division with respect to the wind speed variable; a division that appears more fuzzy in the CDRPM fit. The effects of the covariates contributions can be seen more clearly at time instants 8, 9, and 12. Also with respect to the JDRPM without covariates of Figure 3.28 we can see a minor improvement, which could have been probably more significant in the case of datasets without an already-quite clear division in the target variable, since in any case the standard fits of target plus space values were already quite good, in terms of fitting metrics and clusters interpretation.

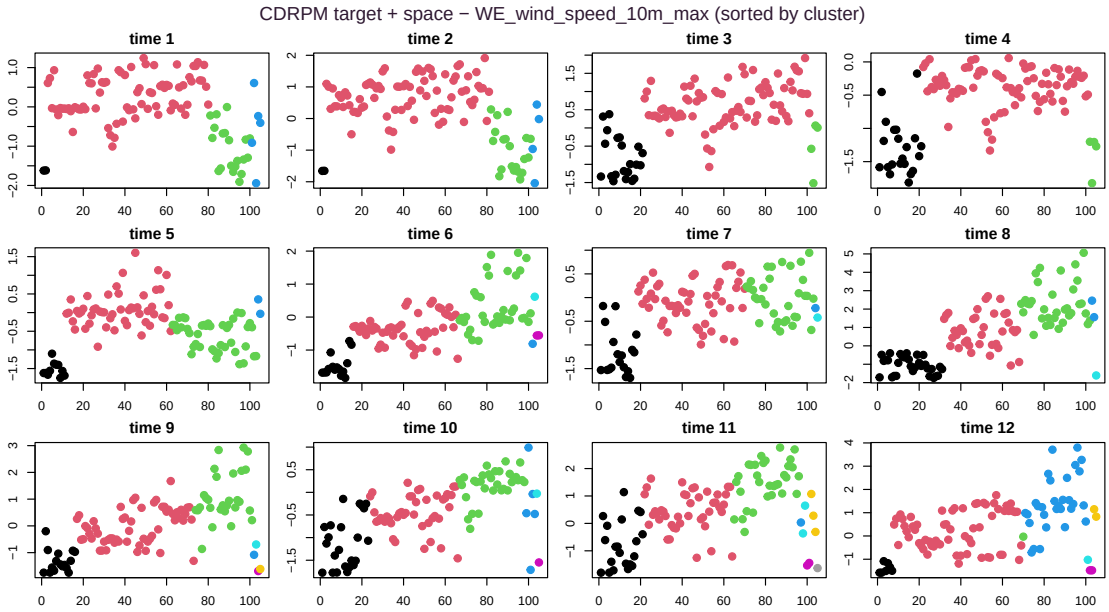

Figure 3.26: Distribution of the clusters according to the JDRPM standard fit, with respect to the wind speed covariate. The indication "sorted by clusters" indicates that the order of the units in the plot is based on their cluster membership and not on their original numbering $1, \ldots, n$.

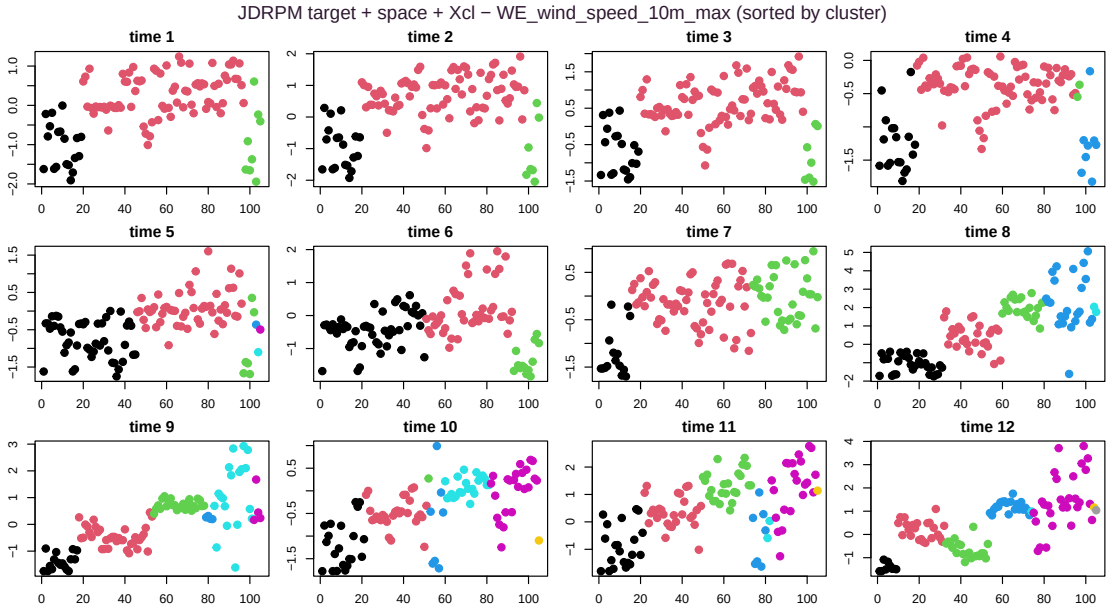

Figure 3.27: Distribution of the clusters according to the JDRPM fit with covariates, with respect to the wind speed covariate. The effects of the covariates contributions can be seen more clearly at time instants 8, 9, and 12.

3.3.3 Inference on a new location

We now conduct a final test which condensates all the improvements added to the original DRPM formulation. To do so, we suppose to study a spatio-temporal dataset in which a new unit, for which we do not have the corresponding target variable measures, is introduced in a new location. Equivalently, this can be seen as removing all the data from a unit already existing in the dataset. In this sort of

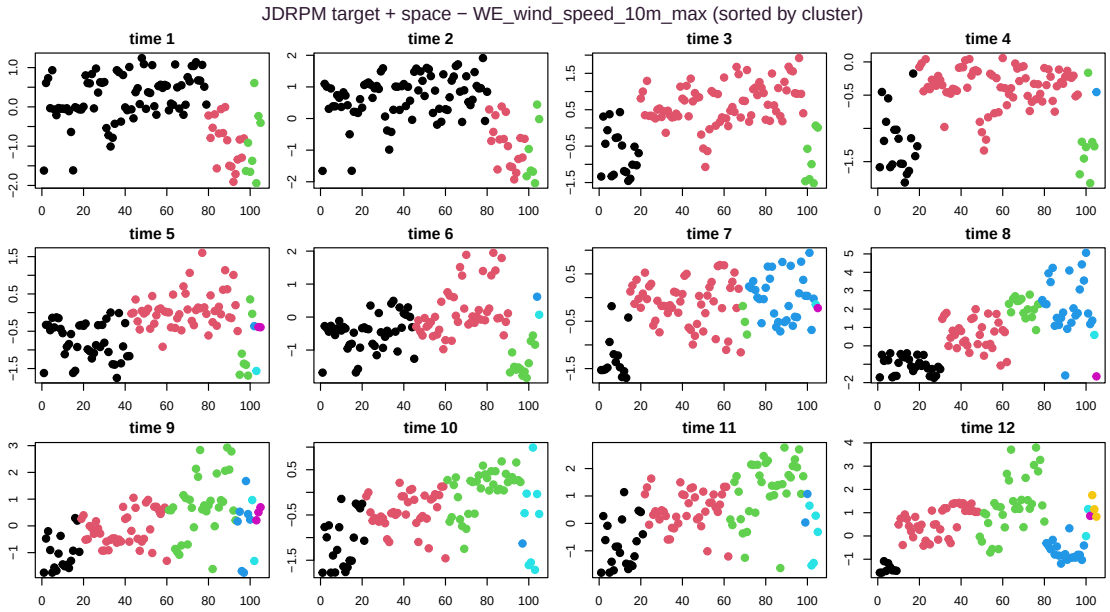

Figure 3.28: Distribution of the clusters according to the JDRPM standard fit, with respect to the wind speed covariate.

kriging (Krige, 1951) context, we want to see how the model is accurate in predicting the behaviour a unit in which a sensor could be absent. We can expect that the estimation will get better with the increasing complexity of the model. Therefore, we will set all the data entries of three randomly selected units to NA, and we will fit JDRPM models in the standard case with just the spatial information, and then with also including covariates. Regarding the covariates, for the likelihood we used the same set of six covariates which was useed in Section 3.3.1, and for the prior the same set of three covariates used in Section 3.3.2.

Table 3.7 shows how indeed the addition of covariates enhanced the estimate of the missing units. The MSEs were computed taking the mean and the median of the fitted values in each model, and comparing them to the true values of the missing units. The best performance seemed to be reached in the fit which includes covariates only in the likelihood.

According to (F. A. Quintana et al., 2015), this only considers the linear effect to the covariate, due to the simple regressor term $\boldsymbol{\beta}_t$. Including covariates only in the prior, instead, accounts for all effects of the covariates when generating the clusters estimates. Therefore this second choice tends to produce an higher number of clusters, while not necessarily improving the fitted estimates. A balance in the number of clusters can be reached by combining the effects of covariates, employng them in both likelihood and prior levels, to accounts for their linear effects through the regressor and for nonlinear effects in the clustering.

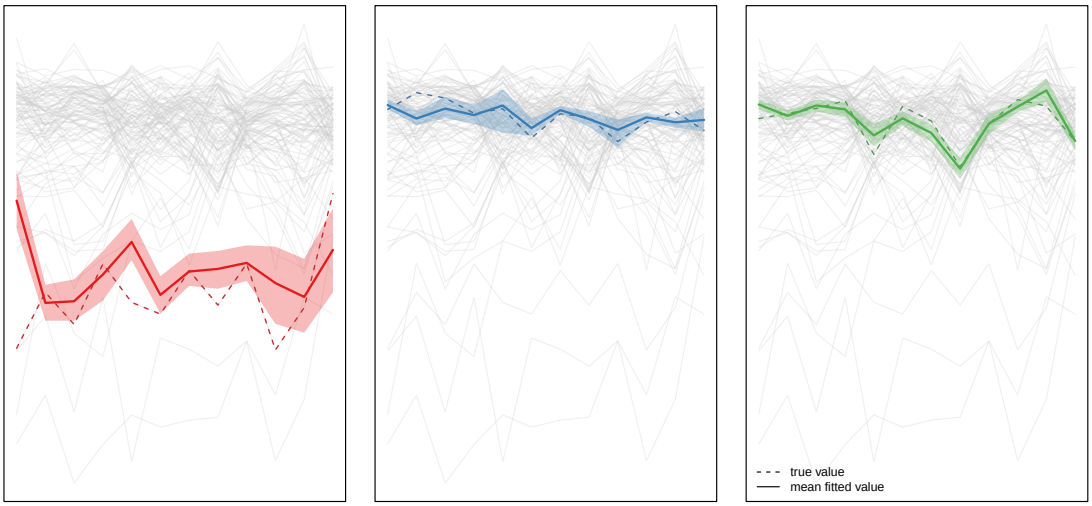

Figure 3.29: Kriging performances of JDRPM, space information

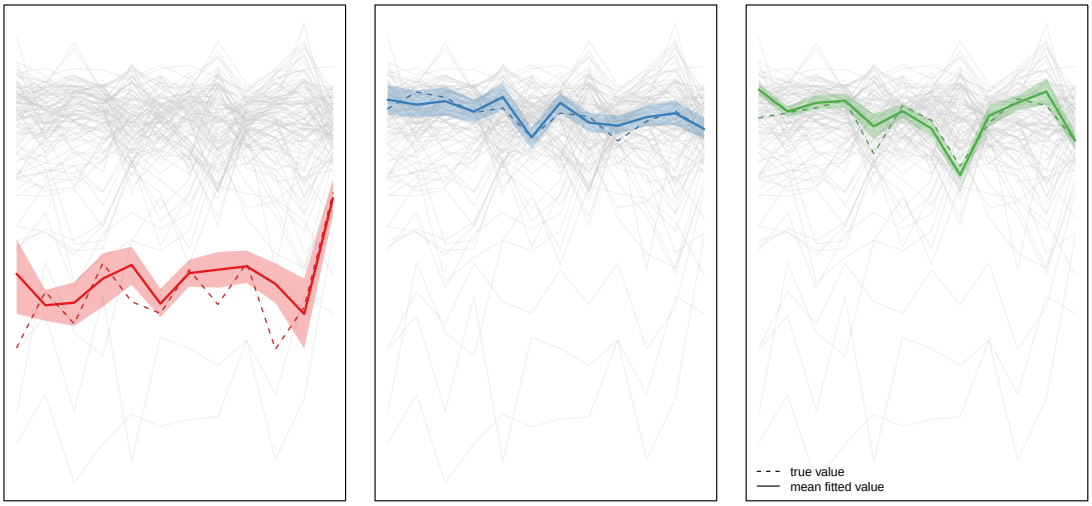

Figure 3.30: Kriging performances of JDRPM, space information plus covariates in the likelihood

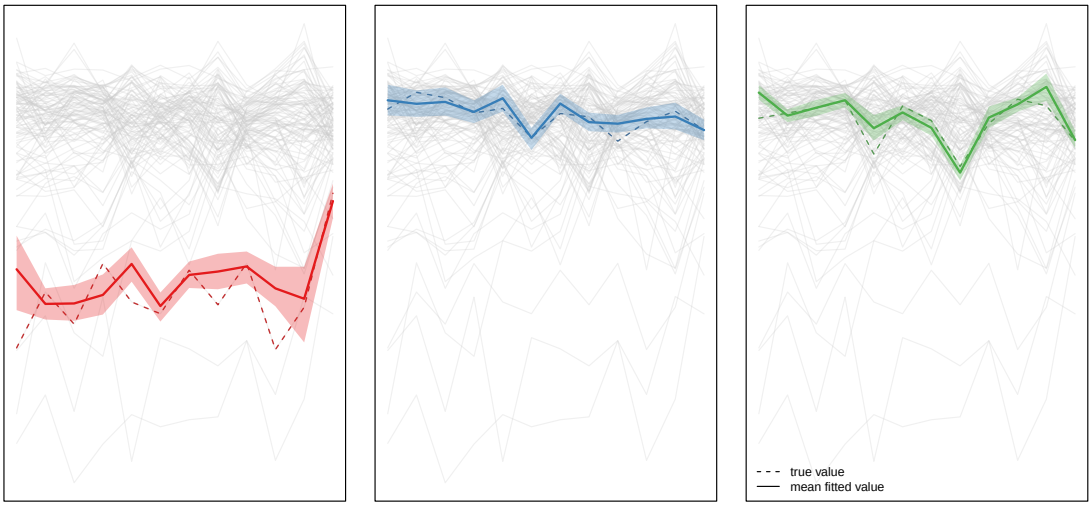

Figure 3.31: Kriging performances of JDRPM, space information plus covariates in the likelihood and in the prior

Table 3.7: Comparison of JDRPM fits in the kriging scenario.

		space	space + Xlk	space + Xlk + Xcl
unit92	MSE mean	0.112452	0.042037	0.044957
	MSE median	0.111573	0.041676	0.045216
unit61	MSE mean	0.004117	0.002449	0.002527
	MSE median	0.004711	0.002547	0.002534
unit44	MSE mean	0.003919	0.006368	0.005945
	MSE median	0.003997	0.006419	0.005950
	execution time	45m	40m	1h15m
	LPML	620.98	758.11	791.86
	WAIC	-1842.48	-2041.95	-1976.73

3.4 Scaling performances

To precisely evaluate whether the objective of faster execution times was accomplished, we established a series of experiments to compare the two models across the various levels of information which they can provide. The original CDRPM allowed clustering based solely on target values or by also incorporating spatial information. The JDRPM introduced the additional option of including covariates at the likelihood and/or prior levels. We recall that, aside from the target values, all other information levels are independent: for instance, one could perform the fit including covariates but disregarding spatial information. However, with an additive perspective in mind, we opted to conduct incremental experiments by progressively append new information on top of the previous ones. Consequently, we will compare fits performed with only the target values, followed by fits that include also the spatial information, followed by fits that incorporate also covariates in the prior, to conclude with fits that incorporate all these elements along with covariates in the likelihood.

As it appeared from Section 2, the Julia implementation seemed to be a little more eager for memory than the C one. This meant that when we ran the larger tests my system could have ran out of RAM memory, resulting in some data needing to be stored in the slower swap space on the disk, and therefore losing performance. However, on newer or just more technical-oriented machines than my simple laptop, this memory limitation should not be an issue.

Accounting all this, in what follows we should consider really accurate just the intermediate-values tests, i.e. the ones with n or T being 10, 50 or 100, and take with a pinch of salt the extreme one of 250, for which my laptop hardware limitations could have concealed the true accurate results. Nonetheless, the analysis is really encouraging for the JDRPM model.

The tests were conducted on randomly generated values, according to n and T, for the target data Y_{it} and the spatial coordinates $\boldsymbol{s}_i$. In this way, we produced a sort of "mesh" of possible fitting parameters, ranging from small number of units and time horizons to larger ones. To record the expected execution time per iteration

of each case we ran each fit with a number of iterations inversely proportional to the size of the test, e.g. 10000 iterations for the case $(n, T) = (10, 10)$ and 16 iterations for $(n, T) = (250, 250)$. This ensured that each fit lasted approximately the same time. Each fit was ran four times, to then save the minimum time observed during those multiple runs. Such practice, common in benchmarking, helps to eliminate bias from the results due to the system computational demands and fluctuations, filtering in this way just the "ideal" execution time in which all the system performance are devoted to that task.

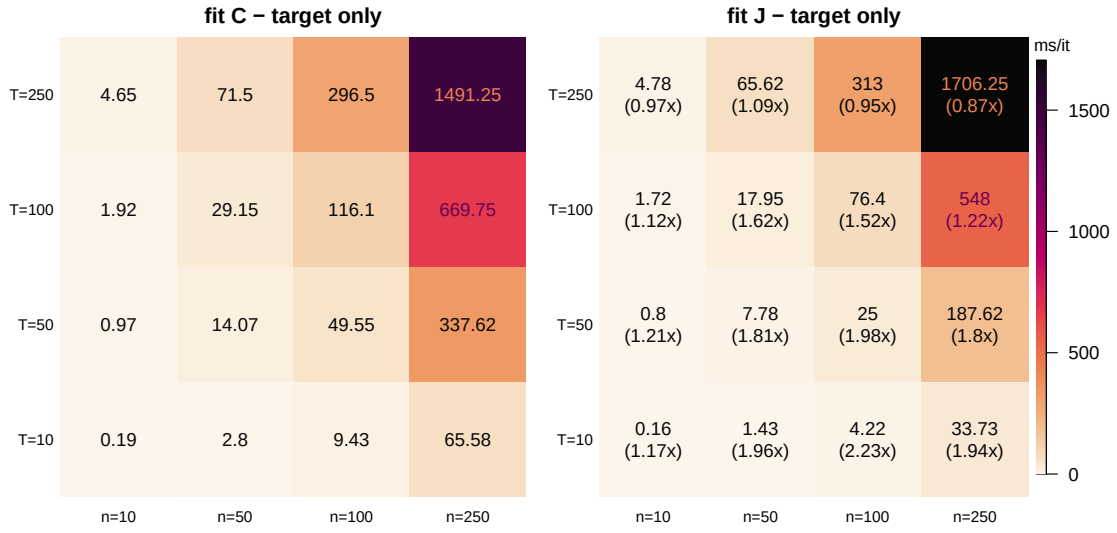

Figure 3.32: Execution times, measured in milliseconds per iteration, when fitting CDRPM and JDRPM using only the target variable. In the JDRPM plot (right), in brackets, are reported the speedups relative to the CDRPM timings (left), where higher values indicate better performance.

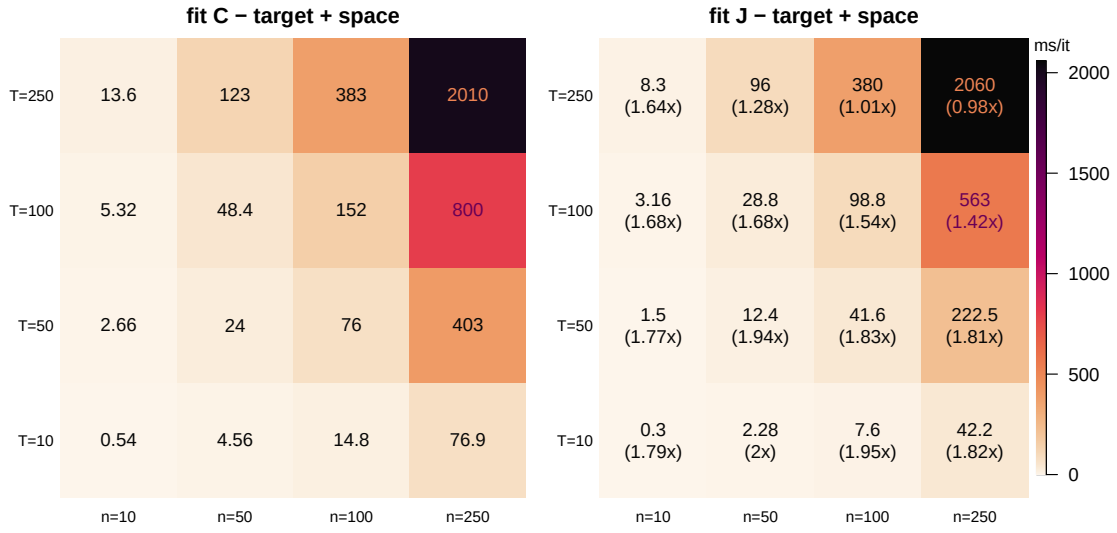

Figure 3.33: Execution times, measured in milliseconds per iteration, when fitting CDRPM and JDRPM using spatial information. In the JDRPM plot (right), in brackets, are reported the speedups relative to the CDRPM timings (left), where higher values indicate better performance.

From Figure 3.32 we can see how the basic fit, with just the target values, perform very quickly in Julia, with peaks even around a 2x speedup. Similar improvements appeared in the case of fits including also the spatial information, as Figure 3.33 shows. Therefore, especially looking at the more reliable non-extreme tests, we can confidently claim that the JDRPM implementation is faster than the CDRPM one.

Regarding fits with covariates, we also generated them randomly by creating matrices of dimensions $n \times p \times T$. For these tests, we avoided to treat different values of p: the previous figures summarizing the fits up to spatial information were in fact projection of 3d information (n, T, and execution time), while if we extended the mesh to also account for p, the number of covariates, we would have ended up with 4d information, or even 5d if we considered separately clustering and likelihood covariates. Therefore, to keep things tidy and understandable, we just fixed $p = 5$ for both cases.

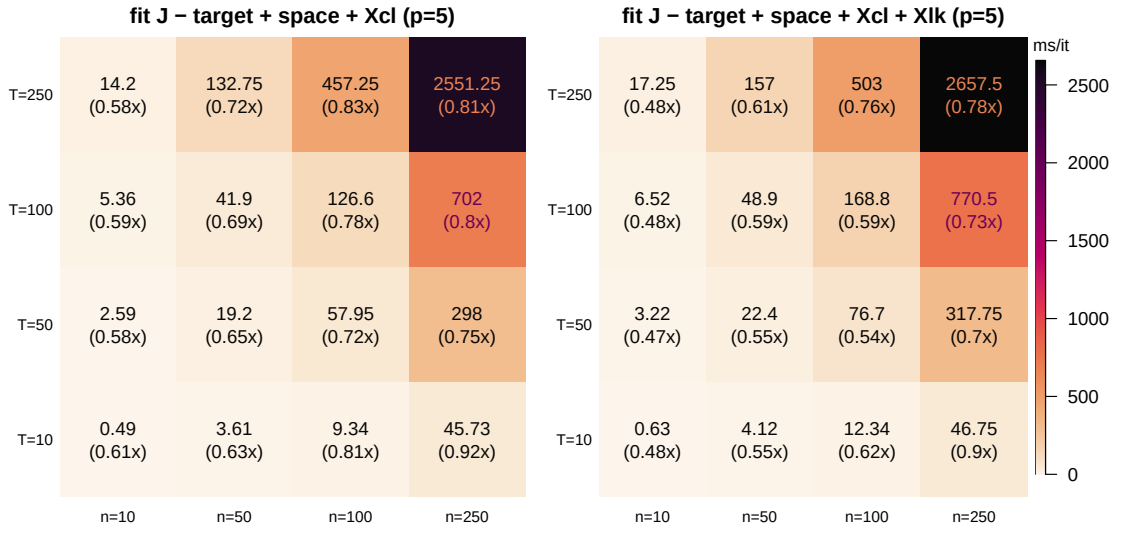

Figure 3.34: Execution times, measured in milliseconds per iteration, when fitting JDRPM using spatial information, covariates in the prior (left), and covariates in both the prior and the likelihood (right). In brackets are reported the speedups relative to the JDRPM timings of the fits with spatial information, with higher values still indicating better performance.

Figure 3.34 shows how fits including covariates saw a drop of performance, which was inevitable due to the additional work to perform, but they still remain at a good performance level. Indeed, Figure 3.36 will point out how some of the fits with all information levels in Julia were actually faster than the basic fits in C; which is quite surprising given the additional complexity and computations introduced by the covariates.

From the encouraging results of Figure 3.36, we also investigated at which model complexity the JDRPM implementation would tie the execution times proposed by CDRPM. To do so, we selected a possibly regular-sized dataset, of $n = 50$ and $T = 50$, and we took as reference the execution time per iteration exhibited by the CDPRM fit in the case of target plus space values. Figure 3.33 retrieves this value to be 24 ms/it. Then, we evaluated the performance of JDRPM fits including

covariates, at likelihood and/or clustering levels, letting now p be varying, to see at which degree of complexity the new implementation match the original one. Figure 3.35 summarizes the result of this analysis. It appears that until we include $p_{\text{cl}} = 5$ covariates in the clustering, we can expect the JDRPM implementation to be faster than the simple spatially-informed fit on CDRPM. This means that in the same time in which the CDRPM performed a spatially-informed fit, JDRPM can perform the same fit plus up to five covariates in the clustering and a possibly indifferent number of covariates in the likelihood, since the increase of p_{lk} did not highlight any significance drop in the performances.

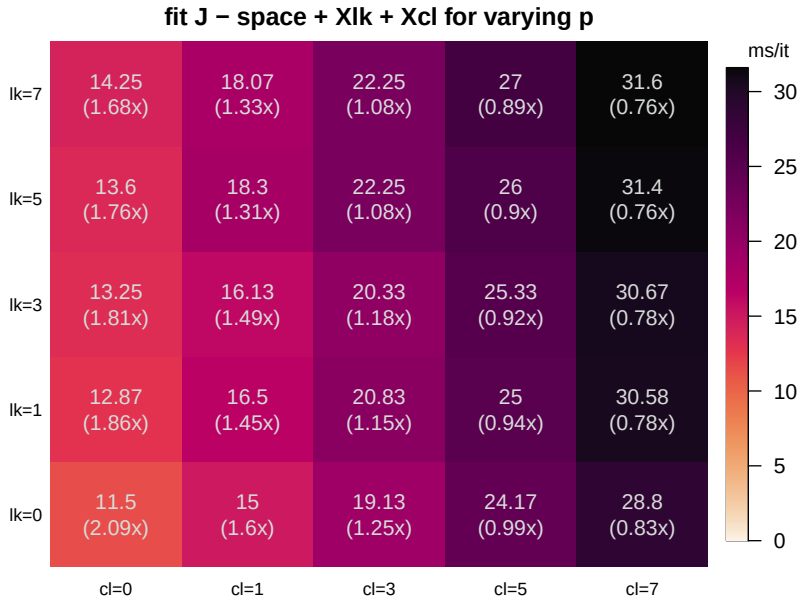

Figure 3.35: Execution times, measured in milliseconds per iteration, when fitting the JDRPM model using target plus space values, plus covariates in the likelihood (symbol lk in the y axis) and/or covariates in the clustering (symbol cl in the x axis). In brackets are reported the speedups relative to the CDRPM timings of the fitting with target and space, with higher values indicating better performance.

As in the previous tests of this section, this analysis was performed trying to devote all the computational resources to the fitting task; therefore the results should be accurate. As a further proof, the comparison performed in Section 3.3.2 and summarized in Table 3.6 showed a fit with JDRPM plus three covariates in the clustering to take 1h20m. Corresponding to this case ($p_{\text{lk}} = 0$, $p_{\text{cl}} = 3$)), Figure 3.35 suggests a speedup factor of 1.25x; and indeed this would imply an expected time of 1h40m in the CDRPM fit, which is practically matching the measured one of 1h38m.

Also in the noisier environment in which the real-application fits of Section 3.1.2 were performed, where we did not try, as instead we did in this dedicated section, to devote all the hardware resources to the models fitting, a considerable speedup was observed. In that case, in which the dataset consisted of $n = 105$ units and $T = 12$ time instants, the CDRPM fit with target plus space values took 1 hour and 38 minutes, while both the JDRPM fits, with equivalent setup and

with covariates in the clustering, exhibited faster execution times. Remarkably, the equivalent JDRPM fit more than halved the execution time; while the fit including covariates showed the expected speedup reported by Figure 3.36, if we look at the closest corresponding case of $n = 100$ and $T = 10$. This is definitely a further proof of the effectiveness of the new implementation.

Finally, from Figures 3.34, we can notice how with larger fits the performance drop reduces to roughly around 0.8x, rather than the 0.6x of the small cases. This indicates that on fits with heavy n and T the bottleneck is no more the algorithm complexity, meaning the choice of which information levels to include in the clusters generation, but rather the available hardware resources. Figure 3.36 also validates this idea by looking at the bottom right plot, in which we can observe a shrinkage in the speedup factors, with all fits that tends to get closer to each other, i.e. manifesting similar execution times, regardless of the information levels included.

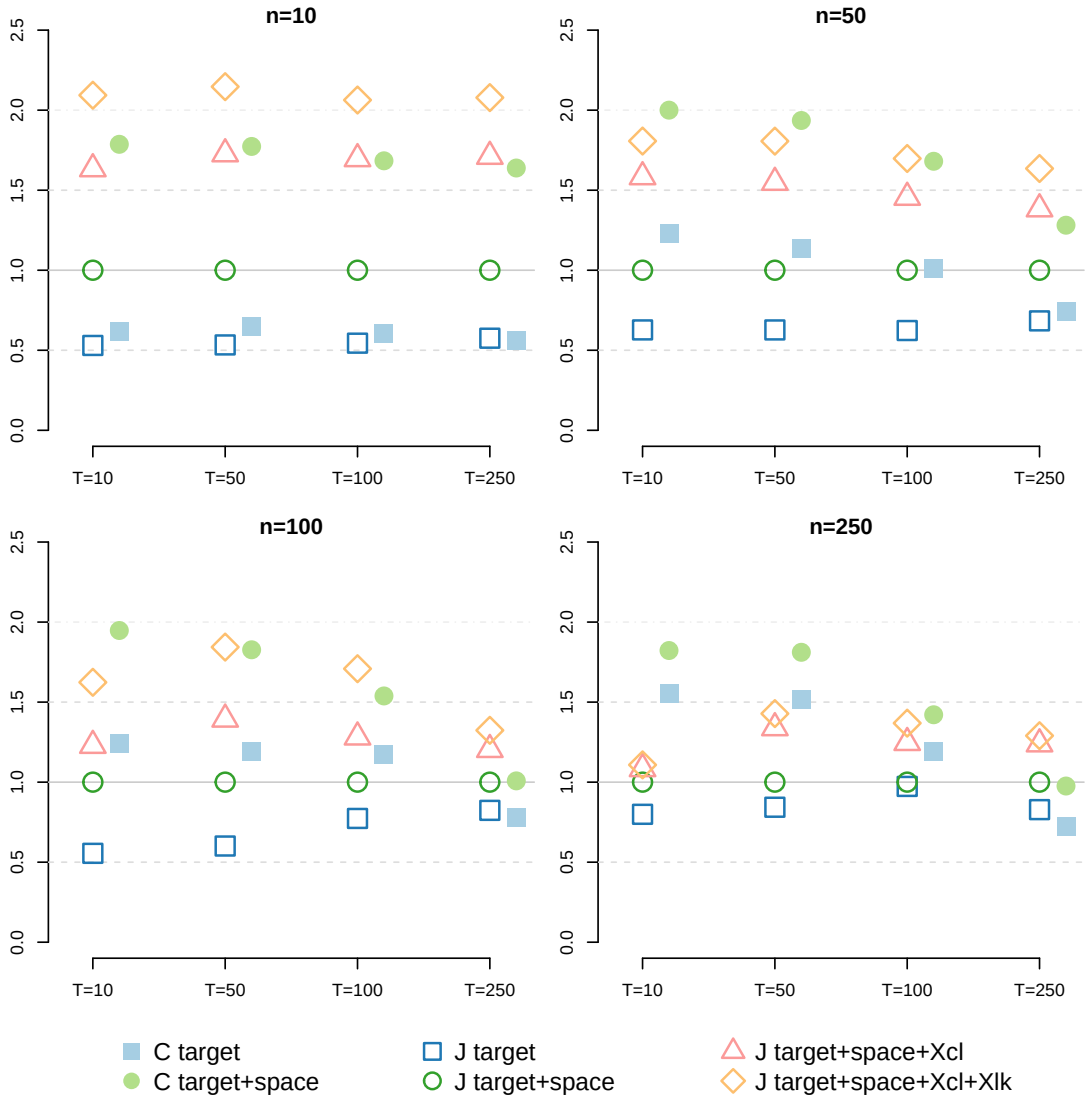

Figure 3.36: Visual representation of the performance of all the fits, for all the n and T cases, relatively to the JDRPM fit using target values and spatial information. Namely, the execution time per iteration metric of that fit has been taken as a reference, to which then all other fits have been compared to derive their speedup (or slowdown) factor. Points above the reference line indicate slower fits, while points below denote faster fits.

Chapter 4

Conclusion

> *And what in human reckoning seems still afar off, may by the Divine ordinance be close at hand, on the eve of its appearance. And so be it, so be it!*
>
> — Fëdor Dostoevskij, *Brothers Karamazov*

In conclusion, the JDRPM represents a significant enhancement over the original CDRPM. From a theoretical perspective, JDRPM retains the foundational structure of its predecessor while introducing the covariates in the prior and likelihood levels. Together with the reduction in the execution times, this is the core upgrade since it should help to yield more accurate and informed results in the partitions. Moreover, the modification on the variances, from a uniform law to an inverse gamma, possibly could enhance the quality of the posterior samples. This choice, in fact, restores conjugacy within the model, thereby improving the mixing properties of the Markov chain during the fitting process.

Despite these improvements, it is important to acknowledge potential drawbacks associated with the increased complexity of the model. The robustness of results may diminish as the intricacies of parameter selection—particularly concerning cohesion and similarity functions—can significantly influence cluster estimates. Striking an appropriate balance between these two sources of information may require empirical testing. In this context, Chapter 1 provides a comprehensive analysis of how tuning parameters for cohesion and similarity impact model performance.

Despite these improvements, it is important to acknowledge potential drawbacks associated with the increased complexity of the model. The robustness of the fits may diminish as the intricacies of parameters selection, particularly concerning the ones regulating cohesion and similarity functions, can significantly influence the cluster estimates. To this end, Chapter 1 provided a comprehensive analysis about how the possible choices on the parameters for cohesions and similarities reflect on their generated values. Moreover, in fits including both space and covariates information, reaching an appropriate balance between these two sources of information may require empirical testing. To address this balance, the Julia function `MCMC_fit` includes an optional argument, `cv_weight`, defaulted to 1, that allows to adjust the influence of covariate similarities.

This complexity is especially evident when defining the prior for the inverse gamma distribution, inherently more delicate than a simpler uniform, of the variance parameters. Other than conducting multiple experiments and studying the trace plots to asses a correct behaviour, a pragmatic approach to address this challenge could be in conducting an initial fit using the original CDRPM to see the expected range in which the variance samples tend to settle, and tune accordingly the inverse gamma parameters. For instance, in the spatio-temporal tests detailed in Section 3.1.2, we observed low variance estimates from the CDRPM fits. Consequently, we assigned an invGamma($a = 1.9, b = 0.4$) for λ^2 and τ_t^2, which has 90% of his density in the interval $[0.109151, 1.58222]$. For the more critical parameter $\sigma_{jt}^{2\star}$ we adopted a less informative prior invGamma($a = 0.01, b = 0.01$) which, despite being not always recommended (Gelman, 2004), proved to be effective and precise relative to sampled reference values from CDRPM. An alternative strategy, albeit less theoretically appealing, could involve truncating the inverse gamma distributions to mitigate the risk of sampling excessively high values when uninformative priors are inadequately adjusted by data. This adjustment can be seamlessly integrated into the Julia code by modifying `rand(InverseGamma(a,b))` to `rand(truncated(InverseGamma(a,b),l,u))`, where l and u define truncation bounds.

From a computational perspective, we successfully reduced execution times by up to 50% compared to the original implementation. Although this occurred with a slight increase in memory requirements, it is a trade-off that is surely manageable with the modern computing resources.

Looking ahead, there remains a wide opportunity for further enhancements, particularly in the usability front given the actual complexity of the model. While the current JDRPM implementation features basic logging capabilities, that allow for stepwise computation tracking, there is potential for more sophisticated profiling and monitoring tools that leverage Julia's flexibility. Possible suggestions could include heuristics about the initialization of the hyperparameters, based on the specific datasets at hand, or visualization tools, using Julia's robust plotting ecosystem, to provide real-time monitoring of the sampled parameters distributions and trace plots directly during execution. Moreover, implementing parallel processing with multiple chains, which is a common in technique implemented in many less heavy Bayesian models, could further enhance performance. Exploring GPU integration through packages within the `JuliaGPU` collection may also yield significant computational efficiencies.

In conclusion, while the JDRPM's complexity may present certain challenges, it also lays the groundwork for significant methodological advancements and practical enhancements. These developments are expected to enhance the model's applicability and ease of use, for more effective research outcomes.

Appendix A

Theoretical details

A.1 Extended computations of the full conditionals

We propose here the extended computations which allowed to extract the full conditionals presented in Chapter 1. We report also the model graph to make it quickly accessible as a reference for the laws involved in the following computations.

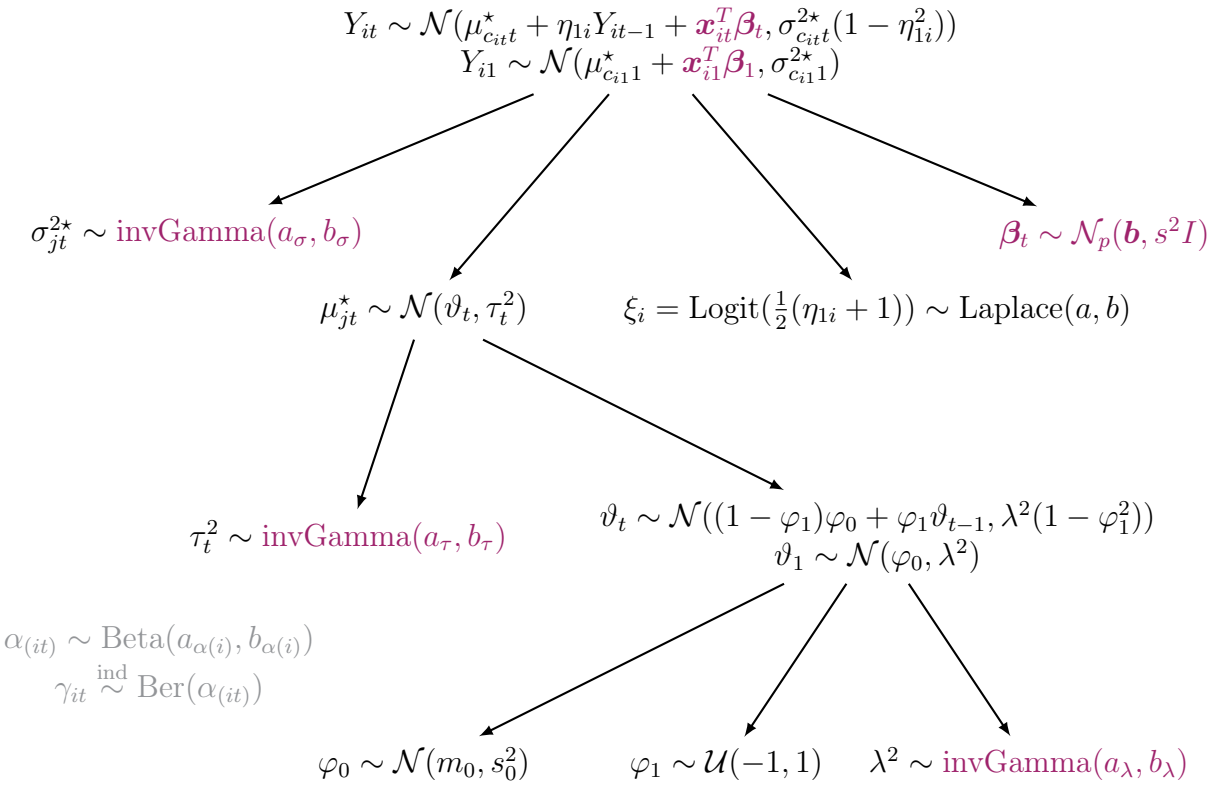

- update $\sigma^{2\star}_{jt}$

  for $t = 1$:
  $f(\sigma^{2\star}_{jt}|-) \propto f(\sigma^{2\star}_{jt}) f(\{Y_{it} : c_{it} = j\}|\sigma^{2\star}_{jt}, -)$

$$
\begin{aligned}
&= \mathcal{L}_{\text{invGamma}(a_\sigma,b_\sigma)}(\sigma^{2\star}_{jt}) \prod_{i\in S_{jt}} \mathcal{L}_{\mathcal{N}(\mu^\star_{c_{it}t}+\boldsymbol{x}_{it}^T\boldsymbol{\beta}_t,\sigma^{2\star}_{c_{it}1})}(Y_{it}) \\
&\propto \left[\left(\frac{1}{\sigma^{2\star}_{jt}}\right)^{a_\sigma+1} \exp\left\{-\frac{1}{\sigma^{2\star}_{jt}}b\right\}\right] \\
&\cdot \left[\prod_{i\in S_{jt}} \left(\frac{1}{\sigma^{2\star}_{jt}}\right)^{1/2} \exp\left\{-\frac{1}{2\sigma^{2\star}_{jt}}(Y_{it}-\mu^\star_{jt}-\boldsymbol{x}_{it}^T\boldsymbol{\beta}_t)^2\right\}\right] \\
&\propto \left(\frac{1}{\sigma^{2\star}_{jt}}\right)^{(a_\sigma+|S_{jt}|/2)+1} \exp\left\{-\frac{1}{\sigma^{2\star}_{jt}}\left(b_\sigma+\frac{1}{2}\sum_{i\in S_{jt}}(Y_{it}-\mu^\star_{jt}-\boldsymbol{x}_{it}^T\boldsymbol{\beta}_t)^2\right)\right\}
\end{aligned}
$$

$$
\begin{aligned}
\implies f(\sigma^{2\star}_{jt}|-) &\propto \text{kernel of a invGamma}(a_{\sigma(\text{post})}, b_{\sigma(\text{post})}) \text{ with} \\
a_{\tau(\text{post})} &= a_\sigma + \frac{|S_{jt}|}{2} \\
b_{\tau(\text{post})} &= b_\sigma + \frac{1}{2}\sum_{i\in S_{jt}}(Y_{it}-\mu^\star_{jt}-\boldsymbol{x}_{it}^T\boldsymbol{\beta}_t)^2
\end{aligned} \tag{A.1}
$$

for $t > 1$:

$$
\begin{aligned}
f(\sigma^{2\star}_{jt}|-) &\propto f(\sigma^{2\star}_{jt}) f(\{Y_{it} : c_{it} = j\}|\sigma^{2\star}_{jt}, -) \\
&= \mathcal{L}_{\text{invGamma}(a_\sigma,b_\sigma)}(\sigma^{2\star}_{jt}) \prod_{i\in S_{jt}} \mathcal{L}_{\mathcal{N}(\mu^\star_{c_{it}t}+\eta_{1i}Y_{it-1}+\boldsymbol{x}_{it}^T\boldsymbol{\beta}_t,\sigma^{2\star}_{c_{it}1})}(Y_{it}) \\
&\propto \left[\left(\frac{1}{\sigma^{2\star}_{jt}}\right)^{a_\sigma+1} \exp\left\{-\frac{1}{\sigma^{2\star}_{jt}}b\right\}\right] \\
&\cdot \left[\prod_{i\in S_{jt}} \left(\frac{1}{\sigma^{2\star}_{jt}}\right)^{1/2} \exp\left\{-\frac{1}{2\sigma^{2\star}_{jt}}(Y_{it}-\mu^\star_{jt}-\eta_{1i}Y_{it-1}-\boldsymbol{x}_{it}^T\boldsymbol{\beta}_t)^2\right\}\right] \\
&\propto \left(\frac{1}{\sigma^{2\star}_{jt}}\right)^{(a_\sigma+|S_{jt}|/2)+1} \\
&\cdot \exp\left\{-\frac{1}{\sigma^{2\star}_{jt}}\left(b_\sigma+\frac{1}{2}\sum_{i\in S_{jt}}(Y_{it}-\eta_{1i}Y_{it-1}-\mu^\star_{jt}-\boldsymbol{x}_{it}^T\boldsymbol{\beta}_t)^2\right)\right\}
\end{aligned}
$$

$$
\begin{aligned}
\implies f(\sigma^{2\star}_{jt}|-) &\propto \text{kernel of a invGamma}(a_{\sigma(\text{post})}, b_{\sigma(\text{post})}) \text{ with} \\
a_{\tau(\text{post})} &= a_\sigma + \frac{|S_{jt}|}{2} \\
b_{\tau(\text{post})} &= b_\sigma + \frac{1}{2}\sum_{i\in S_{jt}}(Y_{it}-\mu^\star_{jt}-\eta_{1i}Y_{it-1}-\boldsymbol{x}_{it}^T\boldsymbol{\beta}_t)^2
\end{aligned} \tag{A.2}
$$

- update $\mu^\star_{jt}$

  for $t = 1$:

  $f(\mu^\star_{jt}|-) \propto f(\mu^\star_{jt}) f(\{Y_{it} : c_{it} = j\}|\mu^\star_{jt}, -)$

$$
\begin{aligned}
&= \mathcal{L}_{\mathcal{N}(\vartheta_t,\tau_t^2)}(\mu_{jt}^\star) \prod_{i\in S_{jt}} \mathcal{L}_{\mathcal{N}(\mu^\star_{c_{it}t}+\boldsymbol{x}_{it}^T\boldsymbol{\beta}_t,\sigma^{2\star}_{c_{it}1})}(Y_{it}) \\
&\propto \exp\left\{-\frac{1}{2\tau_t^2}(\mu_{jt}^\star-\vartheta_t)^2\right\} \exp\left\{-\frac{1}{2\sigma_{jt}^{2\star}}\left(\sum_{i\in S_{jt}}(\mu_{jt}^\star-(Y_{i1}-\boldsymbol{x}_{it}^T\boldsymbol{\beta}_t))^2\right)\right\} \\
&\propto \exp\left\{-\frac{1}{2\tau_t^2}(\mu_{jt}^\star-\vartheta_t)^2\right\} \exp\left\{-\frac{|S_{jt}|}{2\sigma_{jt}^{2\star}}\left(\mu_{jt}^\star-\frac{\mathrm{SUM}_y}{|S_{jt}|}\right)^2\right\} \\
&\text{where } \mathrm{SUM}_y = \sum_{i\in S_{jt}} Y_{i1}-\boldsymbol{x}_{it}^T\boldsymbol{\beta}_t
\end{aligned}
$$

$$
\begin{aligned}
&\implies f(\mu_{jt}^\star|-) \propto \text{kernel of a } \mathcal{N}(\mu_{\mu^\star_{jt}(\text{post})}, \sigma^2_{\mu^\star_{jt}(\text{post})}) \text{ with} \\
&\sigma^2_{\mu^\star_{jt}(\text{post})} = \frac{1}{\frac{1}{\tau_t^2}+\frac{|S_{jt}|}{\sigma_{jt}^{2\star}}} \\
&\mu_{\mu^\star_{jt}(\text{post})} = \sigma^2_{\mu^\star_{jt}(\text{post})}\left(\frac{\vartheta_t}{\tau_t^2}+\frac{\mathrm{SUM}_y}{\sigma_{jt}^{2\star}}\right)
\end{aligned} \tag{A.3}
$$

for $t>1$:

$$
\begin{aligned}
f(\mu_{jt}^\star|-) &\propto f(\mu_{jt}^\star) f(\{Y_{it}: c_{it}=j\}|\mu_{jt}^\star,-) \\
&= \mathcal{L}_{\mathcal{N}(\vartheta_1,\tau_t^2)}(\mu_{jt}^\star) \prod_{i\in S_{jt}} \mathcal{L}_{\mathcal{N}(\mu^\star_{c_{it}t}+\eta_{1i}Y_{it-1}+\boldsymbol{x}_{it}^T\boldsymbol{\beta}_t,\sigma^{2\star}_{c_{it}1})}(Y_{it}) \\
&\propto \exp\left\{-\frac{1}{2\tau_t^2}(\mu_{jt}^\star-\vartheta_t)^2\right\} \\
&\cdot \exp\left\{-\frac{1}{2\sigma_{jt}^{2\star}}\left(\sum_{i\in S_{jt}}\frac{1}{1-\eta_{1i}^2}\left(\mu_{jt}^\star-(Y_{it}-\eta_{1i}Y_{i,t-1}-\boldsymbol{x}_{it}^T\boldsymbol{\beta}_t)\right)^2\right)\right\} \\
&\propto \exp\left\{-\frac{1}{2\tau_t^2}(\mu_{jt}^\star-\vartheta_t)^2\right\} \exp\left\{-\frac{\mathrm{SUM}_{e2}}{2\sigma_{jt}^{2\star}}\left(\mu_{jt}^\star-\frac{\mathrm{SUM}_y}{\mathrm{SUM}_{e2}}\right)^2\right\} \\
&\text{where } \mathrm{SUM}_y = \sum_{i\in S_{jt}}\frac{Y_{it}-\eta_{1i}Y_{i,t-1}-\boldsymbol{x}_{it}^T\boldsymbol{\beta}_t}{1-\eta_{1i}^2},\ \mathrm{SUM}_{e2} = \sum_{i\in S_{jt}}\frac{1}{1-\eta_{1i}^2}
\end{aligned}
$$

$$
\begin{aligned}
&\implies f(\mu_{jt}^\star|-) \propto \text{kernel of a } \mathcal{N}(\mu_{\mu^\star_{jt}(\text{post})}, \sigma^2_{\mu^\star_{jt}(\text{post})}) \text{ with} \\
&\sigma^2_{\mu^\star_{jt}(\text{post})} = \frac{1}{\frac{1}{\tau_t^2}+\frac{\mathrm{SUM}_{e2}}{\sigma_{jt}^{2\star}}} \\
&\mu_{\mu^\star_{jt}(\text{post})} = \sigma^2_{\mu^\star_{jt}(\text{post})}\left(\frac{\vartheta_t}{\tau_t^2}+\frac{\mathrm{SUM}_y}{\sigma_{jt}^{2\star}}\right)
\end{aligned} \tag{A.4}
$$

- update $\boldsymbol{\beta}_t$

for $t=1$:

$$
\begin{aligned}
f(\boldsymbol{\beta}_t|-) &\propto f(\boldsymbol{\beta}_t) f(\{Y_{1t},\ldots,Y_{nt}\}|\boldsymbol{\beta}_t,-) \\
&= \mathcal{L}_{\mathcal{N}(\boldsymbol{b},s^2I)}(\boldsymbol{\beta}_t) \prod_{i=1}^{n} \mathcal{L}_{\mathcal{N}(\mu^\star_{c_{it}t}+\boldsymbol{x}_{it}^T\boldsymbol{\beta}_t,\sigma^{2\star}_{c_{it}t})}(Y_{it})
\end{aligned}
$$

$$
\begin{aligned}
&\propto \exp\left\{-\frac{1}{2}\left[(\boldsymbol{\beta}_t^T-\boldsymbol{b})^T\frac{1}{s^2}(\boldsymbol{\beta}_t-\boldsymbol{b})\right]\right\}\\
&\cdot \exp\left\{-\frac{1}{2}\sum_{i=1}^{n}(Y_{it}-\mu^{\star}_{c_{it}t}-\boldsymbol{x}_{it}^T\boldsymbol{\beta}_t)^2\right\}\\
&\propto \exp\left\{-\frac{1}{2}\left[\boldsymbol{\beta}_t^T\left(\frac{1}{s^2}I+\sum_{i=1}^{n}\frac{\boldsymbol{x}_{it}\boldsymbol{x}_{it}^T}{\sigma^{2\star}_{c_{it}t}}\right)\boldsymbol{\beta}_t\right.\right.\\
&\left.\left.-\ 2\left(\frac{\boldsymbol{b}}{s^2}+\sum_{i=1}^{n}\frac{(Y_{it}-\mu^{\star}_{c_{it}t})\boldsymbol{x}_{it}}{\sigma^{2\star}_{c_{it}t}}\right)\cdot\boldsymbol{\beta}_t\right]\right\}\\
\implies\ & f(\boldsymbol{\beta}_t|-)\propto \text{kernel of a } \mathcal{N}(\boldsymbol{b}_{(\text{post})},A_{(\text{post})}) \text{ with}\\
&A_{(\text{post})}=\left(\frac{1}{s^2}I+\sum_{i=1}^{n}\frac{\boldsymbol{x}_{it}\boldsymbol{x}_{it}^T}{\sigma^{2\star}_{c_{it}t}}\right)^{-1}\\
&\boldsymbol{b}_{(\text{post})}=A_{(\text{post})}\left(\frac{\boldsymbol{b}}{s^2}+\sum_{i=1}^{n}\frac{(Y_{it}-\mu^{\star}_{c_{it}t})\boldsymbol{x}_{it}}{\sigma^{2\star}_{c_{it}t}}\right)\\
\iff\ & f(\boldsymbol{\beta}_t|-)\propto \text{kernel of a } \mathcal{N}\text{Canon}(\boldsymbol{h}_{(\text{post})},J_{(\text{post})}) \text{ with}\\
&\boldsymbol{h}_{(\text{post})}=\left(\frac{\boldsymbol{b}}{s^2}+\sum_{i=1}^{n}\frac{(Y_{it}-\mu^{\star}_{c_{it}t})\boldsymbol{x}_{it}}{\sigma^{2\star}_{c_{it}t}}\right)\\
&J_{(\text{post})}=\left(\frac{1}{s^2}I+\sum_{i=1}^{n}\frac{\boldsymbol{x}_{it}\boldsymbol{x}_{it}^T}{\sigma^{2\star}_{c_{it}t}}\right)
\end{aligned}
\tag{A.5}
$$

for $t>1$:

$$
\begin{aligned}
f(\boldsymbol{\beta}_t|-)&\propto f(\boldsymbol{\beta}_t)f(\{Y_{1t},\dots,Y_{nt}\}|\boldsymbol{\beta}_t,-)\\
&=\mathcal{L}_{\mathcal{N}(\boldsymbol{b},s^2I)}(\boldsymbol{\beta}_t)\prod_{i=1}^{n}\mathcal{L}_{\mathcal{N}(\mu^{\star}_{c_{it}t}+\eta_{1i}Y_{it-1}+\boldsymbol{x}_{it}^T\boldsymbol{\beta}_t,\sigma^{2\star}_{c_{it}t})}(Y_{it})\\
&\propto \exp\left\{-\frac{1}{2}\left[(\boldsymbol{\beta}_t^T-\boldsymbol{b})^T\frac{1}{s^2}(\boldsymbol{\beta}_t-\boldsymbol{b})\right]\right\}\\
&\cdot \exp\left\{-\frac{1}{2}\sum_{i=1}^{n}(Y_{it}-\mu^{\star}_{c_{it}t}-\eta_{1i}Y_{it-1}-\boldsymbol{x}_{it}^T\boldsymbol{\beta}_t)^2\right\}\\
&\propto \exp\left\{-\frac{1}{2}\left[\boldsymbol{\beta}_t^T\left(\frac{1}{s^2}I+\sum_{i=1}^{n}\frac{\boldsymbol{x}_{it}\boldsymbol{x}_{it}^T}{\sigma^{2\star}_{c_{it}t}}\right)\boldsymbol{\beta}_t\right.\right.\\
&\left.\left.-2\left(\frac{\boldsymbol{b}}{s^2}+\sum_{i=1}^{n}\frac{(Y_{it}-\mu^{\star}_{c_{it}t}-\eta_{1i}Y_{it-1})\boldsymbol{x}_{it}}{\sigma^{2\star}_{c_{it}t}}\right)\cdot\boldsymbol{\beta}_t\right]\right\}\\
\implies\ & f(\boldsymbol{\beta}_t|-)\propto \text{kernel of a } \mathcal{N}(\boldsymbol{b}_{(\text{post})},A_{(\text{post})}) \text{ with}\\
&A_{(\text{post})}=\left(\frac{1}{s^2}I+\sum_{i=1}^{n}\frac{\boldsymbol{x}_{it}\boldsymbol{x}_{it}^T}{\sigma^{2\star}_{c_{it}t}}\right)^{-1}\\
&\boldsymbol{b}_{(\text{post})}=A_{(\text{post})}\left(\frac{\boldsymbol{b}}{s^2}+\sum_{i=1}^{n}\frac{(Y_{it}-\mu^{\star}_{c_{it}t}-\eta_{1i}Y_{it-1})\boldsymbol{x}_{it}}{\sigma^{2\star}_{c_{it}t}}\right)
\end{aligned}
$$

$$\begin{aligned}
&\iff f(\boldsymbol{\beta}_t|-) \propto \text{kernel of a } \mathcal{N}\text{Canon}(\boldsymbol{h}_{(\text{post})}, J_{(\text{post})}) \text{ with} \\
&\boldsymbol{h}_{(\text{post})} = \left(\frac{\boldsymbol{b}}{s^2} + \sum_{i=1}^{n} \frac{(Y_{it} - \mu^{\star}_{c_{it}t} - \eta_{1i} Y_{it-1})\boldsymbol{x}_{it}}{\sigma^{2\star}_{c_{it}t}} \right) \\
&J_{(\text{post})} = \left(\frac{1}{s^2} I + \sum_{i=1}^{n} \frac{\boldsymbol{x}_{it}\boldsymbol{x}_{it}^T}{\sigma^{2\star}_{c_{it}t}} \right)
\end{aligned} \tag{A.6}$$

- update τ_t^2

$$\begin{aligned}
f(\tau_t^2|-) &\propto f(\tau_t^2) f((\mu^{\star}_{1t}, \ldots, \mu^{\star}_{k_t t})|\tau_t^2, -) \\
&= \mathcal{L}_{\text{invGamma}(a_\tau, b_\tau)}(\tau_t^2) \prod_{j=1}^{k_t} \mathcal{L}_{\mathcal{N}(\vartheta_t, \tau_t^2)}(\mu^{\star}_{jt}) \\
&\propto \left[\left(\frac{1}{\tau_t^2} \right)^{a_\tau + 1} \exp\left\{ -\frac{b_\tau}{\tau_t^2} \right\} \right] \left[\prod_{j=1}^{k_t} \left(\frac{1}{\tau_t^2} \right)^{1/2} \exp\left\{ -\frac{1}{2\tau_t^2} (\mu^{\star}_{jt} - \vartheta_t)^2 \right\} \right] \\
&\propto \left(\frac{1}{\tau_t^2} \right)^{\left(\frac{k_t}{2} + a_\tau\right) + 1} \exp\left\{ -\frac{1}{\tau_t^2} \left(\frac{\sum_{j=1}^{k_t} (\mu^{\star}_{jt} - \vartheta_t)^2}{2} + b_\tau \right) \right\} \\
\implies f(\tau_t^2|-) &\propto \text{kernel of a invGamma}(a_{\tau(\text{post})}, b_{\tau(\text{post})}) \text{ with} \\
a_{\tau(\text{post})} &= \frac{k_t}{2} + a_\tau \\
b_{\tau(\text{post})} &= \frac{\sum_{j=1}^{k_t} (\mu^{\star}_{jt} - \vartheta_t)^2}{2} + b_\tau
\end{aligned} \tag{A.7}$$

- update ϑ_t

for $t = T$:

$$\begin{aligned}
f(\vartheta_t|-) &\propto f(\vartheta_t) f((\mu^{\star}_{1t}, \ldots, \mu^{\star}_{k_t t})|\vartheta_t, -) \\
&= \mathcal{L}_{\mathcal{N}((1-\varphi_1)\varphi_0 + \varphi_1 \vartheta_{t-1}, \lambda^2(1-\varphi_1^2))}(\vartheta_t) \prod_{j=1}^{k_t} \mathcal{L}_{\mathcal{N}(\vartheta_t, \tau_t^2)}(\mu^{\star}_{jt}) \\
&\propto \exp\left\{ -\frac{1}{2(\lambda^2(1-\varphi_1^2))} \Big(\vartheta_t - ((1-\varphi_1)\varphi_0 + \varphi_1 \vartheta_{t-1}) \Big)^2 \right\} \\
&\cdot \exp\left\{ -\frac{k_t}{2\tau_t^2} \left(\vartheta_t - \frac{\sum_{j=1}^{k_t} \mu^{\star}_{jt}}{k_t} \right) \right\} \\
\implies f(\vartheta_t|-) &\propto \text{kernel of a } \mathcal{N}(\mu_{\vartheta_t(\text{post})}, \sigma^2_{\vartheta_t(\text{post})}) \text{ with} \\
\sigma^2_{\vartheta_t(\text{post})} &= \frac{1}{\frac{1}{\lambda^2(1-\varphi_1^2)} + \frac{k_t}{\tau_t^2}} \\
\mu_{\vartheta_t(\text{post})} &= \sigma^2_{\vartheta_t(\text{post})} \left(\frac{\sum_{j=1}^{k_t} \mu^{\star}_{jt}}{\tau_t^2} + \frac{(1-\varphi_1)\varphi_0 + \varphi_1 \vartheta_{t-1}}{\lambda^2(1-\varphi_1^2)} \right)
\end{aligned} \tag{A.8}$$

for $1 < t < T$:

$$
\begin{aligned}
f(\vartheta_t|-) &\propto \underbrace{f(\vartheta_t)f((\mu^\star_{1t},\dots,\mu^\star_{k_t t})|\vartheta_t,-)}_{\text{as in the case } t=T} f(\vartheta_{t+1}|\vartheta_t,-) \\
&= \mathcal{L}_{\mathcal{N}(\mu_{\vartheta_t(\text{post})},\sigma^2_{\vartheta_t(\text{post})})}(\vartheta_t)\mathcal{L}_{\mathcal{N}((1-\varphi_1)\varphi_0+\varphi_1\vartheta_t,\lambda^2(1-\varphi_1^2))}(\vartheta_{t+1}) \\
&\propto \exp\left\{-\frac{1}{2\sigma^2_{\vartheta_t(\text{post})}}\left(\vartheta_t-\mu_{\vartheta_t(\text{post})}\right)^2\right\} \\
&\cdot \exp\left\{-\frac{1}{2\frac{\lambda^2(1-\varphi_1^2)}{\varphi_1^2}}\left(\vartheta_t-\frac{\vartheta_{t+1}-(1-\varphi_1)\varphi_0}{\varphi_1}\right)^2\right\} \\
\implies & f(\vartheta_t|-) \propto \text{kernel of a } \mathcal{N}(\mu_{\vartheta_t(\text{post})},\sigma^2_{\vartheta_t(\text{post})}) \text{ with} \\
\sigma^2_{\vartheta_t(\text{post})} &= \frac{1}{\frac{1+\varphi_1^2}{\lambda^2(1-\varphi_1^2)}+\frac{k_t}{\tau_t^2}} \\
\mu_{\vartheta_t(\text{post})} &= \sigma^2_{\vartheta_t(\text{post})}\left(\frac{\sum_{j=1}^{k_t}\mu^\star_{jt}}{\tau_t^2}+\frac{\varphi_1(\vartheta_{t-1}+\vartheta_{t+1})+\varphi_0(1-\varphi_1)^2}{\lambda^2(1-\varphi_1^2)}\right) \qquad \text{(A.9)}
\end{aligned}
$$

for $t=1$:

$$
\begin{aligned}
f(\vartheta_t|-) &\propto f(\vartheta_t)f(\vartheta_{t+1}|\vartheta_t,-)f(\boldsymbol{\mu}^\star_t|\vartheta_t,-) \\
&= \mathcal{L}_{\mathcal{N}(\varphi_0,\lambda^2)}(\vartheta_t)\mathcal{L}_{\mathcal{N}((1-\varphi_1)\varphi_0+\varphi_1\vartheta_{t-1},\lambda^2(1-\varphi_1^2))}(\vartheta_{t+1})\prod_{j=1}^{k_t}\mathcal{L}_{\mathcal{N}(\vartheta_t,\tau_t^2)}(\mu^\star_{jt}) \\
&\propto \exp\left\{-\frac{1}{2\lambda^2}(\vartheta_t-\varphi_0)^2\right\} \\
&\cdot \exp\left\{-\frac{1}{2\frac{\lambda^2(1-\varphi_1^2)}{\varphi_1^2}}\left(\vartheta_t-\frac{\vartheta_{t+1}-(1-\varphi_1)\varphi_0}{\varphi_1}\right)^2\right\} \\
&\cdot \exp\left\{-\frac{k_t}{2\tau_t^2}\left(\vartheta_t-\frac{\sum_{j=1}^{k_t}\mu^\star_{jt}}{k_t}\right)\right\} \\
\implies & f(\vartheta_t|-) \propto \text{kernel of a } \mathcal{N}(\mu_{\vartheta_t(\text{post})},\sigma^2_{\vartheta_t(\text{post})}) \text{ with} \\
\sigma^2_{\vartheta_t(\text{post})} &= \frac{1}{\frac{1}{\lambda^2}+\frac{\varphi_1^2}{\lambda^2(1-\varphi_1^2)}+\frac{k_t}{\tau_t^2}} \\
\mu_{\vartheta_t(\text{post})} &= \sigma^2_{\vartheta_t(\text{post})}\left(\frac{\varphi_0}{\lambda^2}+\frac{\varphi_1(\vartheta_{t+1}-(1-\varphi_1)\varphi_0)}{\lambda^2(1-\varphi_1^2)}+\frac{\sum_{j=1}^{k_t}\mu^\star_{jt}}{\tau_t^2}\right) \qquad \text{(A.10)}
\end{aligned}
$$

- update φ_0

$$
\begin{aligned}
f(\varphi_0|-) &\propto f(\varphi_0)f((\vartheta_1,\dots,\vartheta_T)|\varphi_0,-) \\
&= \mathcal{L}_{\mathcal{N}(m_0,s_0^2)}(\varphi_0)\mathcal{L}_{\mathcal{N}(\varphi_0,\lambda^2)}(\vartheta_1)\prod_{t=2}^{T}\mathcal{L}_{\mathcal{N}((1-\varphi_1)\varphi_0+\varphi_1\vartheta_{t-1},\lambda^2(1-\varphi_1^2))}(\vartheta_t) \\
&\propto \exp\left\{\left\{-\frac{1}{2s_0^2}(\varphi_0-m_o)^2\right\}\right\}\exp\left\{\left\{-\frac{1}{2\lambda^2}(\varphi_0-\vartheta_1)^2\right\}\right\}
\end{aligned}
$$

$$\cdot \exp\left\{\left\{-\frac{1}{2\frac{\lambda^2(1-\varphi_1^2)}{(T-1)(1-\varphi_1)^2}}\left(\varphi_0 - \frac{(1-\varphi_1)(\text{SUM}_t)}{(T-1)(1-\varphi_1)^2}\right)^2\right\}\right\}$$

$$\text{where } \text{SUM}_t = \sum_{t=2}^{T}(\vartheta_t - \varphi_1\vartheta_{t-1})$$

$$\implies f(\varphi_0|-) \propto \text{kernel of a } \mathcal{N}(\mu_{\varphi_0(\text{post})}, \sigma^2_{\varphi_0(\text{post})}) \text{ with}$$

$$\sigma^2_{\varphi_0(\text{post})} = \frac{1}{\frac{1}{s_0^2} + \frac{1}{\lambda^2} + \frac{(T-1)(1-\varphi_1)^2}{\lambda^2(1-\varphi_1^2)}}$$

$$\mu_{\varphi_0(\text{post})} = \sigma^2_{\varphi_0(\text{post})}\left(\frac{m_0}{s_0^2} + \frac{\vartheta_1}{\lambda^2} + \frac{1-\varphi_1}{\lambda^2(1-\varphi_1^2)}\text{SUM}_t\right) \tag{A.11}$$

- update λ^2

$$\begin{aligned}
f(\lambda^2|-) &\propto f(\lambda^2)f(\vartheta_1,\ldots,\vartheta_T|\lambda^2,-) \\
&= \mathcal{L}_{\text{invGamma}(a_\lambda,b_\lambda)}(\lambda^2)\mathcal{L}_{\mathcal{N}(\varphi_0,\lambda^2)}(\vartheta_1)\prod_{t=2}^{T}\mathcal{L}_{\mathcal{N}((1-\varphi_1)\varphi_0+\varphi_1\vartheta_{t-1},\lambda^2(1-\varphi_1^2))}(\vartheta_t) \\
&\propto \left[\left(\frac{1}{\lambda_t^2}\right)^{a_\lambda+1}\exp\left\{-\frac{b_\lambda}{\lambda^2}\right\}\right]\left[\left(\frac{1}{\lambda^2}\right)^{1/2}\exp\left\{-\frac{1}{2\lambda^2}(\vartheta_1-\varphi_0)^2\right\}\right] \\
&\cdot \left[\prod_{t=2}^{T}\left(\frac{1}{\lambda^2}\right)^{1/2}\exp\left\{-\frac{1}{2\lambda^2}\left(\vartheta_t-(1-\varphi_1)\varphi_0-\varphi_1\vartheta_{t-1}\right)^2\right\}\right] \\
&\propto \left(\frac{1}{\lambda^2}\right)^{\left(\frac{T}{2}+a_\lambda\right)+1} \\
&\cdot \exp\left\{-\frac{1}{\lambda^2}\left(\frac{(\vartheta_1-\varphi_0)^2}{2} + \sum_{t=2}^{T}\frac{\left(\vartheta_t-(1-\varphi_1)\varphi_0-\varphi_1\vartheta_{t-1}\right)^2}{2} + b_\lambda\right)\right\}
\end{aligned}$$

$$\implies f(\lambda^2|-) \propto \text{kernel of a invGamma}(a_{\lambda(\text{post})}, b_{\lambda(\text{post})}) \text{ with}$$

$$a_{\lambda(\text{post})} = \frac{T}{2} + a_\lambda$$

$$b_{\lambda(\text{post})} = \frac{(\vartheta_1-\varphi_0)^2}{2} + \sum_{t=2}^{T}\frac{\left(\vartheta_t-(1-\varphi_1)\varphi_0-\varphi_1\vartheta_{t-1}\right)^2}{2} + b_\lambda \tag{A.12}$$

- update α

if global α: prior is $\alpha \sim \text{Beta}(a_\alpha, b_\alpha)$

$$\begin{aligned}
f(\alpha|-) &\propto f(\alpha)f((\gamma_{11},\ldots,\gamma_{1T},\ldots,\gamma_{n1},\ldots,\gamma_{nT})|\alpha) \\
&\propto \alpha^{a_\alpha-1}(1-\alpha)^{b_\alpha-1}\prod_{i=1}^{n}\prod_{t=1}^{T}\alpha^{\gamma_{it}}(1-\alpha)^{1-\gamma_{it}} \\
&= \alpha^{(a_\alpha+\sum_{i=1}^{n}\sum_{t=1}^{T}\gamma_{it})-1}(1-\alpha)^{(b_\alpha+nT-\sum_{i=1}^{n}\sum_{t=1}^{T}\gamma_{it})-1}
\end{aligned}$$

$$\implies f(\alpha|-) \propto \text{kernel of a Beta}(a_{\alpha(\text{post})}, b_{\alpha(\text{post})}) \text{ with}$$

$$a_{\alpha(\text{post})} = a_\alpha + \sum_{i=1}^{n}\sum_{t=1}^{T}\gamma_{it} \quad b_{\alpha(\text{post})} = b_\alpha + nT - \sum_{i=1}^{n}\sum_{t=1}^{T}\gamma_{it} \tag{A.13}$$

if time specific α: prior is $\alpha_t \sim \text{Beta}(a_\alpha, b_\alpha)$

$$\begin{aligned} f(\alpha_t|-) &\propto f(\alpha_t) f((\gamma_{1t},\dots,\gamma_{nt})|\alpha_t) \\ &\propto \alpha_t^{a_\alpha-1}(1-\alpha_t)^{b_\alpha-1}\prod_{i=1}^{n}\alpha_t^{\gamma_{it}}(1-\alpha_t)^{1-\gamma_{it}} \\ &= \alpha_t^{(a_\alpha+\sum_{i=1}^{n}\gamma_{it})-1}(1-\alpha_t)^{(b_\alpha+n-\sum_{i=1}^{n}\gamma_{it})-1} \\ \implies f(\alpha_t|-) &\propto \text{kernel of a Beta}(a_{\alpha(\text{post})}, b_{\alpha(\text{post})}) \text{ with} \\ a_{\alpha(\text{post})} &= a_\alpha + \sum_{i=1}^{n}\gamma_{it} \quad b_{\alpha(\text{post})} = b_\alpha + n - \sum_{i=1}^{n}\gamma_{it} \end{aligned} \tag{A.14}$$

if unit specific α: prior is $\alpha_i \sim \text{Beta}(a_{\alpha i}, b_{\alpha i})$

$$\begin{aligned} f(\alpha_i|-) &\propto f(\alpha_i) f((\gamma_{i1},\dots,\gamma_{iT})|\alpha_i) \\ &\propto \alpha_i^{a_{\alpha i}-1}(1-\alpha_i)^{b_{\alpha i}-1}\prod_{t=1}^{T}\alpha_i^{\gamma_{it}}(1-\alpha_i)^{1-\gamma_{it}} \\ &= \alpha_{it}^{(a_{\alpha i}+\sum_{t=1}^{T}\gamma_{it})-1}(1-\alpha_{it})^{(b_{\alpha i}+T-\sum_{t=1}^{T}\gamma_{it})-1} \\ \implies f(\alpha_i|-) &\propto \text{kernel of a Beta}(a_{\alpha(\text{post})}, b_{\alpha(\text{post})}) \text{ with} \\ a_{\alpha(\text{post})} &= a_{\alpha i} + \sum_{t=1}^{T}\gamma_{it} \quad b_{\alpha(\text{post})} = b_{\alpha i} + T - \sum_{t=1}^{T}\gamma_{it} \end{aligned} \tag{A.15}$$

if time and unit specific α: prior is $\alpha_{it} \sim \text{Beta}(a_{\alpha_i}, b_{\alpha_i})$

$$\begin{aligned} f(\alpha_{it}|-) &\propto f(\alpha_{it}) f(\gamma_{it}|\alpha_{it}) \\ &\propto \alpha_{it}^{a-1}(1-\alpha_{it})^{b-1}\alpha_{it}^{\gamma_{it}}(1-\alpha_{it})^{1-\gamma_{it}} \\ &= \alpha_i^{(a+\gamma_{it})-1}(1-\alpha_i)^{(b+1-\gamma_{it})-1} \\ \implies f(\alpha_{it}|-) &\propto \text{kernel of a Beta}(a_{\alpha(\text{post})}, b_{\alpha(\text{post})}) \text{ with} \\ a_{\alpha(\text{post})} &= a_{\alpha i} + \gamma_{it} \quad b_{\alpha(\text{post})} = b_{\alpha i} + 1 - \gamma_{it} \end{aligned} \tag{A.16}$$

- update a missing observation Y_{it}

for $t = 1$:

$$\begin{aligned} f(Y_{it}|-) &\propto f(Y_{it}) f(Y_{it+1}|Y_{it}, -) \\ &= \mathcal{L}_{\mathcal{N}(\mu^\star_{c_{it}t} + \boldsymbol{x}_{it}^T\boldsymbol{\beta}_t, \sigma^{2\star}_{c_{it}t})}(Y_{it}) \\ &\cdot \mathcal{L}_{\mathcal{N}(\mu^\star_{c_{it+1}t+1} + \eta_{1i}Y_{it} + \boldsymbol{x}_{it+1}^T\boldsymbol{\beta}_{t+1}, \sigma^{2\star}_{c_{it+1}t+1}(1-\eta_{1i}^2))}(Y_{it+1}) \\ &\propto \exp\left\{-\frac{1}{2\sigma^{2\star}_{c_{it}t}}(Y_{it} - \mu^\star_{c_{it}t} - \boldsymbol{x}_{it}^T\boldsymbol{\beta}_t)^2\right\} \\ &\cdot \exp\left\{-\frac{1}{2\sigma^{2\star}_{c_{it+1}t+1}(1-\eta_{1i}^2)}(Y_{it+1} - \mu^\star_{c_{it+1}t+1} - \eta_{1i}Y_{it} - \boldsymbol{x}_{it+1}^T\boldsymbol{\beta}_{t+1})^2\right\} \end{aligned}$$

$$
\begin{aligned}
&= \exp\left\{-\frac{1}{2\sigma^{2\star}_{c_{it}t}}\left(Y_{it} - (\mu^{\star}_{c_{it}t} + \boldsymbol{x}_{it}^T\boldsymbol{\beta}_t)\right)^2\right\} \\
&\cdot \exp\left\{-\frac{\eta_{1i}^2}{2\sigma^{2\star}_{c_{it+1}t+1}(1-\eta_{1i}^2)}\left(Y_{it} - \frac{Y_{it+1} - \mu^{\star}_{c_{it+1}t+1} - \boldsymbol{x}_{it+1}^T\boldsymbol{\beta}_{t+1}}{\eta_{1i}}\right)^2\right\} \\
\implies & f(Y_{it}|-) \propto \text{kernel of a } \mathcal{N}(\mu_{Y_{it}(\text{post})}, \sigma^2_{Y_{it}(\text{post})}) \text{ with} \\
\sigma^2_{Y_{it}(\text{post})} &= \frac{1}{\frac{1}{\sigma^{2\star}_{c_{it}t}} + \frac{\eta_{1i}^2}{2\sigma^{2\star}_{c_{it+1}t+1}(1-\eta_{1i}^2)}} \\
\mu_{Y_{it}(\text{post})} &= \sigma^2_{Y_{it}(\text{post})}\left(\frac{\mu^{\star}_{c_{it}t} + \boldsymbol{x}_{it}^T\boldsymbol{\beta}_t}{\sigma^{2\star}_{c_{it}t}} + \frac{\eta_{1i}(Y_{it+1} - \mu^{\star}_{c_{it+1}t+1} - \boldsymbol{x}_{it+1}^T\boldsymbol{\beta}_{t+1})}{\sigma^{2\star}_{c_{it+1}t+1}(1-\eta_{1i}^2)}\right)
\end{aligned}
\tag{A.17}
$$

for $1 < t < T$:

$$
\begin{aligned}
f(Y_{it}|-) &\propto f(Y_{it})f(Y_{it+1}|Y_{it},-) \\
&= \mathcal{L}_{\mathcal{N}(\mu^{\star}_{c_{it}t} + \eta_{1i}Y_{it-1} + \boldsymbol{x}_{it}^T\boldsymbol{\beta}_t, \sigma^{2\star}_{c_{it}t})}(Y_{it}) \\
&\cdot \mathcal{L}_{\mathcal{N}(\mu^{\star}_{c_{it+1}t+1} + \eta_{1i}Y_{it} + \boldsymbol{x}_{it+1}^T\boldsymbol{\beta}_{t+1}, \sigma^{2\star}_{c_{it+1}t+1}(1-\eta_{1i}^2))}(Y_{it+1}) \\
&\propto \exp\left\{-\frac{1}{2\sigma^{2\star}_{c_{it}t}(1-\eta_{1i}^2)}(Y_{it} - \mu^{\star}_{c_{it}t} - \eta_{1i}Y_{it-1} - \boldsymbol{x}_{it}^T\boldsymbol{\beta}_t)^2\right\} \\
&\cdot \exp\left\{-\frac{1}{2\sigma^{2\star}_{c_{it+1}t+1}(1-\eta_{1i}^2)}(Y_{it+1} - \mu^{\star}_{c_{it+1}t+1} - \eta_{1i}Y_{it} - \boldsymbol{x}_{it+1}^T\boldsymbol{\beta}_{t+1})^2\right\} \\
&= \exp\left\{-\frac{1}{2\sigma^{2\star}_{c_{it}t}(1-\eta_{1i}^2)}\left(Y_{it} - (\mu^{\star}_{c_{it}t} + \eta_{1i}Y_{it-1} + \boldsymbol{x}_{it}^T\boldsymbol{\beta}_t)\right)^2\right\} \\
&\cdot \exp\left\{-\frac{\eta_{1i}^2}{2\sigma^{2\star}_{c_{it+1}t+1}(1-\eta_{1i}^2)}\left(Y_{it} - \frac{Y_{it+1} - \mu^{\star}_{c_{it+1}t+1} - \boldsymbol{x}_{it+1}^T\boldsymbol{\beta}_{t+1}}{\eta_{1i}}\right)^2\right\} \\
\implies & f(Y_{it}|-) \propto \text{kernel of a } \mathcal{N}(\mu_{Y_{it}(\text{post})}, \sigma^2_{Y_{it}(\text{post})}) \text{ with} \\
\sigma^2_{Y_{it}(\text{post})} &= \frac{1-\eta_{1i}^2}{\frac{1}{\sigma^{2\star}_{c_{it}t}} + \frac{\eta_{1i}^2}{\sigma^{2\star}_{c_{it+1}t+1}}} \\
\mu_{Y_{it}(\text{post})} &= \sigma^2_{Y_{it}(\text{post})}\left(\frac{\mu^{\star}_{c_{it}t} + \eta_{1i}Y_{it-1} + \boldsymbol{x}_{it}^T\boldsymbol{\beta}_t}{\sigma^{2\star}_{c_{it}t}(1-\eta_{1i}^2)} + \frac{\eta_{1i}(Y_{it+1} - \mu^{\star}_{c_{it+1}t+1} - \boldsymbol{x}_{it+1}^T\boldsymbol{\beta}_{t+1})}{\sigma^{2\star}_{c_{it+1}t+1}(1-\eta_{1i}^2)}\right)
\end{aligned}
\tag{A.18}
$$

for $t = T$:

$$
\begin{aligned}
f(Y_{it}|-) &\propto f(Y_{it}) \\
&= \mathcal{L}_{\mathcal{N}(\mu^{\star}_{c_{it}t} + \eta_{1i}Y_{it-1} + \boldsymbol{x}_{it}^T\boldsymbol{\beta}_t, \sigma^{2\star}_{c_{it}t}(1-\eta_{1i}^2))}(Y_{it}) \\
\implies & f(Y_{it}|-) \text{ is just the likelihood of } Y_{it}
\end{aligned}
\tag{A.19}
$$

Appendix B

Computational details

B.1 Fitting algorithm code

We report here part of the code of the `MCMC_fit` function which implements the updated DRPM model described in this work. We include it to let the readers appreciate the ease, clarity, and even elegance of the Julia language in translating the mathematical formulation into code. All this with the the hope for Julia to become the new natural choice in the statistical, or in general scientific, computing field, giving to it a refreshing approach.

Together with what said in Chapter 2, we also note that the productivity offered by the Julia language is not only obtained through the vast land of packages and documentation, but even through an online active forum[1], where I wrote myself some questions (and received answers) during the development of the thesis. Finally, at `https://github.com/federicomor/Tesi/tree/main/src/JDRPM` there are available all the codes behind this JDRPM update.

Listing 3: Julia code which implements the fitting model algorithm. We report here just the "functional" part, i.e. not all the setup lines regarding the function definition, variable preallocations, input arguments checks, etc.

```
############# start MCMC algorithm #############
println(replace(string(now()),"T" => " ")[1:end-4])
println("Starting MCMC algorithm")

t_start = now()
progresso = Progress(round(Int64(draws)),
      showspeed=true,
      output=stdout, # default is stderr, which turns out in orange color on R
      dt=1, # every how many seconds update the feedback
      barlen=0 # no progress bar
      )

@inbounds for i in 1:draws
   ############# sample the missing values #############
   # from the "update rho" section onwards also the Y[j,t] will be needed (to
   ↪  compute weights, update laws, etc)
   # so we need now to simulate the values for the data which are missing (from
   ↪  their full conditional)
```

[1] `https://discourse.julialang.org/`

```
if Y_has_NA
    # we have to use the missing_idxs to remember which units and at which
    ↪  times had a missing value,
    # in order to simulate just them and instead use the given value for the
    ↪  other units and times
    for (j,t) in missing_idxs
        # Problem: if when filling a NA we occur in another NA value? eg when
        ↪  we also need Y[j,t+1]
        # I decided here to set that value to 0, if occurs, since anyway target
        ↪  should be centered
        # so it seems a reasonable patch
        # We could have decided to ignore this computation and just use the
        ↪  likelihood as proposal
        # filling distribution, but this would have just worked in the Y[j,t+1]
        ↪  case so the general
        # problem would have still been there

        c_it = Si_iter[j,t]
        Xlk_term_t = (lk_xPPM ? dot(view(Xlk_covariates,j,:,t), beta_iter[t]) :
        ↪  0)
        aux1 = eta1_iter[j]^2

        if t==1
            c_itp1 = Si_iter[j,t+1]
            Xlk_term_tp1 = (lk_xPPM ? dot(view(Xlk_covariates,j,:,t+1),
            ↪  beta_iter[t+1]) : 0)

            sig2_post = 1 / (1/sig2h_iter[c_it,t] +
            ↪  aux1/(sig2h_iter[c_itp1,t+1]*(1-aux1)))
            mu_post = sig2_post * (
                (1/sig2h_iter[c_it,t])*(muh_iter[c_it,t] + Xlk_term_t) +
                (eta1_iter[j]/(sig2h_iter[c_itp1,t+1]*(1-aux1)))*((ismissing(Y[j,t+1])
                ↪  ? 0 : Y[j,t+1]) - muh_iter[c_itp1,t+1] - Xlk_term_tp1)
                )

            Y[j,t] = rand(Normal(mu_post,sqrt(sig2_post)))

        elseif 1<t<T
            c_itp1 = Si_iter[j,t+1]
            Xlk_term_tp1 = (lk_xPPM ? dot(view(Xlk_covariates,j,:,t+1),
            ↪  beta_iter[t+1]) : 0)

            sig2_post = (1-aux1) / (1/sig2h_iter[c_it,t] +
            ↪  aux1/sig2h_iter[c_itp1,t+1])
            mu_post = sig2_post * (
                (1/(sig2h_iter[c_it,t]*(1-aux1)))*(muh_iter[c_it,t] +
                ↪  eta1_iter[j]*(ismissing(Y[j,t-1]) ? 0 : Y[j,t-1]) +
                ↪  Xlk_term_t) +
                (eta1_iter[j]/(sig2h_iter[c_itp1,t+1]*(1-aux1)))*((ismissing(Y[j,t+1])
                ↪  ? 0 : Y[j,t+1]) - muh_iter[c_itp1,t+1] - Xlk_term_tp1)
                )

            Y[j,t] = rand(Normal(mu_post,sqrt(sig2_post)))

        else # t==T
            Y[j,t] = rand(Normal(
                muh_iter[c_it,t] + eta1_iter[j]*(ismissing(Y[j,t-1]) ? 0 :
                ↪  Y[j,t-1]) + Xlk_term_t,
                sqrt(sig2h_iter[c_it,t]*(1-aux1))
                ))
        end
    end
```

```
    end


    for t in 1:T
        ############# update gamma #############
        for j in 1:n
            if t==1
                gamma_iter[j,t] = 0
                # at the first time units get reallocated
            else
                # we want to find rho_t^{R_t(-j)} ...
                indexes = findall_faster(jj -> jj != j && gamma_iter[jj, t] == 1,
                ↪  1:n)
                Si_red = Si_iter[indexes, t]
                copy!(Si_red1, Si_red)
                push!(Si_red1, Si_iter[j,t]) # ... and rho_t^R_t(+j)}

                # get also the reduced spatial info if sPPM model
                if sPPM
                    sp1_red = @view sp1[indexes]
                    sp2_red = @view sp2[indexes]
                end
                # and the reduced covariates info if cl_xPPM model
                if cl_xPPM
                    Xcl_covariates_red = @view Xcl_covariates[indexes,:,t]
                end

                # compute n_red's and nclus_red's and relabel
                n_red = length(Si_red) # = "n" relative to here, i.e. the
                ↪  sub-partition size
                n_red1 = length(Si_red1)
                relabel!(Si_red,n_red)
                relabel!(Si_red1,n_red1)
                nclus_red = isempty(Si_red) ? 0 : maximum(Si_red) # = number of
                ↪  clusters
                nclus_red1 = maximum(Si_red1)

                # save the label of the current working-on unit j
                j_label = Si_red1[end]

                # compute also nh_red's
                nh_red .= 0
                nh_red1 .= 0
                for jj in 1:n_red
                    nh_red[Si_red[jj]] += 1 # = numerosities for each cluster label
                    nh_red1[Si_red1[jj]] += 1
                end
                nh_red1[Si_red1[end]] += 1 # account for the last added unit j, not
                ↪  included in the above loop

                # start computing weights
                lg_weights .= 0

                # unit j can enter an existing cluster...
                for k in 1:nclus_red

                    # filter the indexes of the units of label k
                    aux_idxs = findall(Si_red .== k)
                    lC .= 0.
                    if sPPM
                        copy!(s1o, sp1_red[aux_idxs])
                        copy!(s2o, sp2_red[aux_idxs])
```

```
            copy!(s1n,s1o); push!(s1n, sp1[j])
            copy!(s2n,s2o); push!(s2n, sp2[j])

            spatial_cohesion!(spatial_cohesion_idx, s1o, s2o,
            ↪  sp_params_struct, true, M_dp, S,1,false,lC)
            spatial_cohesion!(spatial_cohesion_idx, s1n, s2n,
            ↪  sp_params_struct, true, M_dp, S,2,false,lC)
         end

         lS .= 0.
         if cl_xPPM
            for p in 1:p_cl
               if isa(first(Xcl_covariates[j,p,t]),Real) # numerical
               ↪  covariate
                  copy!(Xo, @view Xcl_covariates_red[aux_idxs,p])
                  copy!(Xn, Xo); push!(Xn,Xcl_covariates[j,p,t])

                  if covariate_similarity_idx == 4
                     covariate_similarity!(covariate_similarity_idx, Xo,
                     ↪  cv_params_sim4[p], Rs[p,t],
                     ↪  true,1,true,lS,cv_weight)
                     covariate_similarity!(covariate_similarity_idx, Xn,
                     ↪  cv_params_sim4[p], Rs[p,t],
                     ↪  true,2,true,lS,cv_weight)
                  else
                     covariate_similarity!(covariate_similarity_idx, Xo,
                     ↪  cv_params, Rs[p,t], true,1,true,lS,cv_weight)
                     covariate_similarity!(covariate_similarity_idx, Xn,
                     ↪  cv_params, Rs[p,t], true,2,true,lS,cv_weight)
                  end
               else # categorical covariate
                  copy!(Xo_cat, @view Xcl_covariates_red[aux_idxs,p])
                  copy!(Xn_cat, Xo_cat);
                  ↪  push!(Xn_cat,Xcl_covariates[j,p,t])

                  covariate_similarity!(covariate_similarity_idx, Xo_cat,
                  ↪  cv_params, Rs[p,t], true,1,true,lS,cv_weight)
                  covariate_similarity!(covariate_similarity_idx, Xn_cat,
                  ↪  cv_params, Rs[p,t], true,2,true,lS,cv_weight)
               end
            end
         end

         lg_weights[k] = log(nh_red[k]) + lC[2] - lC[1] + lS[2] - lS[1]
      end

      # ... or unit j can create a singleton
      lC .= 0.
      if sPPM
         spatial_cohesion!(spatial_cohesion_idx, SVector(sp1[j]),
         ↪  SVector(sp2[j]), sp_params_struct, true, M_dp, S,2,false,lC)
      end
      lS .= 0.
      if cl_xPPM
         for p in 1:p_cl
            if covariate_similarity_idx == 4
               covariate_similarity!(covariate_similarity_idx,
               ↪  SVector(Xcl_covariates[j,p,t]), cv_params_sim4[p],
               ↪  Rs[p,t], true, 2,true,lS,cv_weight)
            else
               covariate_similarity!(covariate_similarity_idx,
               ↪  SVector(Xcl_covariates[j,p,t]), cv_params, Rs[p,t],
               ↪  true, 2,true,lS,cv_weight)
```

```
            end
         end
      end
      lg_weights[nclus_red+1] = log_Mdp + lC[2] + lS[2]

      # now use the weights towards sampling the new gamma_jt
      max_ph = maximum(@view lg_weights[1:(nclus_red+1)])
      sum_ph = 0.0

      # exponentiate...
      for k in 1:(nclus_red+1)
          # for numerical purposes we subract max_ph
         lg_weights[k] = exp(lg_weights[k] - max_ph)
         sum_ph += lg_weights[k]
      end
      # ... and normalize
      lg_weights ./= sum_ph

      # compute probh
      probh::Float64 = 0.0
      if time_specific_alpha==false && unit_specific_alpha==false
         probh = alpha_iter / (alpha_iter + (1 - alpha_iter) *
         ↪  lg_weights[j_label])
      elseif time_specific_alpha==true && unit_specific_alpha==false
         probh = alpha_iter[t] / (alpha_iter[t] + (1 - alpha_iter[t]) *
         ↪  lg_weights[j_label])
      elseif time_specific_alpha==false && unit_specific_alpha==true
         probh = alpha_iter[j] / (alpha_iter[j] + (1 - alpha_iter[j]) *
         ↪  lg_weights[j_label])
      elseif time_specific_alpha==true && unit_specific_alpha==true
         probh = alpha_iter[j,t] / (alpha_iter[j,t] + (1 -
         ↪  alpha_iter[j,t]) * lg_weights[j_label])
      end

      # compatibility check for gamma transition
      if gamma_iter[j, t] == 0
         # we want to find rho_(t-1)^{R_t(+j)} ...
         indexes = findall_faster(jj -> jj==j || gamma_iter[jj, t]==1,
         ↪  1:n)
         Si_comp1 = @view Si_iter[indexes, t-1]
         Si_comp2 = @view Si_iter[indexes, t] # ... and rho_t^R_t(+j)}

         rho_comp = compatibility(Si_comp1, Si_comp2)
         if rho_comp == 0
            probh = 0.0
         end
      end
      # sample the new gamma
      gt = rand(Bernoulli(probh))
      gamma_iter[j, t] = gt
   end
end # for j in 1:n

############## update rho #############
# we only update the partition for the units which can move (i.e. with
↪  gamma_jt=0)
movable_units = findall(gamma_iter[:,t] .== 0) # fast

for j in movable_units
   # remove unit j from the cluster she is currently in

   if nh[Si_iter[j,t],t] > 1 # unit j does not belong to a singleton
   ↪  cluster
```

```
        nh[Si_iter[j,t],t] -= 1
        # no nclus_iter[t] change since j's cluster is still alive
    else # unit j belongs to a singleton cluster
        j_label = Si_iter[j,t]
        last_label = nclus_iter[t]

        if j_label < last_label
            # here we enter if j_label is not the last label, so we need to
            # relabel clusters in order to then remove j's cluster
            # eg: units 1 2 3 4 5 j 7 -> units 1 2 3 4 5 j 7
            #     label 1 1 2 2 2 3 4    label 1 1 2 2 2 4 3

            # swap cluster labels...
            for jj in 1:n
                if Si_iter[jj, t] == last_label
                    Si_iter[jj, t] = j_label
                end
            end
            Si_iter[j, t] = last_label
            # ... and cluster-specific parameters
            sig2h_iter[j_label, t], sig2h_iter[last_label, t] =
            ↪  sig2h_iter[last_label, t], sig2h_iter[j_label, t]
            muh_iter[j_label, t], muh_iter[last_label, t] =
            ↪  muh_iter[last_label, t], muh_iter[j_label, t]
            nh[j_label, t] = nh[last_label, t]
            nh[last_label, t] = 1

        end
        # remove the j-th observation and the last cluster (being j in a
        ↪  singleton)
        nh[last_label, t] -= 1
        nclus_iter[t] -= 1
    end

    # setup probability weights towards the sampling of rho_jt
    ph .= 0.0
    resize!(ph,nclus_iter[t]+1)
    copy!(rho_tmp, @view Si_iter[:,t])

    # compute nh_tmp (numerosities for each cluster label)
    copy!(nh_tmp, @view nh[:,t])
    # unit j contribute is already absent from the change we did above
    nclus_temp = 0

    # we now simulate the unit j to be assigned to one of the existing
    ↪  clusters...
    for k in 1:nclus_iter[t]
        rho_tmp[j] = k
        indexes = findall(gamma_iter[:,t+1] .== 1) # fast
        # we check the compatibility between rho_t^{h=k,R_(t+1)} ...
        Si_comp1 = @view rho_tmp[indexes]
        Si_comp2 = @view Si_iter[indexes,t+1] # and rho_(t+1)^{R_(t+1)}
        rho_comp = compatibility(Si_comp1, Si_comp2)

        if rho_comp != 1
            ph[k] = log(0) # assignment to cluster k is not compatible
        else
            # update params for "rho_jt = k" simulation
            nh_tmp[k] += 1
            nclus_temp = count(a->(a>0), nh_tmp)

            lPP .= 0.
```

```
        for kk in 1:nclus_temp
            aux_idxs = findall(rho_tmp .== kk)
            if sPPM
                copy!(s1n, @view sp1[aux_idxs])
                copy!(s2n, @view sp2[aux_idxs])
                spatial_cohesion!(spatial_cohesion_idx, s1n, s2n,
                ↪  sp_params_struct, true, M_dp, S,1,true,lPP)
            end
            if cl_xPPM
                for p in 1:p_cl
                    Xn_view = @view Xcl_covariates[aux_idxs,p,t]
                    if covariate_similarity_idx == 4
                        covariate_similarity!(covariate_similarity_idx,
                        ↪  Xn_view, cv_params_sim4[p], Rs[p,t],
                        ↪  true,1,true,lPP,cv_weight)
                    else
                        covariate_similarity!(covariate_similarity_idx,
                        ↪  Xn_view, cv_params, Rs[p,t],
                        ↪  true,1,true,lPP,cv_weight)
                    end
                end
            end
            lPP[1] += log_Mdp + lgamma(nh_tmp[kk])
        end

        if t==1
            ph[k] = loglikelihood(Normal(
                muh_iter[k,t] + (lk_xPPM ? dot(view(Xlk_covariates,j,:,t),
                ↪  beta_iter[t]) : 0),
                sqrt(sig2h_iter[k,t])),
                Y[j,t]) + lPP[1]
        else
            ph[k] = loglikelihood(Normal(
                muh_iter[k,t] + eta1_iter[j]*Y[j,t-1] + (lk_xPPM ?
                ↪  dot(view(Xlk_covariates,j,:,t), beta_iter[t]) : 0),
                sqrt(sig2h_iter[k,t]*(1-eta1_iter[j]^2))),
                Y[j,t]) + lPP[1]
        end

        # restore params after "rho_jt = k" simulation
        nh_tmp[k] -= 1
    end
end

# ... plus the case of being assigned to a new (singleton for now)
↪  cluster
k = nclus_iter[t]+1
rho_tmp[j] = k
# declare (for later scope accessibility) the new params here
muh_draw = 0.0; sig2h_draw = 0.0

indexes = findall(gamma_iter[:,t+1] .== 1)
Si_comp1 = @view rho_tmp[indexes]
Si_comp2 = @view Si_iter[indexes,t+1]
rho_comp = compatibility(Si_comp1, Si_comp2)

if rho_comp != 1
    ph[k] = log(0) # assignment to a new cluster is not compatible
else
    # sample new params for this new cluster
    muh_draw = rand(Normal(theta_iter[t], sqrt(tau2_iter[t])))
    sig2h_draw = rand(InverseGamma(sig2h_priors[1],sig2h_priors[2]))
```

```
        # update params for "rho_jt = k" simulation
        nh_tmp[k] += 1
        nclus_temp = count(a->(a>0), nh_tmp)

        lPP .= 0.
        for kk in 1:nclus_temp
            aux_idxs = findall(rho_tmp .== kk) # fast
            if sPPM
                copy!(s1n, @view sp1[aux_idxs])
                copy!(s2n, @view sp2[aux_idxs])
                spatial_cohesion!(spatial_cohesion_idx, s1n, s2n,
                ↪  sp_params_struct, true, M_dp, S,1,true,lPP)
            end
            if cl_xPPM
                for p in 1:p_cl
                    Xn_view = @view Xcl_covariates[aux_idxs,p,t]
                    if covariate_similarity_idx == 4
                        covariate_similarity!(covariate_similarity_idx, Xn_view,
                        ↪  cv_params_sim4[p], Rs[p,t],
                        ↪  true,1,true,lPP,cv_weight)
                    else
                        covariate_similarity!(covariate_similarity_idx, Xn_view,
                        ↪  cv_params, Rs[p,t], true,1,true,lPP,cv_weight)
                    end
                end
            end
            lPP[1] += log_Mdp + lgamma(nh_tmp[kk])
        end

        if t==1
            ph[k] = loglikelihood(Normal(
                muh_draw + (lk_xPPM ? dot(view(Xlk_covariates,j,:,t),
                ↪  beta_iter[t]) : 0),
                sqrt(sig2h_draw)),
                Y[j,t]) + lPP[1]
        else
            ph[k] = loglikelihood(Normal(
                muh_draw + eta1_iter[j]*Y[j,t-1] + (lk_xPPM ?
                ↪  dot(view(Xlk_covariates,j,:,t), beta_iter[t]) : 0),
                sqrt(sig2h_draw*(1-eta1_iter[j]^2))),
                Y[j,t]) + lPP[1]
        end

        # restore params after "rho_jt = k" simulation
        nh_tmp[k] -= 1
    end

    # now exponentiate the weights...
    max_ph = maximum(ph)
    sum_ph = 0.0
    for k in eachindex(ph)
        # for numerical purposes we subract max_ph
        ph[k] = exp(ph[k] - max_ph)
        sum_ph += ph[k]
    end
    # ... and normalize them
    ph ./= sum_ph

    # now sample the new label Si_iter[j,t]
    u = rand(Uniform(0,1))
    cph = cumsum(ph)
```

```
        cph[end] = 1 # fix numerical problems of having sums like 0.999999etc
        new_label = 0
        for k in eachindex(ph)
            if u <= cph[k]
                new_label = k
                break
            end
        end

        if new_label <= nclus_iter[t]
            # we enter an existing cluster
            Si_iter[j, t] = new_label
            nh[new_label, t] += 1
        else
            # we create a new singleton cluster
            nclus_iter[t] += 1
            cl_new = nclus_iter[t]
            Si_iter[j, t] = cl_new
            nh[cl_new, t] = 1
            muh_iter[cl_new, t] = muh_draw
            sig2h_iter[cl_new, t] = sig2h_draw
        end

        # now we need to relabel after the possible mess created by the
        ↪  sampling
        # eg: (before sampling)  (after sampling)
        #     units j 2 3 4 5 ->  units j 2 3 4 5
        #    labels 1 1 1 2 2    labels 3 1 1 2 2
        # the after case has to be relabelled
        Si_tmp = @view Si_iter[:,t]

        relabel_full!(Si_tmp,n,Si_relab, nh_reorder, old_lab)
        # - Si_relab gives the relabelled partition
        # - nh_reorder gives the numerosities of the relabelled partition, ie
        ↪  "nh_reorder[k] = #(units of new cluster k)"
        # - old_lab tells "the index in position i (which before was cluster i)
        ↪  is now called cluster old_lab[i]"
        # eg:             Original labels (Si): 4 2 1 1 1 3 1 4 5
        #          Relabeled groups (Si_relab): 1 2 3 3 3 4 3 1 5
        # Reordered cluster sizes (nh_reorder): 2 1 4 1 1 0 0 0 0
        #                 Old labels (old_lab): 4 2 1 3 5 0 0 0 0

        # now fix everything (morally permute params)
        Si_iter[:,t] = Si_relab
        # discard the zeros at the end of the auxiliary vectors nh_reorde and
        ↪  old_lab
        copy!(muh_iter_copy, muh_iter)
        copy!(sig2h_iter_copy, sig2h_iter)
        len = findlast(x -> x != 0, nh_reorder)
        for k in 1:nclus_iter[t]
            muh_iter[k,t] = muh_iter_copy[old_lab[k],t]
            sig2h_iter[k,t] = sig2h_iter_copy[old_lab[k],t]
            nh[k,t] = nh_reorder[k]
        end

    end # for j in movable_units

    ############# update muh #############
    if t==1
        for k in 1:nclus_iter[t]
            sum_Y = 0.0
            for j in 1:n
```

```
            if Si_iter[j,t]==k
               sum_Y += Y[j,t] - (lk_xPPM ? dot(view(Xlk_covariates,j,:,t),
               ↪  beta_iter[t]) : 0.0)
            end
         end
         sig2_star = 1 / (1/tau2_iter[t] + nh[k,t]/sig2h_iter[k,t])
         mu_star = sig2_star * (theta_iter[t]/tau2_iter[t] +
         ↪  sum_Y/sig2h_iter[k,t])

         muh_iter[k,t] = rand(Normal(mu_star,sqrt(sig2_star)))
      end

   else # t>1
      for k in 1:nclus_iter[t]
         sum_Y = 0.0
         sum_e2 = 0.0
         for j in 1:n
            if Si_iter[j,t]==k
               aux1 = 1 / (1-eta1_iter[j]^2)
               sum_e2 += aux1
               sum_Y += (Y[j,t] - eta1_iter[j]*Y[j,t-1] - (lk_xPPM ?
               ↪  dot(view(Xlk_covariates,j,:,t), beta_iter[t]) : 0.0)) *
               ↪  aux1
            end
         end
         sig2_star = 1 / (1/tau2_iter[t] + sum_e2/sig2h_iter[k,t])
         mu_star = sig2_star * (theta_iter[t]/tau2_iter[t] +
         ↪  sum_Y/sig2h_iter[k,t])

         muh_iter[k,t] = rand(Normal(mu_star,sqrt(sig2_star)))
      end
   end

   ############## update sigma2h ##############
   if t==1
      for k in 1:nclus_iter[t]
         a_star = sig2h_priors[1] + nh[k,t]/2
         sum_Y = 0.0
         S_kt = findall(Si_iter[:,t] .== k)
         for j in S_kt
            sum_Y += (Y[j,t] - muh_iter[k,t] - (lk_xPPM ?
            ↪  dot(view(Xlk_covariates,j,:,t), beta_iter[t]) : 0.0))^2
         end

         b_star = sig2h_priors[2] + sum_Y/2
         sig2h_iter[k,t] = rand(InverseGamma(a_star, b_star))
      end

   else # t>1
      for k in 1:nclus_iter[t]
         a_star = sig2h_priors[1] + nh[k,t]/2
         sum_Y = 0.0
         S_kt = findall(Si_iter[:,t] .== k)
         for j in S_kt
            sum_Y += (Y[j,t] - muh_iter[k,t] - eta1_iter[j]*Y[j,t-1] -
            ↪  (lk_xPPM ? dot(view(Xlk_covariates,j,:,t), beta_iter[t]) :
            ↪  0.0))^2
         end

         b_star = sig2h_priors[2] + sum_Y/2
         sig2h_iter[k,t] = rand(InverseGamma(a_star, b_star))
      end
```

```
end

############# update beta #############
if lk_xPPM && i>=beta_update_threshold
   if t==1
      sum_Y = zeros(p_lk)
      A_star = I(p_lk)/s2_beta
      for j in 1:n
         X_jt = @view Xlk_covariates[j,:,t]
         sum_Y += (Y[j,t] - muh_iter[Si_iter[j,t],t]) * X_jt /
         ↪  sig2h_iter[Si_iter[j,t],t]
         A_star += (X_jt * X_jt') / sig2h_iter[Si_iter[j,t],t]
      end
      b_star = beta0/s2_beta + sum_Y
      A_star = Symmetric(A_star)
      # Symmetric is needed for numerical problems
      # but A_star is indeed symm and pos def (by construction) so there
      ↪  is no problem
      beta_iter[t] = rand(MvNormalCanon(b_star, A_star))
      # this is the quicker and more accurate method

      # old method with the MvNormal and the inversion required
      # Am1_star = inv(A_star)
      # beta_iter[t] = rand(MvNormal(inv(Symmetric(A_star))*b_star,
      ↪  inv(Symmetric(A_star))))
   else
      sum_Y = zeros(p_lk)
      A_star = I(p_lk)/s2_beta
      for j in 1:n
         X_jt = @view Xlk_covariates[j,:,t]
         sum_Y += (Y[j,t] - muh_iter[Si_iter[j,t],t] -
         ↪  eta1_iter[j]*Y[j,t-1]) * X_jt / sig2h_iter[Si_iter[j,t],t]
         A_star += (X_jt * X_jt') / sig2h_iter[Si_iter[j,t],t]
      end
      b_star = beta0/s2_beta + sum_Y
      A_star = Symmetric(A_star)
      beta_iter[t] = rand(MvNormalCanon(b_star, A_star))
   end
end

############# update theta #############
aux1::Float64 = 1 / (lambda2_iter*(1-phi1_iter^2))
kt = nclus_iter[t]
sum_mu=0.0
for k in 1:kt
   sum_mu += muh_iter[k,t]
end

if t==1
   sig2_post = 1 / (1/lambda2_iter + phi1_iter^2*aux1 + kt/tau2_iter[t])
   mu_post = sig2_post * (phi0_iter/lambda2_iter + sum_mu/tau2_iter[t] +
   ↪  (phi1_iter*(theta_iter[t+1] - (1-phi1_iter)*phi0_iter))*aux1)

   theta_iter[t] = rand(Normal(mu_post, sqrt(sig2_post)))

elseif t==T
   sig2_post = 1 / (aux1 + kt/tau2_iter[t])
   mu_post = sig2_post * (sum_mu/tau2_iter[t] + ((1- phi1_iter)*phi0_iter
   ↪  + phi1_iter*theta_iter[t-1])*aux1)

   theta_iter[t] = rand(Normal(mu_post, sqrt(sig2_post)))
```

```
      else # 1<t<T
         sig2_post = 1 / ((1+phi1_iter^2)*aux1 + kt/tau2_iter[t])
         mu_post = sig2_post * (sum_mu/tau2_iter[t] +
         ↪  (phi1_iter*(theta_iter[t-1]+theta_iter[t+1]) +
         ↪  phi0_iter*(1-phi1_iter)^2)*aux1)

         theta_iter[t] = rand(Normal(mu_post, sqrt(sig2_post)))
      end

      ############# update tau2 #############
      kt = nclus_iter[t]
      aux1 = 0.0
      for k in 1:kt
         aux1 += (muh_iter[k,t] - theta_iter[t])^2
      end
      a_star_tau = tau2_priors[1] + kt/2
      b_star_tau = tau2_priors[2] + aux1/2
      tau2_iter[t] = rand(InverseGamma(a_star_tau, b_star_tau))

   end # for t in 1:T

   ############# update eta1 #############
   # the input argument eta1_priors[2] is already the std dev
   if update_eta1
      for j in 1:n
         eta1_old = eta1_iter[j]
         eta1_new = rand(Normal(eta1_old,eta1_priors[2])) # proposal value

         if (-1 <= eta1_new <= 1)
            ll_old = 0.0
            ll_new = 0.0
            for t in 2:T
               # likelihood contribution
               ll_old += loglikelihood(Normal(
                  muh_iter[Si_iter[j,t],t] + eta1_old*Y[j,t-1] + (lk_xPPM ?
                  ↪  dot(view(Xlk_covariates,j,:,t), beta_iter[t]) : 0),
                  sqrt(sig2h_iter[Si_iter[j,t],t]*(1-eta1_old^2))
                  ), Y[j,t])
               ll_new += loglikelihood(Normal(
                  muh_iter[Si_iter[j,t],t] + eta1_new*Y[j,t-1] + (lk_xPPM ?
                  ↪  dot(view(Xlk_covariates,j,:,t), beta_iter[t]) : 0),
                  sqrt(sig2h_iter[Si_iter[j,t],t]*(1-eta1_new^2))
                  ), Y[j,t])
            end
            logit_old = aux_logit(eta1_old)
            logit_new = aux_logit(eta1_new)

            # prior contribution
            ll_old += -log(2*eta1_priors[1]) -1/eta1_priors[1]*abs(logit_old)
            ll_new += -log(2*eta1_priors[1]) -1/eta1_priors[1]*abs(logit_new)

            ll_ratio = ll_new-ll_old
            u = rand(Uniform(0,1))
            if (ll_ratio > log(u))
               eta1_iter[j] = eta1_new # accept the candidate
               acceptance_ratio_eta1 += 1
            end
         end
      end
   end

   ############# update alpha #############
```

```
if update_alpha
   if time_specific_alpha==false && unit_specific_alpha==false
      # a scalar
      sumg = sum(@view gamma_iter[:,1:T])
      a_star = alpha_priors[1] + sumg
      b_star = alpha_priors[2] + n*T - sumg
      alpha_iter = rand(Beta(a_star, b_star))

   elseif time_specific_alpha==true && unit_specific_alpha==false
      # a vector in time
      for t in 1:T
         sumg = sum(@view gamma_iter[:,t])
         a_star = alpha_priors[1] + sumg
         b_star = alpha_priors[2] + n - sumg
         alpha_iter[t] = rand(Beta(a_star, b_star))
      end

   elseif time_specific_alpha==false && unit_specific_alpha==true
      # a vector in units
      for j in 1:n
         sumg = sum(@view gamma_iter[j,1:T])
         a_star = alpha_priors[1,j] + sumg
         b_star = alpha_priors[2,j] + T - sumg
         alpha_iter[j] = rand(Beta(a_star, b_star))
      end
   elseif time_specific_alpha==true && unit_specific_alpha==true
      # a matrix
      for j in 1:n
         for t in 1:T
            sumg = gamma_iter[j,t] # nothing to sum in this case
            a_star = alpha_priors[1,j] + sumg
            b_star = alpha_priors[2,j] + 1 - sumg
            alpha_iter[j,t] = rand(Beta(a_star, b_star))
         end
      end
   end
end

############# update phi0 #############
aux1 = 1/lambda2_iter
aux2 = 0.0
for t in 2:T
   aux2 += theta_iter[t] - phi1_iter*theta_iter[t-1]
end
sig2_post = 1 / ( 1/phi0_priors[2] + aux1 * (1 +
↪  (T-1)*(1-phi1_iter)/(1+phi1_iter)) )
mu_post = sig2_post * ( phi0_priors[1]/phi0_priors[2] + theta_iter[1]*aux1 +
↪  aux1/(1+phi1_iter)*aux2 )
phi0_iter = rand(Normal(mu_post, sqrt(sig2_post)))

############# update phi1 #############
# the input argument phi1_priors is already the std dev
if update_phi1
   phi1_old = phi1_iter
   phi1_new = rand(Normal(phi1_old, phi1_priors)) # proposal value

   if (-1 <= phi1_new <= 1)
      ll_old = 0.0; ll_new = 0.0
      for t in 2:T
         # likelihood contribution
         ll_old += loglikelihood(Normal(
            (1-phi1_old)*phi0_iter + phi1_old*theta_iter[t-1],
```

```
            sqrt(lambda2_iter*(1-phi1_old^2))
            ), theta_iter[t])
         ll_new += loglikelihood(Normal(
            (1-phi1_new)*phi0_iter + phi1_new*theta_iter[t-1],
            sqrt(lambda2_iter*(1-phi1_new^2))
            ), theta_iter[t])
      end

      # prior contribution
      ll_old += loglikelihood(Uniform(-1,1), phi1_old)
      ll_new += loglikelihood(Uniform(-1,1), phi1_new)

      ll_ratio = ll_new-ll_old
      u = rand(Uniform(0,1))
      if (ll_ratio > log(u))
         phi1_iter = phi1_new # accept the candidate
         acceptance_ratio_phi1 += 1
      end
   end
end

############## update lambda2 ##############
aux1 = 0.0
for t in 2:T
   aux1 += (theta_iter[t] - (1-phi1_iter)*phi0_iter -
   ↪  phi1_iter*theta_iter[t-1])^2
end
a_star_lambda2 = lambda2_priors[1] + T/2
b_star_lambda2 = lambda2_priors[2] + ((theta_iter[1] - phi0_iter)^2 + aux1) /
↪  2
lambda2_iter = rand(InverseGamma(a_star_lambda2,b_star_lambda2))

############## save MCMC iterates ##############
if i>burnin && i%thin==0
   Si_out[:,:,i_out] = Si_iter[:,1:T]
   gamma_out[:,:,i_out] = gamma_iter[:,1:T]
   if time_specific_alpha==false && unit_specific_alpha==false
      # for each iterate, a scalar
      alpha_out[i_out] = alpha_iter
   elseif time_specific_alpha==true && unit_specific_alpha==false
      # for each iterate, a vector in time
      alpha_out[:,i_out] = alpha_iter[1:T]
   elseif time_specific_alpha==false && unit_specific_alpha==true
      # for each iterate, a vector in units
      alpha_out[:,i_out] = alpha_iter
   elseif time_specific_alpha==true && unit_specific_alpha==true
      # for each iterate, a matrix
      alpha_out[:,:,i_out] = alpha_iter[:,1:T]
   end
   for t in 1:T
      for j in 1:n
         sigma2h_out[j,t,i_out] = sig2h_iter[Si_iter[j,t],t]
         muh_out[j,t,i_out] = muh_iter[Si_iter[j,t],t]
      end
   end
   eta1_out[:,i_out] = eta1_iter
   if lk_xPPM
      for t in 1:T
         beta_out[t,:,i_out] = beta_iter[t]
      end
   end
   theta_out[:,i_out] = theta_iter[1:T]
```

```
      tau2_out[:,i_out] = tau2_iter[1:T]
      phi0_out[i_out] = phi0_iter
      phi1_out[i_out] = phi1_iter
      lambda2_out[i_out] = lambda2_iter

      ############# save fitted values and metrics #############
      for j in 1:n
         for t in 1:T
            muh_jt = muh_iter[Si_iter[j,t],t]
            sig2h_jt = sig2h_iter[Si_iter[j,t],t]
            X_lk_term = lk_xPPM ? dot(view(Xlk_covariates,j,:,t), beta_iter[t])
            ↪  : 0.0

            if t==1
               llike[j,t,i_out] = logpdf(Normal(
                  muh_jt + X_lk_term,
                  sqrt(sig2h_jt)
                  ), Y[j,t])
               fitted[j,t,i_out] = muh_jt + X_lk_term
            else # t>1
               llike[j,t,i_out] = logpdf(Normal(
                  muh_jt + eta1_iter[j]*Y[j,t-1] + X_lk_term,
                  sqrt(sig2h_jt*(1-eta1_iter[j]^2))
                  ), Y[j,t])
               fitted[j,t,i_out] = muh_jt + eta1_iter[j]*Y[j,t-1] + X_lk_term
            end

            mean_likelhd[j,t] += exp(llike[j,t,i_out])
            mean_loglikelhd[j,t] += llike[j,t,i_out]
            CPO[j,t] += exp(-llike[j,t,i_out])
         end
      end

      i_out += 1
   end

next!(progresso)

end # for i in 1:draws

println("\ndone!")
t_end = now()
println("Elapsed time: ",
↪  Dates.canonicalize(Dates.CompoundPeriod(t_end-t_start)))

############# compute LPML and WAIC #############
for j in 1:n
   for t in 1:T
      LPML += log(CPO[j,t])
   end
end
LPML -= n*T*log(nout) # scaling factor
LPML = -LPML # fix sign
println("LPML: ", LPML, " (the higher the better)")

# adjust mean variables
mean_likelhd ./= nout
mean_loglikelhd./= nout
for j in 1:n
   for t in 1:T
      WAIC += 2*mean_loglikelhd[j,t] - log(mean_likelhd[j,t])
   end
```

```
end
WAIC *= -2
println("WAIC: ", WAIC, " (the lower the better)")

if update_eta1 @printf "acceptance ratio eta1: %.2f%%\n"
↪  acceptance_ratio_eta1/(n*draws) *100 end
if update_phi1 @printf "acceptance ratio phi1: %.2f%%"
↪  acceptance_ratio_phi1/draws*100 end
println()

if perform_diagnostics
   chn = Chains(
      hcat(lambda2_out,phi0_out,tau2_out',theta_out',eta1_out',alpha_out'),
      ["lambda2","phi0",
      [string("tau2_t", i) for i in 1:T]...,
      [string("theta_t", i) for i in 1:T]...,
      [string("eta1_j", i) for i in 1:n]...,
      [string("alpha_t", i) for i in 1:T]...,
      ]
   )
   ss = DataFrame(summarystats(chn))
   println("\nDiagnostics:")
   @show ss[!,[1,4,5,6,7]];
   if logging CSV.write(log_file,ss[!,[1,4,5,6,7]]) end
end

close(log_file)

if simple_return
   return Si_out, LPML, WAIC
else
   return Si_out, Int.(gamma_out), alpha_out, sigma2h_out, muh_out, include_eta1
   ↪  ? eta1_out : NaN,
      lk_xPPM ? beta_out : NaN, theta_out, tau2_out, phi0_out, include_phi1 ?
      ↪  phi1_out : NaN, lambda2_out,
      fitted, llike, LPML, WAIC
end
```

B.2 Interface

Now some more technical details about the whole implementation design. The fitting code was written in Julia, but its main intended use is from R. This choice was made because R is currently the best language for statistical purposes, or at least the most spread; in fact all other models "competitors" to the DRPM are available through some R package. Therefore we thought that letting our work be also accessible from R, and not only from Julia, would have eased the possibilities of testing and comparisons with other models or datasets.

To do so, we relied on the `JuliaConnectoR` on R which allows the interaction between the two languages. In this sense, we can load in R the Julia package `JDRPM`, which stores the Julia project (i.e. all codes and packages dependencies) about the improved version of the DRPM model, and call it using data and arguments from R. The output produced by the Julia functions has then to be converted back into R structures, which is done automatically through a dedicated function of the

package. The structure of this workflow is summarized in Listing 4.

Listing 4: Instructions on how to use the `JDRPM` model from R.

```
############# Requirements #############
# install the required pacakge
install.packages("JuliaConnectoR")

############# Setup #############
# load the package
library(JuliaConnectoR)
# check it returns TRUE
juliaSetupOk()

# load the Package manager on Julia
juliaEval("using Pkg")
# enter into the JDRPM project
juliaEval("Pkg.activate(\"<path/to/where/you/stored/JDRPM>\")")

# downloads and install, only once, all the depdendencies
juliaEval("Pkg.instantiate()")
# now, as a check, this should print the list of packages that JDRPM uses,
# such as Distributions, Statistics, LinearAlgebra, SpecialFunctions, etc.
juliaEval("Pkg.status()")

# locate the "main" file
module = normalizePath("<path/to/where/you/stored/JDRPM>/src/JDRPM.jl")
# load the "main" file into a callable R object
module_JDRPM = juliaImport(juliaCall("include", module))

# trigger the compilation of the function, otherwise all first runs
# will be slow since the function still would have to be compiled
module_JDRPM$trigger_compilation()

############# Fit #############
# perform the fit
out = module_JDRPM$MCMC_fit(...)

# convert the output to R structures
rout = juliaGet(out)
names(rout)  = c("Si","gamma","alpha", "sigma2h", "muh", "eta1","beta","theta",
↪  "tau2", "phi0", "phi1","lambda2","fitted","llike","lpml","waic")

# and reshape it to uniform to the DRPM output form
rout$Si = aperm(rout$Si, c(2, 1, 3))
rout$gamma = aperm(rout$gamma, c(2, 1, 3))
rout$sigma2h = aperm(rout$sigma2h, c(2, 1, 3))
rout$muh = aperm(rout$muh, c(2, 1, 3))
rout$fitted = aperm(rout$fitted, c(2, 1, 3))
rout$llike = aperm(rout$llike, c(2, 1, 3))
rout$alpha = aperm(rout$alpha, c(2, 1))
rout$theta = aperm(rout$theta, c(2, 1))
rout$tau2 = aperm(rout$tau2, c(2, 1))
rout$eta1 = aperm(rout$eta1, c(2, 1))
rout$phi0 = matrix(rout$phi0, ncol = 1)
rout$phi1 = matrix(rout$phi1, ncol = 1)
rout$lambda2 = matrix(rout$lambda2, ncol = 1)
```

```
# this reshape works in the case of full model fit, but in the case of special
# fitting options (e.g. unit_specific_alpha=true) it needs to be adjusted
```

The `trigger_compilation` function runs the fitting function on a small test case to simply give Julia a friendly nudge to compile the function, making all the subsequent and more serious fits faster. In fact, especially for more complex projects, there are packages such as `PrecompileTools` and `PackageCompiler` which helps to solve this "time to first execution" problem of Julia.

Regarding instead the visual interface, in the sense of the feedback provided by the function, we decided to make it more user-friendly and possibly informative than the original C implementation. The most relevant add-ons are the possibility to perform diagnostics on a subset of the sampled parameters, and the real-time progress monitoring, which updates itself every second to show the estimated remaining time to complete the fit. As a further proof of the ease of this language, these features were just a simple insertion of few lines of code, thanks to the Julia packages `MCMCChains` (Ge et al., 2018) and `ProgressMeter`.

Listing 5: Feedback from the JDRPM implementation.

```
# if verbose=true this initial parameter section is also printed
Parameters:
sig2h ~ invGamma(0.01, 0.01)
Logit(1/2(eta1+1)) ~ Laplace(0, 0.9)
tau2 ~ invGamma(1.9, 0.4)
phi0 ~ Normal(μ=0.0, σ=10.0)
lambda2 ~ invGamma(1.9, 0.4)
alpha ~ Beta(2.0, 2.0)

- using seed 113.0 -
fitting 110000 total iterates (with burnin=90000, thinning=5)
thus producing 4000 valid iterates in the end

on n=105 subjects
for T=12 time instants

[✓] with space? true (cohesion 3.0)
[✗] with covariates in the likelihood? false
[✗] with covariates in the clustering process? false
[✗] are there missing data in Y? false

2024-10-14 09:33:11
Starting MCMC algorithm
Progress: 100% Time: 0:25:39 (15.40 ms/it)

done!
Elapsed time: 48 minutes, 45 seconds, 862 milliseconds
LPML: 624.9135200152505 (the higher the better)
WAIC: -1898.049549751033 (the lower the better)
acceptance ratio eta1: 51.72%
acceptance ratio phi1: 36.99%

# if perform_diagnostics=true this final diagnostics section is also printed
Diagnostics:
```

```
ss[!, [1, 4, 5, 6, 7]] = 143×5 DataFrame
 Row | parameters  mcse         ess_bulk   ess_tail   rhat
     | Symbol      Float64      Float64    Float64    Float64
-----------------------------------------------------------------
   1 | lambda2     0.000817173  4243.04    3970.25    0.999769
   2 | phi0        0.00218706   3533.95    3675.99    1.00018
   3 | tau2_t1     0.00540064   3716.56    3645.99    0.999968
         ⋮
  14 | tau2_t12    0.00259168   3965.77    3655.55    0.999951
  15 | theta_t1    0.00404988   3603.34    3765.78    0.999834
         ⋮
  26 | theta_t12   0.00337843   3588.83    3907.13    0.999866
  27 | eta1_j1     0.0112187     451.588   1107.96    1.00163
         ⋮
 131 | eta1_j105   0.00328424   1539.36    2194.83    1.00002
 132 | alpha_t1    0.000213087  3774.24    3920.48    1.00044
         ⋮
 143 | alpha_t12   0.00266005    541.427   1867.54    1.0084
```

Appendix C

Fits interpretation

We provide here some comments and insights about the air pollution levels in Lombardy that we can derive from the spatio-temporal fits performed in Chapter 3. We recall that they refer to the weekly averages concentrations of PM_{10}, recorded for $n = 105$ monitoring stations and on a time period of $T = 12$ corresponding to the first three months of 2018.

tipo notare che l'area di brescia magari è inquinata, poi che invece il cluster più inquinato diventa verso milano o bergamo, ecc, commenti ambientali sui fit

Non so se questa parte è utile/interessante da inserire

Bibliography

Aldous, David J. (1985). "Exchangeability and related topics". In: *École d'Été de Probabilités de Saint-Flour XIII — 1983*. Ed. by P. L. Hennequin. Berlin, Heidelberg: Springer Berlin Heidelberg, pp. 1–198. ISBN: 978-3-540-39316-0 (cit. on p. 3).

Antoniano Villalobos, Isadora and Stephen Walker (Aug. 2015). "A Nonparametric Model for Stationary Time Series". In: *Journal of Time Series Analysis* 63. DOI: 10.1111/jtsa.12146 (cit. on p. 5).

Barajas, Luis E Nieto, Peter Muller, Yuan Ji, Yiling Lu, and Gordon B. Mills (Jan. 2012). "A Time-Series DDP for Functional Proteomics Profiles". In: *Biometrics* 68.3, pp. 859–868. DOI: 10.1111/j.1541-0420.2011.01724.x (cit. on p. 5).

Barry, Daniel and J. A. Hartigan (1993). "A Bayesian Analysis for Change Point Problems". In: *Journal of the American Statistical Association* 88.421, pp. 309–319. ISSN: 01621459, 1537274X. URL: http://www.jstor.org/stable/2290726 (cit. on p. 12).

Besançon, Mathieu, Theodore Papamarkou, David Anthoff, Alex Arslan, Simon Byrne, Dahua Lin, and John Pearson (2021). "Distributions.jl: Definition and Modeling of Probability Distributions in the JuliaStats Ecosystem". In: *Journal of Statistical Software* 98.16, pp. 1–30. ISSN: 1548-7660. DOI: 10.18637/jss.v098.i16 (cit. on p. 23).

Bezanson, Jeff, Alan Edelman, Stefan Karpinski, and Viral B Shah (2017). "Julia: A fresh approach to numerical computing". In: *SIAM Review* 59.1, pp. 65–98. DOI: 10.1137/141000671 (cit. on p. 23).

Blackwell, David and James B. MacQueen (1973). "Ferguson Distributions Via Polya Urn Schemes". In: *The Annals of Statistics* 1.2, pp. 353–355. DOI: 10.1214/aos/1176342372 (cit. on p. 3).

Caron, François, Willie Neiswanger, Frank Wood, Arnaud Doucet, and Manuel Davy (Jan. 2017). "Generalized Pólya urn for time-varying Pitman-Yor processes". In: *Journal of Machine Learning Research* 18.1, pp. 836–867. ISSN: 1532-4435 (cit. on p. 5).

Chen, Jiahao and Jarrett Revels (Aug. 2016). "Robust benchmarking in noisy environments". In: *arXiv e-prints*, arXiv:1608.04295. arXiv: 1608.04295 [cs.PF] (cit. on p. 25).

Christensen, Ronald, Wesley Johnson, Adam Branscum, and Timothy Hanson (2010). *Bayesian ideas and data analysis. An introduction for scientists and statisticians*. CRC Press. DOI: 10.1201/9781439894798 (cit. on p. 12).

Crowley, Evelyn M. (1997). "Product Partition Models for Normal Means". In: *Journal of the American Statistical Association* 92.437, pp. 192–198. ISSN: 01621459. URL: http://www.jstor.org/stable/2291463 (cit. on p. 12).

David B. Dahl, Devin J. Johnson and Peter Müller (2022). "Search Algorithms and Loss Functions for Bayesian Clustering". In: *Journal of Computational and Graphical Statistics* 31.4, pp. 1189–1201. DOI: 10.1080/10618600.2022.2069779 (cit. on p. 33).

De Blasi, Pierpaolo, Stefano Favaro, Antonio Lijoi, Ramses H. Mena, Igor Prunster, and Matteo Ruggiero (Feb. 2015). "Are Gibbs-Type Priors the Most Natural Generalization of the Dirichlet Process?" In: *IEEE Trans. Pattern Anal. Mach. Intell.* 37.2, pp. 212–229. ISSN: 0162-8828. DOI: 10.1109/TPAMI.2013.217 (cit. on p. 15).

De Iorio, Maria, Stefano Favaro, Alessandra Guglielmi, and Lifeng Ye (Oct. 2019). *Bayesian nonparametric temporal dynamic clustering via autoregressive Dirichlet priors*. DOI: 10.48550/arXiv.1910.10443 (cit. on p. 5).

De Iorio, Maria and Athanasios Kottas (2018). "Modeling for Dynamic Ordinal Regression Relationships: An Application to Estimating Maturity of Rockfish in California". In: *Journal of the American Statistical Association* 113.521, pp. 68–80. DOI: 10.1080/01621459.2017.1328357 (cit. on p. 5).

Denison, D. and C Holmes (Apr. 2001). "Bayesian Partitioning for Estimating Disease Risk". In: *Biometrics* 57, pp. 143–9. DOI: 10.1111/j.0006-341X.2001.00143.x (cit. on p. 14).

Duncan, Earl (2016). *Deriving the Full Conditionals*. BRAG: Bayesian Research & Application Group. URL: https://bragqut.wordpress.com/wp-content/uploads/2018/04/deriving-the-full-conditionals.pdf (cit. on p. 9).

Fassò, A., J. Rodeschini, A. Fusta Moro, Q. Shaboviq, P. Maranzano, M. Cameletti, F. Finazzi, N. Golini, R. Ignaccolo, and P. Otto (2023). *AgrImOnIA: Open Access dataset correlating livestock and air quality in the Lombardy region, Italy (3.0.0)*. DOI: https://doi.org/10.5281/zenodo.7956006 (cit. on pp. v, vii, 4, 34, 39).

Ferguson, Thomas S. (1973). "A Bayesian Analysis of Some Nonparametric Problems". In: *The Annals of Statistics* 1.2, pp. 209–230. DOI: 10.1214/aos/1176342360. URL: https://doi.org/10.1214/aos/1176342360 (cit. on p. 2).

Franzén, Jessica (2008). "Bayesian Cluster Analysis : Some Extensions to Non-standard Situations". In: URL: https://api.semanticscholar.org/CorpusID:12397258 (cit. on p. 2).

Ge, Hong, Kai Xu, and Zoubin Ghahramani (2018). "Turing: a language for flexible probabilistic inference". In: *International Conference on Artificial Intelligence and Statistics, AISTATS 2018, 9-11 April 2018, Playa Blanca, Lanzarote, Canary Islands, Spain*, pp. 1682–1690. URL: http://proceedings.mlr.press/v84/ge18b.html (cit. on p. 94).

Gelman, Andrew (Jan. 2004). "Prior Distributions for Variance Parameters in Hierarchical Models". In: *Economics and Econometrics Research Institute (EERI), EERI Research Paper Series* 1 (cit. on p. 66).

Gelman, Andrew, Jessica Hwang, and Aki Vehtari (July 2013). "Understanding predictive information criteria for Bayesian models". In: *Statistics and Computing* 24. DOI: 10.1007/s11222-013-9416-2 (cit. on p. 12).

Gormley, Isobel, Thomas Murphy, and Adrian Raftery (Oct. 2022). "Model-Based Clustering". In: *Annual Review of Statistics and Its Application* 10. DOI: 10.1146/annurev-statistics-033121-115326 (cit. on p. 2).

Gower, J. C. (1971). "A General Coefficient of Similarity and Some of Its Properties". In: *Biometrics* 27.4, pp. 857–871. ISSN: 0006341X, 15410420. URL: http://www.jstor.org/stable/2528823 (cit. on p. 19).

Grazian, Clara (Mar. 2023). *A review on Bayesian model-based clustering*. DOI: 10.48550/arXiv.2303.17182 (cit. on p. 3).

Gutiérrez, Luis, Ramsés H. Mena, and Matteo Ruggiero (2016). "A time dependent Bayesian nonparametric model for air quality analysisa". In: *Computational Statistics & Data Analysis* 95.C, pp. 161–175. DOI: 10.1016/j.csda.2015.10.00. URL: https://ideas.repec.org/a/eee/csdana/v95y2016icp161-175.html (cit. on p. 5).

Hartigan, J.A. (1990). "Partition models". In: *Communications in Statistics - Theory and Methods* 19.8, pp. 2745–2756. DOI: 10.1080/03610929008830345 (cit. on p. 12).

Hubert, Lawrence J. and Phipps Arabie (1985). "Comparing partitions". In: *Journal of Classification* 2, pp. 193–218. URL: https://api.semanticscholar.org/CorpusID:189915041 (cit. on p. 31).

Jo, Seongil, Jaeyong Lee, Peter Müller, Fernando Quintana, and Lorenzo Trippa (May 2016). "Dependent Species Sampling Models for Spatial Density Estimation". In: *Bayesian Analysis* 12. DOI: 10.1214/16-BA1006 (cit. on p. 5).

Kalli, Maria and Jim Griffin (Jan. 2018). "Bayesian nonparametric vector autoregressive models". In: *Journal of Econometrics* 203. DOI: 10.1016/j.jeconom.2017.11.009 (cit. on p. 5).

Krige, Daniel G (1951). "A statistical approach to some basic mine valuation problems on the Witwatersrand". In: *Journal of the Southern African Institute of Mining and Metallurgy* 52.6, pp. 119–139 (cit. on p. 57).

Lawson, C. L., R. J. Hanson, D. R. Kincaid, and F. T. Krogh (Sept. 1979). "Basic Linear Algebra Subprograms for Fortran Usage". In: *ACM Trans. Math. Softw.* 5.3, pp. 308–323. ISSN: 0098-3500. DOI: 10.1145/355841.355847 (cit. on p. 23).

Lenz, Stefan, Maren Hackenberg, and Harald Binder (2022). "The JuliaConnectoR: A Functionally-Oriented Interface for Integrating Julia in R". In: *Journal of Statistical Software* 101.6, pp. 1–24. DOI: 10.18637/jss.v101.i06 (cit. on p. 31).

Lin, Dahua, John Myles White, Simon Byrne, Douglas Bates, Andreas Noack, John Pearson, Alex Arslan, Kevin Squire, David Anthoff, Theodore Papamarkou, Mathieu Besançon, Jan Drugowitsch, Moritz Schauer, and other contributors (July 2019). *JuliaStats/Distributions.jl: a Julia package for probability distributions and associated functions*. DOI: 10.5281/zenodo.2647458 (cit. on p. 23).

Müller, Peter, Fernando Quintana, and Gary Rosner (Mar. 2011). "A Product Partition Model With Regression on Covariates". In: *Journal of computational and graphical statistics: a joint publication of American Statistical Association, Institute of Mathematical Statistics, Interface Foundation of North America* 20, pp. 260–278. DOI: 10.1198/jcgs.2011.09066 (cit. on p. 15).

Page, Garrit L., Fernando A. Quintana, and David B. Dahl (2022). "Dependent Modeling of Temporal Sequences of Random Partitions". In: *Journal of Com-*

putational and Graphical Statistics 31.2, pp. 614–627. DOI: 10.1080/10618600.2021.1987255 (cit. on pp. v, vii, 3, 5, 9, 32, 36).

Page, Garritt and Fernando Quintana (Sept. 2018). "Calibrating covariate informed product partition models". In: *Statistics and Computing* 28, pp. 1–23. DOI: 10.1007/s11222-017-9777-z (cit. on pp. 18, 19).

— (Apr. 2015). "Spatial Product Partition Models". In: *Bayesian Analysis* 11. DOI: 10.1214/15-BA971 (cit. on pp. 14, 22).

Quintana, Fernando, Peter Müller, and Ana Luisa Papoila (Mar. 2015). "Cluster-Specific Variable Selection for Product Partition Models". In: *Scandinavian Journal of Statistics* 42. DOI: 10.1111/sjos.12151 (cit. on p. 15).

Quintana, Fernando A., Peter Müller, and Ana Luisa Papoila (2015). "Cluster-Specific Variable Selection for Product Partition Models". In: *Scandinavian Journal of Statistics* 42.4, pp. 1065–1077. DOI: https://doi.org/10.1111/sjos.12151 (cit. on p. 57).

R Core Team (2024). *R: A Language and Environment for Statistical Computing*. R Foundation for Statistical Computing. Vienna, Austria. URL: https://www.R-project.org/ (cit. on p. 31).

Teh, Yee Whye (2010). "Dirichlet Process". In: *Encyclopedia of Machine Learning*. Ed. by Claude Sammut and Geoffrey I. Webb. Boston, MA: Springer US, pp. 280–287. ISBN: 978-0-387-30164-8. DOI: 10.1007/978-0-387-30164-8_219 (cit. on p. 3).

Wade, Sara (Mar. 2023). "Bayesian cluster analysis". In: *Philosophical transactions. Series A, Mathematical, physical, and engineering sciences* 381, p. 20220149. DOI: 10.1098/rsta.2022.0149 (cit. on p. 2).

Acknowledgements

"This is to be my haven for many long years, my niche which I enter with such a mistrustful, such a painful sensation... And who knows? Maybe when I come to leave it many years hence I may regret it!"

— Fëdor Dostoevskij, *The House of the Dead*

I would like to thank my advisors Alessandra Guglielmi and Alessandro Carminati, primarily for having made me feel, during the entire course of the thesis, in a very calm, lovely atmosphere, in which I have been able to feel perfectly at ease (which is notoriously a NP-hard problem). The epigraphs of my beloved author Dostoevsky and the title inspired by the Star Wars films, as well as some poetic licenses and easter eggs scattered across the chapters (which they have kindly allowed me to keep) I think prove this feeling of sweet and respectful confidence.

I thank professor Alessandra Guglielmi for having guided me through the fog of uncertainty and puzzlement that often the thesis brings, or in general the final period of university. From the beginning she shared a genuine interest in the work that we would have done and a confidence in my chances of really carrying it out.

I thank Alessandro Carminati for having assisted me in many of the most critical phases of the thesis. His action always precise and effective has been necessary to solve the various theoretical puddles in which I got stuck. Moreover, we share the same passion for Julia and, I believe, the delight for having overthrown the not-so-missed C of the old model implementation.

I thank my family for having helped me, in different ways, during these years of university, and my friends and fellows who have always and wisely brought to light my highest potential and resources. The passion for solving problems, inventing creative solutions, getting lost in calculations, wandering through the magical world of the most advanced mathematics, sharing doubts and reasonings: all this has always found in you a wonderful and unforeseen companion.

I also thank all the boys and girls with whom I have had the honour to work and play in the various summer camps, for steadily reminding me of the cheerful and soft spirit with which all the various challenges can be faced.

Ringraziamenti

> *"Ecco il mio ponte d'approdo per molti lunghi anni, il mio angoletto, nel quale faccio il mio ingresso con una sensazione così diffidente, così morbosa... Ma chi lo sa? Forse, quando tra molti anni mi toccherà abbandonarlo, magari potrei anche rimpiangerlo!"*
>
> — Fëdor Dostoevskij, *Memorie da una casa di morti*

Vorrei ringraziare innanzitutto i miei relatori Alessandra Guglielmi e Alessandro Carminati, principalmente per avermi fatto sentire, durante l'intero svolgimento della tesi, in un clima molto tranquillo, sereno, in cui ho avuto modo di trovarmi pienamente a mio agio. Le epigrafi del mio caro autore Dostoevskij e il titolo ispirato alla saga di Star Wars, nonché alcune licenze poetiche sparse nei vari capitoli (che loro mi hanno gentilmente concesso di tenere) credo dimostrino questa atmosfera di piacevole ma rispettosa confidenza.

Ringrazio la professoressa Alessandra Guglielmi per avermi guidato attraverso la nebbia di incertezza e confusione che spesso accompagna la tesi, o in senso lato gli ultimi mesi di università. Fin dall'inizio ha infatti condiviso un sincero interesse per il lavoro che avremmo dovuto svolgere e una fiducia nelle mie possibilità di condurlo a termine.

Ringrazio Alessandro Carminati per avermi aiutato in molte delle fasi più critiche della tesi. Il suo intervento sempre preciso e puntuale è stato necessario per risolvere le varie pozzanghere teoriche in cui mi ero impantanato. Inoltre, condividiamo la stessa passione per Julia e, credo, la soddisfazione per aver battuto il non-così-compianto C della vecchia implementazione del modello.

Ringrazio la mia famiglia per avermi aiutato, in vari modi, durante questi anni di università, e i miei amici e compagni di studio, i quali hanno sempre sapientemente fatto emergere le mie migliori potenzialità e risorse. La passione per risolvere problemi, ideare soluzioni creative, perdersi nei calcoli, addentrarsi nel magico mondo della matematica più avanzata, condividere dubbi e ragionamenti: tutto questo ha sempre trovato in voi un'ottima e inaspettata compagnia.

Ringrazio anche tutti i bambini e ragazzi con cui ho avuto modo di lavorare e giocare nei vari campi estivi, per farmi sempre ricordare dello spirito gioioso e leggero con cui si possono approcciare tutte le varie sfide.